DEMOLDING OF
MICRO-STRUCTURED SURFACES
IN THE INJECTION MOLDING PROCESS

by

Tobias Struklec

A Dissertation
in Candidacy for the Degree of
Doktor der montanistischen Wissenschaften

Montanuniversitaet Leoben
Department of Polymer Engineering and Science

Chair of Polymer Processing
Head: Prof. Dr. Clemens Holzer

Supervisor: Prof. Dr. Clemens Holzer

May 2015

I hereby declare on oath that I did this dissertation
in hand by myself using only the literature cited at
the end of this thesis

Tobias Struklec

Abstract

Modern medical applications attempt to scale down entire diagnostic laboratories to a single polymer chip the size of a credit card. This is an enormous challenge for the manufacturing process because very small structures have to be realized. The demolding of the polymer part containing these structures in the injection molding is often the bottle neck for the part quality. Structures can be damaged and in some cases the continuous manufacturing process can be disturbed. Understanding the demolding is therefore essential for the final part quality.

To analyze this step, a special measurement device has been developed. Using this measurement tool, demolding forces can be measured in a reproducible way under process conditions. Demolding energies are calculated from this force. The demolding energy is shown to be an important indicator for the demolding step where lower energies mean better demolding and therefore less risk of damage to the part.

The measurement device was used to investigate four influencing factors that affect the demolding step: a) *polymer*, b) *geometry*, c) *mold surface* and d) *process conditions*. Concerning a) the *polymer*, three thermoplastic polymers, one thermoplastic elastomere and two polymer blends were tested. To investigate b) the *geometry*, four different micro-structures in six configurations were tested. To look into c) the injection *mold surface*, several different coatings were tested to look into how different surface properties affect demolding. Finally, for d) the injection molding *process*, specifically the temperature management for the demolding step was emphasized.

The investigations showed that there is not one coating ideal for all polymers but different suitable coatings for each investigated polymer. PMMA works well with TiN while TiN does not improve the demolding of COP. The placement of the micro-structure is also important, especially in combination with the process settings. High mold temperatures increase the demolding energy which can add to the effect of an unsuitable structure placement. Due to the complexity of the interactions improving the demoldability is not a straightforward process. Using this measurement device, suitable coatings for the application and polymer can be found easily. Additionally, an optimization of the processing parameters can be performed, reducing the number of substandard goods.

Kurzfassung

Moderne medizinische Anwendungen können mittlerweile ein gesamtes diagnostisches Labor auf einen Polymerchip der Größe einer Kreditkarte zu bringen. Die Herstellung dieser kleine Strukturen ist eine enorme Herausforderung für den Prozess. Die Entformung dieser strukturierten Bauteile im Spritzgussverfahren ist oft ein kritischer Schritt für die Funktionalität. Strukturen können beschädigt werden und in manchen Fällen kann der kontinuierliche Prozess unterbrochen werden. Das grundlegende Verständnis des Entformungsschrittes ist daher unerlässlich für die Bauteilqualität.

Um die Entformung zu analysieren wurde ein spezielles Messwerkzeug entwickelt, mit dem Entformungskräfte reproduzierbar unter realen Prozessbedingungen gemessen werden können. Aus diesen Kräften wird anschließend die Entformungsenergie berechnet, welche ein wichtiger Indikator für den Entformungsschritt ist. Hierbei bedeuten niedrigere Energien eine bessere Entformbarkeit und damit ein geringeres Risiko für eine Beschädigung des Teils.

Dieses Messgerät wurde verwendet, um vier Einflussfaktoren, die den Entformungsschritt bestimmen, zu untersuchen: a) *Polymer*, b) *Geometrie*, c) *Werkzeugoberfläche* und d) *Prozessbedingungen*. Bezüglich a) dem *Polymer* wurden drei thermoplastische Polymere, ein thermoplastisches Elastomer und zwei Polymermischungen getestet. Um b) die *Geometrie* zu untersuchen wurden vier verschiedene Mikrostrukturen in sechs Konfigurationen getestet. Für c) die *Oberfläche*, wurden verschiedene Beschichtungen getestet. Damit wurde untersucht wie unterschiedliche Oberflächeneigenschaften die Entformung beeinflussen. Schließlich liegt für d) im *Spritzgussverfahren* der Fokus insbesondere auf der Temperaturführung des Entformungsschrittes.

Die Untersuchungen zeigten, dass es keine ideale Beschichtung gibt, die für alle Polymere den Entformungsvorgang verbessert. Statt dessen zeigt sich, dass das Entformungsverhalten für jedes der untersuchten Polymer unterschiedlich ist. PMMA funktioniert gut mit TiN, während TiN nicht in der Lage ist, die Entformung beim Einsatz von COP zu verbessern. Die Anordnung der Mikrostruktur ist ebenfalls wichtig, insbesondere in Kombination mit den Prozesseinstellungen. Hohe Werkzeugtemperaturen erhöhen die Entformungsenergie, was sich zusätzlich zu einer ungeeigneten Struktur Platzierung negativ auswirkt. Aufgrund der Komplexität der Wechselwirkungen ist eine Verbesserung der Entformbarkeit schwierig und kein geradliniger Prozess. Trotzdem können mit dieser Messvorrichtung geeignete Beschichtungen für bestimmte Anwendung und Polymere leichter gefunden werden. Außerdem können Prozessparameter optimiert werden, um möglichen Ausschuss zu reduzieren.

Acknowledgments

I want to thank all the people that helped me to get where i am now.

First of all I want to thank the Sony DADC Austria AG for the opportunity to conduct my PhD thesis at this interesting field of research, which connected medical applications, mold technology, injection molding processing, material selection and micro-structures. I want to thank my supervisors Prof. Clemens Holzer and Dr. Thomas Lucyshyn of the Chair of Polymer Processing for their excellent support and help during the thesis.

For their commitment and enthusiasm I thank Martin Burgsteiner without whom the mold design would not have been possible and Barbara Strohmyer who worked with me on the project and helped me in the execution of the experiments. On the side of Sony I want to thank Dr. Werner Balika, Stefan Moderegger and Martin Karl who had not only initiated this project but also supported and helped me during the research. For their support in the injection molding lab and a lot of troubleshooting I want to thank Eduard Leitner, Rudolf Schatzer. Furthermore, I want to thank all the colleagues at the University for their help, numerous discussions and inputs: Dr. Martin Pletz, Dr. Florian Mueller and Marian Janko

At last I want to thank my family, especially my parents and my girlfriend for their support, help and patience through all the years of studying.

Contents

Chapter 1

Introduction and objectives

An important part of modern medical applications is based on 'lab-on-a-chip' or similar technologies. These 'chips' are used for disposables or life-science applications in different medical areas (e.g. diagnostics). To enhance their functionality as many features as possible are placed on the smallest possible space [3, 5, 36, 76]. This miniaturization continuously increased the possibilities for these applications and is still ongoing. To support this fast paced progress the micro-geometries for the application (e.g. micro channel) as well as the part macro-geometry (e.g. slide for microscopy) have to become more and more accurate. Subsequently, the dimensional tolerances for the polymer applications are going down fast. By now tolerances for the macro-geometry of only a few micrometers are required with the tolerances for the micro-geometry set even lower. In addition to these geometric requirements, the applications in the medical sector have many restrictions. In most applications the polymer material choice is limited to only a few or even one eligible polymer. These polymers have to pass strict standards and must not be altered in any way. This means that any additives or enhancements to aid in the manufacturing process are inadmissible. The resulting injection molding process often is very limited and not ready for large scale production [58]. Therefore, the goal of this thesis is to better understand the acting mechanisms that occur in large scale production units, especially focusing on injection molding. In particular the focus is on the demolding and the demoldability of micro-structured surfaces.

These surface interactions during the demolding step are critical as they define the demoldability (i.e. the final part quality after demolding) of the part. The demolding can lead to different kinds of problems, most prominently the ripping of micro-structures. These interacting forces that can rip the polymer might also induce bending of the polymer chip, or inhibit demolding altogether. All of these effects can occur in different setups and will

render the application unusable. Despite the importance of the demolding step, there is a lack of thorough investigation. Most studies focus on the replication grade of different micro-structures and rely mainly on the hot embossing process.

The main objective of this work is to address this issue and focus on demoldability of the micro-structures especially in the large scale oriented injection molding process. To make this possible, the interaction mechanisms and the demolding step were investigated. The next and most important step was to quantitate the demoldability and to devise a method that can be implemented in a regular injection molding environment. To put this into practice an injection mold was developed to measure the mechanisms that affect the demolding. This device was used to systematically study the demolding step and pinpoint the parameters most important for manufacturing different micro-structures in different polymers. Additionally, this makes distinctions in the demoldability between different setups (e.g. designs, polymers) possible. So far the demoldability was characterized as either 'good' (usable part) or 'bad' (unusable, broken part). Measuring a specific value (i.e. demolding force or demolding energy) to describe the demoldability makes establishing a viable process window easier and more precise.

Finally, the understanding of the effects that play a crucial role in the demolding step provides the information necessary to understand the underlying injection molding process. This can directly be used to reduce the number of defective parts and thereby making competitive injection molding for micro-structured applications feasible and new applications possible.

Chapter 2

State of the art

2.1 Replication of micro-structured surfaces

To produce micro-structured polymer devices in large numbers, replication methods are used. This means a negative of the desired design is manufactured and replicated over and over again. The negative carrying the micro-structure used in polymer processing is commonly called 'stamper'. This stamper can be manufactured in a variety of ways including micromachining from silicon, different forms of LIGA (Lithography electroplating and molding) or machining using a CNC micro-milling tool (used for larger features). For the manufacturing of a certain micro-structure a suitable manufacturing technology has to be chosen. Among the different methods used for manufacturing only a few suit the purposes of producing high precision micro-structures [76]. Depending on the choice of geometry methods like wet silicon etching are inferior to LIGA mainly because they are limited in the freedom of design. Micro milling (mechanical micromachining) for comparison can be used for a large variety of different designs but is restricted by the minimum feature size, which is defined by the size of the drill. Regarding the design of micro-channels or similar structures the LIGA technology would fulfill all necessary requirements perfectly. Unfortunately, low availability and high cost make it unfeasible or even inaccessible for stamper manufacturing. The best alternative is the optical lithography and electroforming method, which is apart from the used wavelength basically identical to the LIGA process. Using longer wavelengths makes the process comparably cheap and available and all needed structures can be manufactured using this process.

An alternative to replication methods that require a stamper or other form of negative is available as well. The technology uses a thermo-active polymer resin that is located on a plane surface. A focused light beam cures

the polymer at desired positions. This creates a hardened three-dimensional construct of any desirable design. Although this process allows for almost any structure to be manufactured, it is limited by the large production times, small areas and high cost. Therefore, the commonly used industrial processes for replication are *injection molding* and *hot embossing*.

2.1.1 Hot embossing

Hot embossing is defined as the stamping of a pattern into a polymer which has been softened before by raising the temperature of the polymer above its glass transition or melt temperature. For this, the polymer substrate is placed in the hot embossing unit (see Figure 2.1 a). Unlike injection molding the polymer is not pressured by injection and therefore flowing into the micro-structure. For the replication the stamper is pressed into the polymer and thereby replicates the structured area (see Figure 2.1 b). After a certain holding time (see Figure 2.1 c) and sufficient cooling, the embossed polymer becomes stiff enough for the last processing step. The last step, as shown in Figure 2.1 d, is the demolding. Similarly to the injection molding process the polymer is cooled down until the stamper can be pulled out without damaging the micro-structure.

The main advantages of hot embossing are low material strain due to the low shearing as well as homogenous shrinkage due to the missing material orientations that occur in the injection molding process. This helps in avoiding internal stress which can induce scattering centers unfavorable for optical applications or other applications. Additionally, lower stresses enable the production of more delicate or fragile structures. This includes free standing thin columns or narrow or long walls.

Despite these superior possibilities regarding the feature size, industrial large scale fabrication of plastics components is usually done using injection molding. The sole reason for this is the hot embossing cycle time. The average cycle time of a hot embossing process is rarely lower then a few minutes and more often ranges in the area of half an hour. The good controllability of the hot embossing process however makes it favorable for scientific purposes [79]. This is represented in the number of publications on the topic of demoldability [4, 17, 18, 37, 42]. Additional use for hot embossing is rapid prototyping, which helps to reduce the time to market for new applications. Despite the differences of hot embossing to injection molding, the demolding problems that occur are similar for both methods.
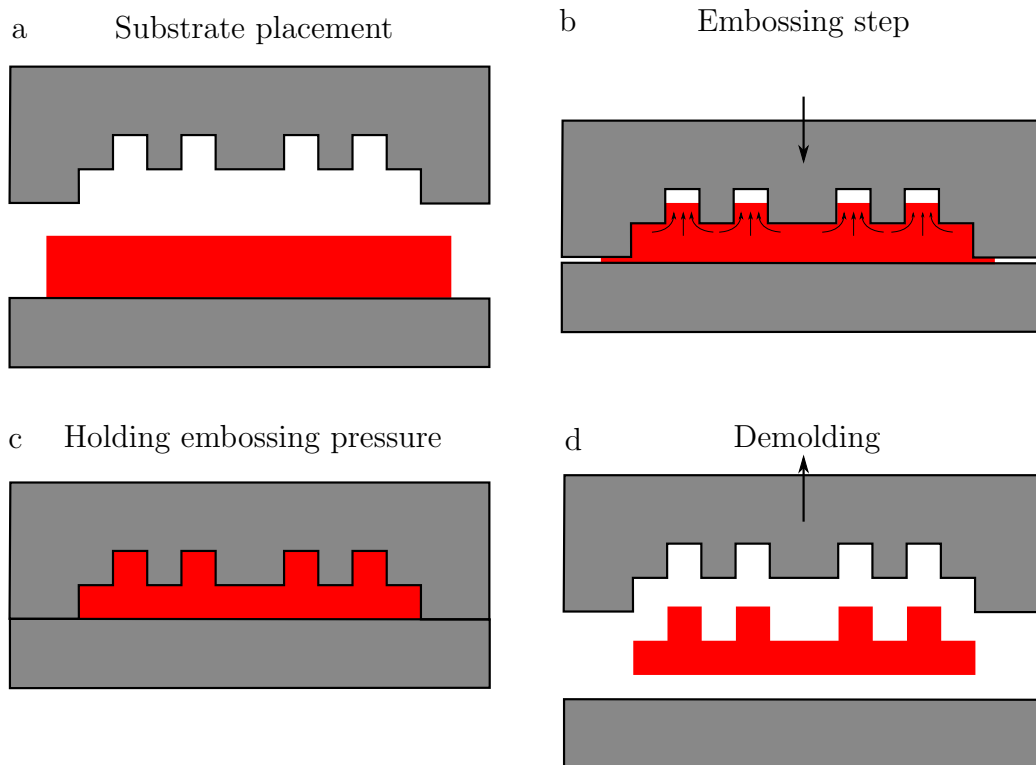
a   Substrate placement   b   Embossing step

c   Holding embossing pressure   d   Demolding

Figure 2.1. Hot embossing of a micro-structured part.

2.1.2 Injection molding

Injection molding is a manufacturing process for producing parts in large
numbers commonly using thermoplastic polymer materials. It is a perfect
process for the mass production of micro-structured surfaces [74] with high
precision [32]. The polymer material is fed into a heated barrel. In the
barrel the polymer is transported by a screw leading to the nozzle. During
transportation, the heat of the barrel and the shear deformation are mixing
and melting the polymer. The retracting screw doses a defined amount of
polymer in front of the closed nozzle. Figure 2.2 illustrates the injection
molding process starting with the closing of the mold (a. Mold closing). The
forward motion of the screw forces the polymer melt into a mold cavity (b.
Injecting polymer). Once the cavity is filled, a holding pressure is maintained
to compensate for material shrinkage (c. Holding pressure). This is done to
ensure good molding of the structured area. In the cavity that defines the
macro-geometry, the polymer cools down and solidifies in the given form.
Simultaneously to the cooling, the screw starts dosing material again to pre-
pare for the next shot. Once the part has cooled down, the mold opens and

the part is ejected (d. Demolding). The cycle then starts again with the closing of the mold. Common injection molding cycle times range from a few seconds to a few minutes.

a   Mold closing   b   Injecting polymer

c   Holding pressure   d   Demolding
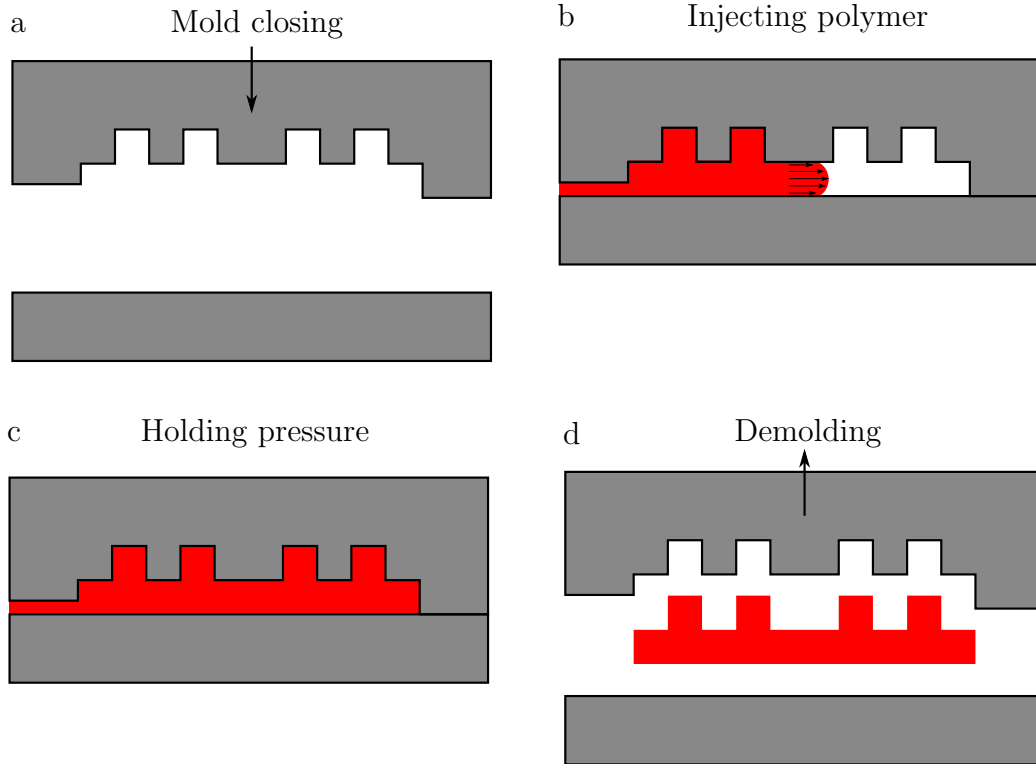
Figure 2.2. Injection molding of a micro-structured part.

For the manufacturing of micro-structured surfaces this 'common' injection molding process is adapted using a micro-structured stamper (as investigated by Griffiths et al. [33]). This stamper is placed in the cavity and fixed using some sort of frame system. This structure is then replicated in the injected polymer. Each stamper is designed for a certain application making it easy to swap out different stampers for different applications using the same injection mold.

2.1.3   Variotherm processing

In the variotherm process cycle the temperature of the mold cavity can be changed over time depending on the process cycle and the necessities. For example right after the ejection and before the next injection step the mold starts heating up to a certain injection temperature. This temperature is usually slightly above the glass transition temperature of the polymer (or in

the range of the melting temperature in case of semi-crystalline polymers). When this set temperature is reached, the polymer is injected immediately. Due to the fact that the mold temperature is now above the glass transition temperature, the polymer remains fluid during the entire filling-phase as no frozen layer can appear at the contact area. This effect will lead for example to a significantly better replication of micro-structures. Immediately after the injection of the polymer is completed, the cooling of the entire mold starts. The heating is disabled and the built in cooling lowers the temperature back to the initial mold temperature. This will then slowly cool down the already molded polymer below the ejection temperature. Once the polymer is sufficiently solidified the mold opens and the polymer part is ejected. This step as well as the rest of the injection molding cycle is identical to the common injection molding cycle. The variotherm process handling is used especially for optical applications, like contact lenses, which need to have a homogeneous crystallinity. This is necessary to achieve a homogeneous refraction index. It has also found its way into the production of polished surfaces on everyday products like modern TV-screen frames. Some of the main benefits of variotherm processing are [70]:

- The molding of the polymer - especially of micro-structures - can be improved (e.g. no frozen layer at the mold contact).
- The injection flow resistance and pressure can be lowered.
- Polymer part quality can be improved, e.g. surface quality, state of stress, reduction of sink marks.
- Increasing of weld line strength due to higher polymer contact temperatures at the weld line.

With a cold mold surface and a process with no variothermal heating, the polymer solidifies instantly at the contact surface. This increases the local viscosity and affect the crystallization. Using a variotherm system a homogenius crystallization can be achived. This leads to a polished looking polymer surface. Additionally, the variotherm heating decreasing the viscosity at the contact surface and therefore decreases the flow resistance. This improves the molding of micro-structures, as a completely frozen layer at the contact area can even completely prevent molding of micro-structures.

This is one of the reasons why variotherm process handling is essential for the production of nano- and micro-structured surfaces [80]. Additionally, micro-structures with high aspect-ratios (compare Chapter 3.2 Terminology for micro-structures) will need a heated mold to achieve a good replication quality. Figure 2.3 shows that the variotherm process can be used to realize these high aspect ratios.

This evaluation done by Fu et al. [28] tested the moldability of certain micro-structures with and without the variotherm system. As in other studies he relies on a metal polymer feedstock but draws conclusions that should apply to similar injected polymers. Unfortunately, it is not described how the maximum attainable aspect ratio was defined or determined. The evaluation of several scanning electron microscope (SEM) pictures by Fu suggests that the moldability was determined by optical means. Important to note is, that Fu found, that smaller micro-structures (micro features) yield better moldability for high aspect ratios. One would expect small features to exhibit a bad filling behavior. Still Fu makes no effort to explain this not obvious behavior in any of the papers quoted in this thesis. Nevertheless, the important conclusion of Fu's study that remains valid despite that is, that variotherm systems will enhance the moldability of micro-structures.
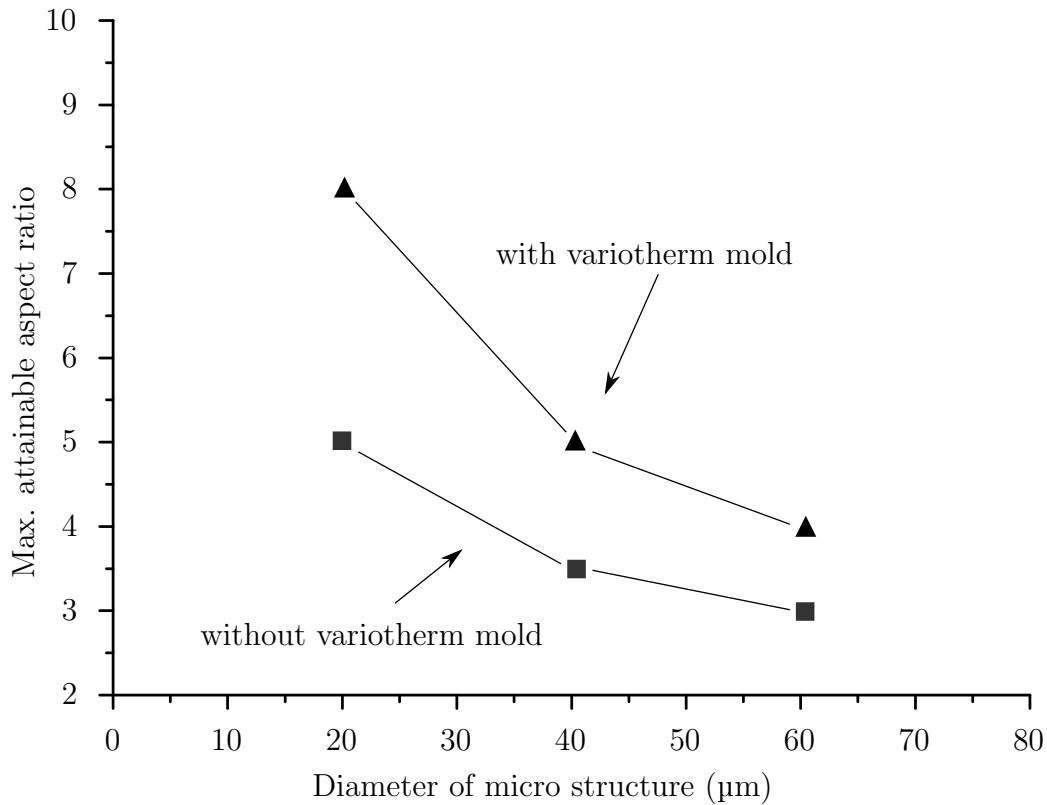

Figure 2.3. Maximum attainable aspect ratios with and without the variotherm mold [28].

2.2 Medical applications

A medical device is an instrument, apparatus, implant, in vitro reagent, or similar or related article that is used to diagnose, prevent, or treat disease or other conditions, and does not achieve its purposes through chemical action within or on the body (which would make it a drug) [16]. Therefore any device that is in contact with a patient directly or indirectly is classified as medical device. This classification brings constraints depending on the risk level associated with the device. An overview of some devices and their associated risk class can be seen in Table 2.1. The risk is defined only by the intended use following several rules defined by the state. In case of Table 2.1 the classification is based on the guidelines of the European Union [25]. Class I items are generally applications that can do little harm, while Class III is almost exclusively for invasive devices that bear a lot more risk for the patients. Class IIa and IIb cover all devices ranging in-between.

Table 2.1. Overview of different sample devices from all the risk categories as defined by the European Union [26].

Class I	Class IIa	Class IIb	Class III
Medical instruments	Dental materials	Anaesthetic equipment	Cardiac catheters
Walking aids	Disinfectants	Condoms	Artificial joints
Wheelchairs	Ultrasonic devices	Radiation equipment	Stents
Care beds	Syringes	Blood bags	Pacemakers
Bandages	Contact lenses	Defibrillators	Breast implants

In this thesis the main focus is on the utilization of structured surfaces for medical devices. These are mostly diagnostic devices for different purposes like blood analysis. Depending on the use, most applications count as in-vitro diagnostics and belong to risk group IIa especially when handling bodily fluids. In polymer processing the most general term is *chip* which in

the field of medical applications mostly refers to more specific *lab-on-a-chip*. This term can be further divided into disposables or life science applications. The term medical also states that all of these 'parts' need to be approved according to the respective risk class to ensure they cause no harm to a patient or compromise medical tests. In America this is commonly done by the Food and Drug administration (FDA) which provides an index for medical applicability. Polymer based applications, like any others are strictly regulated. Besides the polymer type (monomer) every used additive is relevant for the approval process. Table 2.2 shows a material study done by Attia et al. [3] that points out a number of polymers that are feasible for micro injection molding and molding of micro-structures. This list covers a mainly polymers used for medical applications that have already been reported in other publications. This excerpt shows some of the more prominent polymer from the semi-crystalline and amorphous category. This list is the basis for choosing relevant materials for the experiments.

These mentioned strict regulations and the associated very thorough testing process leads to long times to market. This makes it hard to enter a well established or saturated market with a new or improved product. Despite that, polymer applications become more and more popular even replacing their glass predecessors in many areas. There are mainly two fields for medical application that are significant for competitors of polymer devices in this market. Both still have a growing demand and are scientifically of great interest. The scientific interest comes from the small basic knowledge regarding small scale structures and the ways they can be produced. This entails a lot of potential for future applications as well as the miniaturization progresses.

Recently, a trend towards high aspect ratios in these 'life-science' applications can be seen. Some reasons are:

- A higher active surface area per unit can be achieved, which generally means higher concentrations. This is particularly important for chemical or biochemical applications like micro-reactors, micro-mixers, chromatographic columns or DNA concentrators.
- The packing density of micro-structure elements can be increased to parallelize different functions of MEMS (micro-electro-mechanical system) on one chip, eg. in DNA separation or nano-well-plates.
- An increase in flow rate can be achieved, as the miniaturization provides a higher cross-sections per unit substrate area .

Table 2.2. Excerpt of polymers used for micro-injection molding based on the research of Attia et al. [3].

Amorphous polymers	
Polymer	**Full name**
PMMA	Polymethylmethacrylate
PC	Polycarbonate
PSU	Polysulfone
PS	Polystyrene
COC / COP	Cyclic olefin (co)polymer
SAN	Styrene acrylonitrile
SBS	Styrene-butadiene-styrene
Semi-crystalline polymers	
Polymer	**Full name**
PP	Polypropylene
PE	Polyethylene
POM	Polyoxymethylene
PBT	Polybutyleneterephthalate
PA	Polyamide
PEEK	Polyetheretherketone

2.2.1 Disposables

Disposable refers to a device that is intended for one use and is discarded afterward. Usually that relates to point-of-care devices that are meant for a specific purpose to be used directly at the point of need instead of a laboratory. Most commonly this is a diagnostic test (e.g. blood test) that can be performed on a predefined lab-on-chip. The goal of these applications is to manufacture a consumer good that not only brings an entire lab to the patient but also allows a fast diagnosis. An example is a lab-on-a-chip urine test that no longer requires for the specimen to be sent to a laboratory. Additionally, the patient can get a feedback on the results immediately. A similar example would be a test for the blood type that can be carried out at home.

Both of these examples can be realized as a micro-fluidic application [68]. Figure 2.4 is an example of a typical micro-fluidic application. The function of this chip is to dilute a sample in a buffer solution for further analyzing. The buffer solution and sample are provided by the two wells on the left and top side of the chip. They travel along the channels and are mixed when they meet up at the intersection. The mixture then moves along the separation channel which functions similar to a chromatography. Overflowing or unneeded sample will flow into the waste chamber to ensure the separation process is not influenced. In the detection area the desired quantities are measured after separation using for example light absorption to measure the amount of a given substance in the sample. These applications can be distributed in a large quantity and have a high efficiency in use. The price is usually very low and can compete with laboratory costs. The demand is estimated to be several millions for individual application. Despite the high number of manufactured polymer parts, a high yield of properly functioning chips has to be achieved. This adds to the high manufacturing complexity. To provide functionality the tolerances of the design are very tight, making it a challenge to realize all applications in terms of polymer processing.
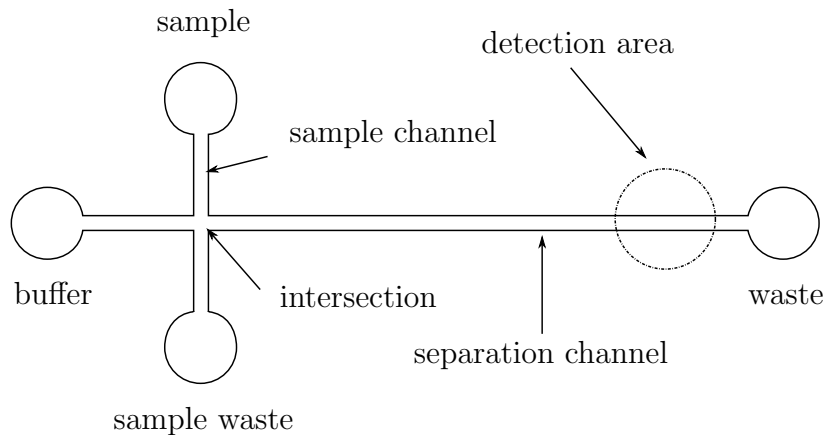
Figure 2.4. Setup and functional principle of a disposable lab-on-a-chip system for capillary electrophoresis [36].

2.2.2 Life science applications

The goal of life science products is not necessarily to be a consumer product. Unlike disposable point-of-care applications, life science is mostly used for scientific/research purposes. This means in most cases it is sophisticated equipment that often cannot be used without a laboratory and is usually

intended for research purpose. An example here would be a chip for the analysis of the genome. In this case the application would contain several features. At one point it would make use of a channel distribution system to enhance the yield of the polymerase chain reaction (PCR). At a later point a patterned structure is used to generate a desired DNA distribution after a separation step. The price range is usually higher then for disposable applications combined with a lower demand that rarely exceeds half a million. Both applications have in common that they try to miniaturize current applications to perform more and more functions on a single chip, which subsequently makes the name 'lab on a chip' evident. Besides the benefits of 'lab on a chip' applications there are other important advantages compared to similar glass applications. Due to the higher cost glass applications are usually cleaned and reused. The cheaper polymer applications are designed for only one use, provide a sterile environment and therefore do not need cleaning. Additionally, there is no risk of contamination, which is critical for most diagnostic applications. Polymers are an ideal basis for these applications because the need to adapt and implement new innovations is high. This means rapid prototyping, short time to market and a low material and manufacturing price is necessary. Polymer replication, especially injection molding offers all of these means.

2.3 Example micro-fluidic devices

As mentioned, micro-fluidic devices can be used for a wide range of applications. The applications range from micro total analysis systems (μTAS), miniaturized drug delivery systems to tissue engineering. Most applications are predominantly passive micro-components. In conventional micro-titer plates simple micro-depressions act as reservoir areas, the so-called wells. Often these miniaturized analysis systems are additionally equipped with capillary micro-channel structures. Mostly they work as inlet or supply channels or as reaction or separation section. They may also contain integrated micro-components, which take over mixing or filter functions. Thereby, precise sample transfer into and from the system can be achieved [36]. More complex μTAS include small pumps or valves.

Some examples for polymer-based micro-fluidic devices are [85]:

- *Flow cells:* Geometrically simple micro-channel configurations of the order of 100 μm with networks or manifolds are successfully utilized in microfluidics. They can be used to extract a component with a

high diffusion coefficient from a sample stream or to measure a sample concentration solely by using the diffusion properties of the substances involved. This concept is applied in a diffusion-based immunoassay for example. Moreover, the different diffusion coefficients between smaller antibodies and larger antigens are utilized to create a color change of an indicator, that can be detected optically. Less complicated microchannel networks, which encapsulate other functional elements such as DNA-arrays, fulfill simple tasks like metering, dosing or distribution [5, 40, 92].

- *Capillary electrophoresis:* Another major expample of microfluidic systems is miniaturized capillary electrophoresis (CE). By means of CE, substance mixtures such as biomolecules (DNA, proteins, etc.) or inorganic ions can be seperated and split up into their components by applying a high voltage [5, 36, 54, 68].

- *Miniaturized PCR:* Polymerase chain reaction (PCR) is commonly used in biotechnology for the amplification of specific DNA fragments. As the PCR process involves elevated temperatures (up to 95 ℃), only polycarbonate (PC) and cyclic olefine copolymer (COC) can be utilized, due to their thermal stability [5, 97].

- *Clinical chemistry and diagnostics:* Polymer devices are particularly suited for diagnostics disposables to avoid contamination. On commercial basis portable 'lab-on-a-chip' systems for blood diagnostics are produced. These include functions such as sample absorption, separation, mixing with reagent, analysis and waste absorption [5, 40, 68].

- *Cell handling:* For biological applications the handling of (living) cells is of great interest. For example for cell counting, flow cytometry or even manipulation is performed on these applications. [1, 66, 72, 86].

- *Micro reactors and containers:* In contrast to the devices and applications described so far, many reactions can take place in a static environment in miniaturized reaction vessels. An example for this device is the open micro-titer plate [5].

2.4 Surface interaction

2.4.1 Friction

All primary interaction between objects is through contact. Objects in contact exhibit forces depending on the interaction. These interactions can either be sliding, rolling or collision. For all practical purposes in this work contact interaction is only defined by sliding. The determining force resulting from a sliding interaction is the friction force which is a force resisting the relative motion of the surfaces in contact [60]. There are several types of friction [6, 44, 60]:

- *Dry friction* is defined as the resistance to relative lateral motion of two solid surfaces in contact.
- *Lubricated friction* is a case of fluid friction where a lubricant fluid separates two solid surfaces.
- *Fluid friction* describes the friction between layers of a viscous fluid that are moving relative to each other.
- *Skin friction* is a component of drag, the force resisting the motion of a fluid across the surface of a body.
- *Internal friction* is the force resisting motion between the elements making up a solid material while it undergoes deformation.

While all of these interactions are friction per definition the most relevant interaction in mechanical setups is dry friction. Figure 2.5 shows a simple free body diagram to visualize the dry friction for two different bodies. In this case the object is on a tilted surface trying to move according to its own weight (acting gravity). Resulting from the gravity a proportional normal force N will act on between the bodies. This normal forces leads to a friction force preventing movement or acting against the downward movement on the tilted surface.
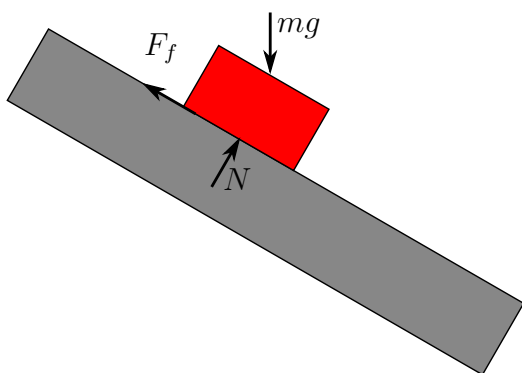

Figure 2.5. Simple free body diagram. N is the normal force, mg the gravitational force, and F_f is the force of friction.

The behavior of dry friction can be expressed using these three empirical laws:

- Amontons' First Law:
  The force of friction is directly proportional to the applied load.
- Amontons' Second Law:
  The force of friction is independent of the apparent area of contact.
- Coulomb's Law of Friction:
  Kinetic friction is independent of the sliding velocity.

The Coulomb law can be easily described in a simple equation using a dimensionless coefficient of friction (compare Equation 2.1). Additionally, dry friction can be divided further into static friction (between non-moving objects) and kinetic friction (in an established sliding motion). This can also be realized in the Coulomb equation using different coefficients of friction for the static and dynamic case (compare Equation 2.1)

$$
F_f = \begin{cases} \mu_s \cdot F_n & \text{at the start of the movement} \\ \mu_k \cdot F_n & \text{for a moving object} \end{cases} \tag{2.1}
$$

Where:

F_f: Friction force acting against the movement

F_n: Normal force acting between the contact surfaces

μ_s: Static friction coefficient

μ_k: Kinetic friction coefficient ($\mu_k \leq \mu_s$)

The friction coefficient to describe similar systems is measured using a simple setup. A body is forced into a controlled sliding motion while the normal force and the force to keep up a constant velocity (i.e. friction force) is measured. Figure 2.6 shows the result of a friction force measurement as described by Worgull [94]. The friction coefficient was measured for different metallic components with a PMMA polymer counterpart. The two measured curves represent the two tested materials. The curves both show a peak that represents the static friction that has to be overcome to initiate movement. The rest of the curve after the peak corresponds to the moving body. For a perfect setup the friction force in the kinetic case should be constant. The oscillation that can be seen for the moving body are slip-stick effects, leading to a varying friction force over the sliding distance. Additionally, the figure shows that the friction force for brass is lower than that for copper.
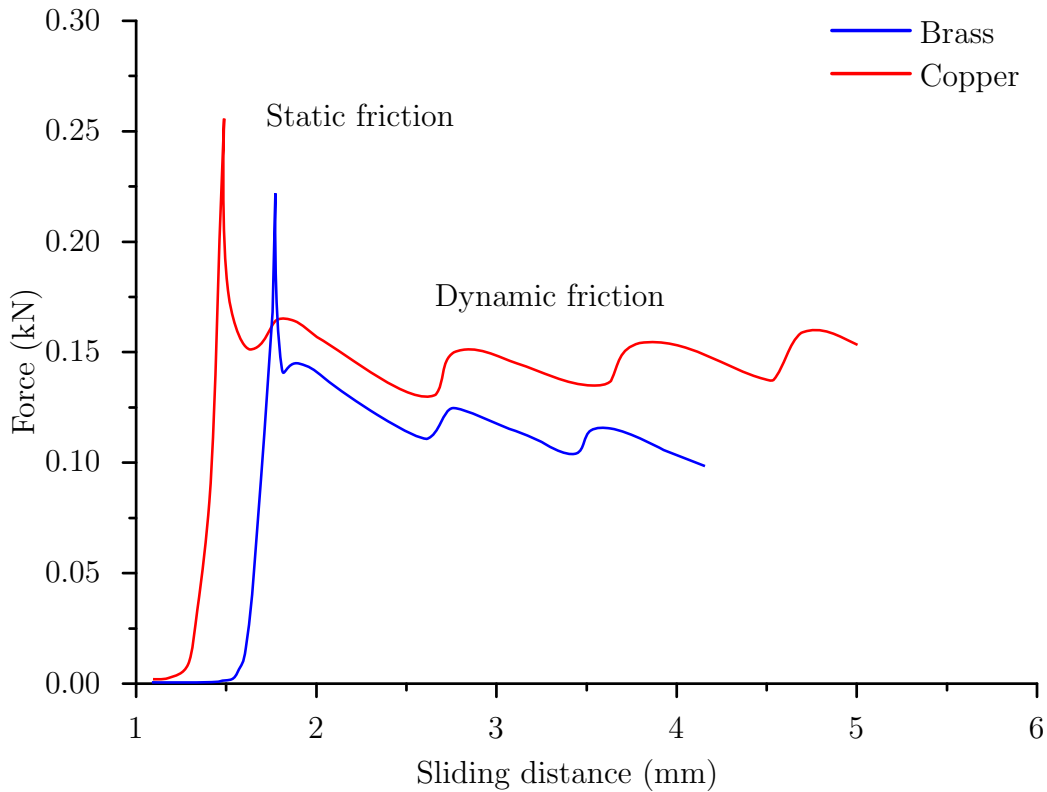
Figure 2.6. Friction of PMMA and the metal counterpart during the demold-
ing process [94].

Measurements like this are commonly performed in tribology where the
measurement setups are often more refined to deal with several of the draw-
backs the very simple Coulomb law has [23]. Therefore, the most important
step for this work is to transfer this simple concept of friction to a regu-
lar injection molding setup and finally make use of this concept for micro-
structures.

To measure friction in the injection molding setup a system has been
proposed by Berger [7]. This system uses the demolding step in the injection
process to induce a sliding motion on the just molded polymer part. The
counterpart can be changed to test different materials with different sur-
face properties. This way arbitrary polymer and metal combinations can be
tested.

To describe the friction that occurs between a micro-structured surface
and the mold horizontal friction measurement will not suffice. The reason
is that micro-structures are placed on a bigger polymer part and are there-
fore subject to shrinkage. Depending on the position of the micro-structure

they can either shrink away or onto the respective sidewalls which changes
the interacting force. Figure 2.7 shows an example setting where the poly-
mer base shrinks towards its geometrical center pressing the micro-structure
against the inner sidewall (Figure 2.7 (a)). The resulting force equilibrium is
illustrated in Figure 2.7 (b). The demolding force F_D, required for ejection is
determined by the release force F_R and the vacuum force F_V (compare Equa-
tion 2.2). F_R represents the friction between the surfaces and is composed
of the pressure between the surfaces p_c due to shrinking, the contact area
A_c and the friction coefficient µ. F_V is an additional force due to vacuum
effects. To measure these combined forces different measurement methods
which are currently used are described in chapter 3.5 'Demolding force and
measurement methods'.
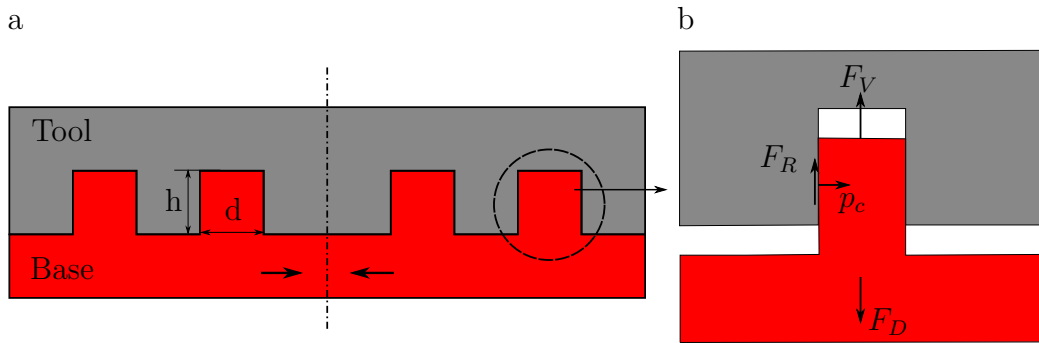
Figure 2.7. Shrinking direction of the molded part and the micro-structure
(a), model of demolding a single micro-structure (b) [27].

$$F_D = F_R + F_V = \mu \cdot A_c \cdot p_c + S \cdot p_v, \tag{2.2}$$

Where:

F_D:	Overall demolding force
F_R:	Release force
F_V:	Vacuum force
μ:	Friction coefficient
A_c:	Sidewall contact area
p_c:	Shrinkage pressure
S:	Cross sectional area
p_v:	Vacuum pressure

The fact that all friction laws are approximations brings a few restrictions. Especially in complex cases like micro-structures with polymeric materials there are many effects that can not be approximated with a simple friction coefficient alone. The most problematic and disregarded phenomena of the Coulomb friction law are:

- There is a temperature dependence of the friction behavior that is especially prominent for polymer materials [77].
- For polymers especially for rubbers the friction coefficient is dependent on the contact area and the normal force [75].
- Even with the distinction of a static and kinematic friction coefficient effects like friction drop after the initial movement or slip stick cannot be described (compare Figure 2.7).
- There is a proven velocity dependence of the friction behavior [77].

These are the main reasons why friction in a micro-structure demolding setup as a stand alone parameter is insufficient. Especially movement and normal force dependance of the friction coefficient poses a huge problem. This means that most standardized measurements can not be transfered to the used setup in this work and sometimes even lack comparability to the performed measurements to friction coefficient measured in a different setup. The 'environmental variables' for the demolding step in the injection molding process are completely different which means that a single Coulomb friction coefficient can not be used to describe the process.

Additionally, a friction simulation done by Fu shows the stress situation that occurs in the micro-structure [27]. This simulation provides results for the stress situation of the micro-structure depending on its placement. This shows as expected that micro-structures farther from the shrinkage center exhibit a higher stress. This means that the friction coefficient is most likely different for each structure as the stress varies. Moreover the critical friction value for failure in the demolding process is the static friction force because it has the higher value. Static friction only occurs at the beginning of the demolding. Therefore, the occurrence of ripping or large deformations of replicated micro-structures will most likely be at the onset of the demolding (compare Figure 3.1 b). Ongoing deformation however happens in the dynamic phase, especially due to slip-stick effects during the demolding (compare Figure 3.1 e). To circumvent these problems a good approach could be to sum all of these small interactions to one global interaction. This is attempted in this work by using the work of friction as a parameter for the interaction (compare Chapter 5.7 'Signal evaluation').

2.4.2 Adhesion

Adhesion in general describes the tendency of two objects or in most cases surfaces to attach to each other. The forces that are responsible for this mutual attraction can be divided into several types [57]:

- *Mechanical adhesion*: Adhesive materials fill the voids or pores of the surfaces and hold surfaces together by interlocking.
- *Chemical adhesion*: Two materials may form a compound at the interface and bond chemically. This can go as far as two materials swapping or sharing electrons (i.e. ionic bonding or covalent bonding).
- *Dispersive adhesion*: In dispersive adhesion the interaction between the two materials is defined by the van der Waals forces.
- *Electrostatic adhesion*: For conducting materials a difference in electrical charge can act similarly to a capacitor and create an attractive electrostatic force between the materials.
- *Diffusive adhesion*: For materials where the molecules are mobile and soluble in each other a bond initiated by diffusion can be established.

For all the relevant interaction in this work (polymer - mold) the adhesion is caused by dispersive interactions. The dispersive adhesion mechanism is a weak interaction that occurs between molecules at close range. These interactions are again split up into different acting disperse interaction which includes the London dispersion forces, Keesom forces, Debye forces and hydrogen bonds. While these attractions are not very strong on an individual basis, they become significant when summed over larger surfaces. [50] To sum up all these dispersive mechanisms and describe a surface the surface energy is used. The surface energy is conventionally defined as the work that is required to create a unit area of a particular surface. The key parameters that are measured are the wettability and the surface roughness.

A good indicator for wettability is the contact angle which is also used as a representation for the surface energy. A higher contact angle means a lower surface energy. This in turn describes a surface that interacts less with others. Figure 2.8 a) shows a schematic contact angle on a flat surface. As the surface energy gets lower the contact angle increases, and the wetted surface decreases. Bormashenko [9] shows that there is an interrelation between the surface energy and the contact angle for different materials. This was first described by Baxter and later refined by Cassie and is now used as the Baxter-Cassie Equation [45]. This equation is derived from the variation of the free energy per surface. For simple calculations a simplified model of the thermodynamic equilibrium leads to the Young relation (see Equation 2.3). Due to the fast and easy measurement of the contact angle as well as easy

evaluation and high availability this measurement method is well suited as practical characterization method.

$$\gamma_{lv} \cdot \cos \Theta_Y = \gamma_{sv} - \gamma_{sl}, \quad (2.3)$$

Where:

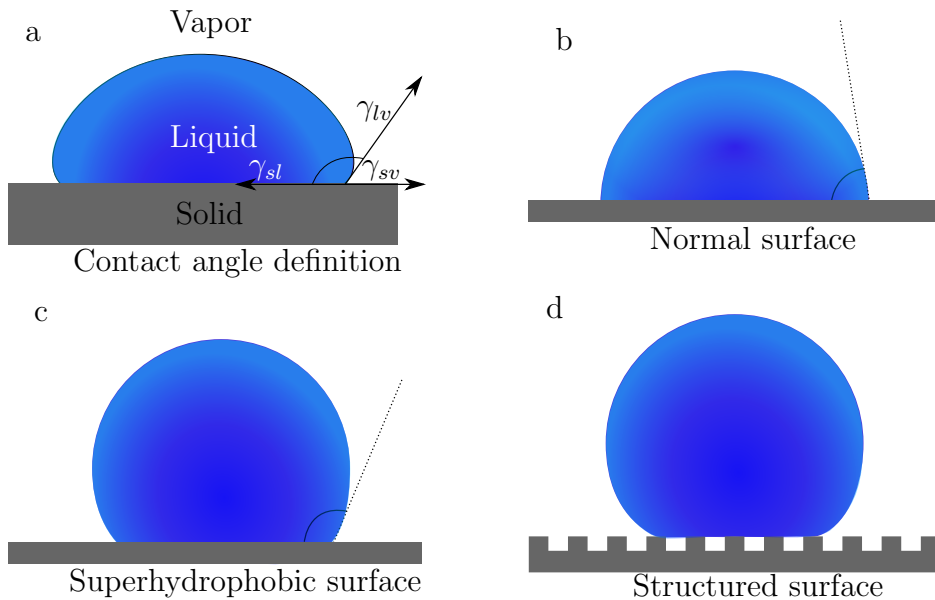|	
Θ_Y:	Contact angle
γ_{lv}:	Surface tension between liquid and vapor
γ_{sv}:	Surface tension between solid and vapor
γ_{sl}:	Surface tension between solid and liquid

Figure 2.8. Different contact angles for different surfaces [53].

The contact angle (surface energy) varies with different surface properties [59]. While a normal, untreated surface exhibits a low contact angle, super hydrophobic surfaces that do not interact with polar water will exhibit high contact angles (see Figure 2.8 b,c and d).

Wolansky shows that for a homogeneous surface higher roughness leads to a larger contact angle [93]. This effect is similar to the lotus effect, the 'self-cleaning' effect of the leaf of the lotus flower. Relatively rough surfaces yield comparably low surface energies. This connection was first described by Wenzel. He proposed equation 2.4 to describe the apparent contact angle formed by a liquid wetting a rough surface for any given intrinsic contact

angle. The apparent contact angle Θ_W describes the measured surface angle that is representative for the given surface. Θ_Y describes the intrinsic surface angle as property of the material without roughness (contact angle on the perfectly plain and smooth surface).

$$\cos \Theta_W = r \cdot \Theta_Y, \tag{2.4}$$

Where:

Θ_Y: Intrinsic contact angle

Θ_W: Apparent contact angle

r: Average roughness ratio

The transition to manufacturing polymer part is similar to the one for friction. Although this parameter does not describe the reality perfectly it is suitable for initial predictions for the experiments. The validity has also been shown in demolding tests done by Kawata [48]. These show that there is indeed a great impact of the surface roughness on the demoldability of polymer parts. Figure 2.9 shows that different processing conditions (in this case inductively coupled plasma etching) led to different surface roughness (top row roughness: a > b > c). The different properties caused by the surfaces can lead to the deterioration of the demolded polymer part. The bottom row of Figure 2.9 shows that the polymer part can be totally defective after demolding if the surface parameters are unfavorable. The upper row shows that roughness that is a critical parameter for the demolding step. This is evident because the roughest surface (a) has the worst demolding properties. Additionally, the demolding force drops from 71 N for (a) to 16 N for case (c). Unfortunately these tests, lack some additional information about the results. It is not evident if the destruction of the demolded polymer in case (a) is only locally or all over the polymer part. An estimated percentage or statistical evaluation would be helpful, as one expects even in case (c) minor defects of the demolded polymer. It is also misleading that case (a) and (b) are undercut which would be an explanation for the significantly worse demolding behavior. But a follow up study done by Kawata strengthens the assumption of the surface roughness influence. Further investigation on the mold influence will be discussed in Chapter 3 'demolding of micro-structures'.
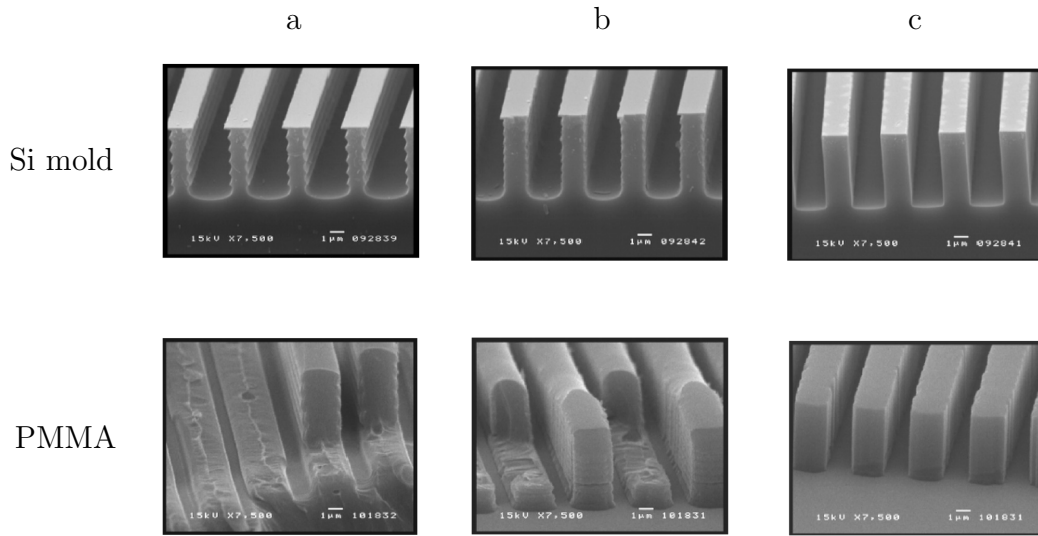
Figure 2.9. Different surface treatements of the Si mold leading to different demolding results [48].

2.4.3 Friction and adhesion in injection molding

The following enumeration provides an overview of the research done in the area of friction and adhesion in injection molding. The goals of these puplications vary greatly they are necessary to show the importance of surface properties in polymer processing:

- *Bruzzone et al.* show that surface phenomena play a decisive role in the behavior of engineering parts; Engineered surfaces rely on the control of surface characteristics to obtain a desired functional performance. Their work shows the importance of surface energy measurements for the advances in polymer applications and the technologies to engineer surfaces with specific properties [11].

- *Critchlow et al.* investigated a number of abhesion-promoting coatings that were selected in terms of their physicochemical and release properties. They performed several tests like adhesion and mechanical tests to determine surface release properties. They found that many of the selected flour based coatings (different PTFE types) proved extremely effective in terms of release against a cured epoxide applied under pressure [19].

- *Dearnley* investigated the ejection stage of polymer injection molding for macroscopic polymer parts (a 40 mm ring). He showed that CrN

23

coatings cause a significant reduction in the frictional forces that act during the ejection of an acetal polymer test ring. He also investigated the wetting behavior of the CrN coating and showed that lower chemical wetting of the CrN surface while in contact with acetal is the reason for the lower frictional force despite having a slightly higher surface roughness. In contrast the TiN or MoS_2 coatings he tested showed higher friction forces [21].

- *Dearnley et al.* also emphasized the importance of interfacial characteristics between the polymer and the tool. They investigated the work of adhesion for several polymers and tried to predict the demolding behavior from these values [22].

- *Duan et al.* investigated the interaction between a resist and template with regard to the surface roughness of the template and the application of a fluorinated release coating. The surface free energy of the template was 16.6 mN/m, and less than that of PTFE (18 mN/m). The imprint experiment results also showed that the anti-adhesion performance of treated template was improved greatly during detaching procedure and the demolding force, measured in the imprinting setup, decreased by 56.64% for the coated template [24].

- *Hall et al.* investigated LIGA fabricated parts for micro-mechanical systems. For the system reliability the friction between contacting sidewall surfaces was studied. This knowledge was used to discuss potential friction, adhesion, and wear management strategies [39].

- *Pouzada et al.* investigated the demolding step for deep core molding and for different polymers. Their work reviews research on the static coefficient of friction in molding conditions and the results obtained with a prototype apparatus that reproduces the conditions occurring during the ejection phase [73].

- *Amirsadeghi et al.* investigated the demolding for molded resists in ultraviolet nanoimprint lithography (UV-NIL). The demolding force was measured using a tensile test machine with homemade fixtures after imprinting the UV resist on a silicone stamp. They measured compositions with different amounts of cross-linking agent content and found that it has little effect on the resist surface energy but reduces the resist's elastic modulus drastically. The decrease in elastic modulus results in a decreased adhesion force at the resist/stamp interface thereby facilitating the demolding [2].

- *Peng et al.* investigated the micro-moulding and demolding of high aspect ratio micro structures. Their main regard was the friction between the molding insert and the thermoplastic material (PMMA). The experiments showed that the PTFE coated nickel insert performed better than the uncoated Ni inserts and thus increases the possibility of successful demolding [71].

- *Yoo et al.* investigated the manufacturing of nano-scale structures in the injection molding process. They used a high temperature ($\geq$ Tg of the molding material) mold or a rapid heating (up to 200 °C) and cooling ($\leq$ 70 °C) mold was used to fill the high aspect ratio nano-holes with thermoplastic melt for the injection molding. They proposed a new simple and efficient rapid heating and cooling that heats the stamper by means of the electrical resistance of the stamper itself. In addition, the contact angle of the water and the adhesion force on the molded surfaces was measured to investigate the effect of the surface nano-structures on the hydrophobicity or dry adhesiveness [98].

- *Yoon et al.* investigated the use of thermoplastic polyurethane (TPU) for the replication of micro-scale features and the impact of three factors on the quality of injection molded microscale features: the optimized process parameters, the use of a more flexible thermoplastic material, and the used as an antistiction coating. With medium aspect ratio (2.3:1) trenches, the antistiction coating doubled depth ratios, enhanced the edge definition and flatness of the features, and significantly reduced tearing of the features during ejection. The flexibility of the TPU permitted easier part ejection and left less polymer residue on the tooling surface in comparison to polycarbonate and other thermoplastic polymers [99].

All these investigations utilized friction measurement or contact angle measurement to show influences on the injection molding process. The research confirms that the demolding can be enhanced with the lowering of the friction between the polymer and the contact surface. What is missing is relevant research that links these well known surface parameters and micro-structured surfaces to the demolding step. This means that the influence of the micro-structure cannot be deduced from these findings.

Chapter 3

Demolding of micro-structures

3.1 Demolding mechanisms

Many different process steps need to be controlled properly to ensure the desired quality of the final product. One major bottle-neck for micro-structured applications, due to a lack of understanding, are often the final steps in the injection molding process, i.e. the molding and the demolding of the polymer part [3]. Most difficulties in polymer micro molding are not caused by the filling of the mold, but by demolding. While molding defines the accuracy in which the polymer can reproduce a given structure, demolding defines the separation process of the polymer and the mold. If either one of these two steps is poorly executed the desired quality can not be achieved. The worst case is that during the demolding process micro-structures are plastically deformed or torn apart [38].

Furthermore, a better molding of the micro-structure induces worse demoldability. This can be explained by the different friction forces that occur in the micro-structure, a perfect molding will fill out the micro-structure and therefore increase the exerted pressure on the contact surface and subsequently the friction force. The molding can be managed by adjusting process parameters; e.g. high injection speed and high melt or mold temperature lead to better molding. No simple relations are known for demolding and at some point demolding becomes impossible without major damage to the structured part. The molding of a micro-structure as well as the demolding of a micro-structured polymer part has been discussed in different scientific articles. The exerted influence of the demolding on the quality of the final product is described. Figure 3.1 shows the different mechanisms that occur while demolding the micro-structure in the hot embossing process. The mechanisms that define the demolding are [78]:

a) A completely sealed channel structure will be air tight. The impossibility for air to get into the micro-structure inhibits the demolding due to the vacuum voids generated (shown as (v)) inside the closed off structure. This can lead to structural defects like ripping at the micro structure ground or partial ripping. It can also lead to the deformation of the micro-structure, e.g. the elongation of an element until the internal stress and vacuum are released.

b) A single structure is ripped apart or elongated due to the high stress level that occurs at the bottom of the micro structure. In addition to the stress induced by the vacuum, the local adhesion and friction exert a strain on the micro-structure. This can lead to ripping or narrowing at the bottom of the micro-structures where the strain is usually the highest.

c) Polymers with higher stiffness will show different mechanisms. Due to the effects from a) or b) the micro structure is under a certain level of stress but in this case the micro-structure can withstand the occurring stress level. Instead of deforming or ripping the micro-structure, the holding forces between the polymer and the tool is overcome. In this event the polymer is ripped off the tool surface. For injection molding this could mean that the polymer part sticks to the nozzle side of the mold preventing the indented release using the ejector pins.

d) The draft angles that are often inherent to the manufacturing process of the mold can alter the main mechanisms for the demolding step. The draft angle will allow air to get into the voids easily. This will reduce the initial force needed for demolding. Furthermore, the detaching of polymer and tool will happen almost immediately leading to reduced dynamic friction as well.

e) Despite the stress reduction due to the draft angle stresses on the micro-structure will occur. The directional shrinking, which cannot be prevented in the injection molding process, will induce stresses on the interacting surface between polymer and tool. In this case the stresses at the base of the polymer are also lower due to the geometry. In this case plastic deformation will occur less likely compared to b). When it does, the draft angle can generate rims in the process of demolding. This can lead to an inhomogeneous deformation of the micro-structure.

f) Similar to e) a stress reduction due to the draft angle stresses on the micro-structure will occur. The symmetrical shrinking, which will occur in the hot embossing process, will induce stresses on the interacting surface between polymer and tool. In this case the stresses at the base of the polymer are also lower due to the geometry. In this case deformation

will occur less likely compared to b). The same deformations as in e) will occur, but unlike e) the effects will diminish towards the shrinkage center, which is therefore best placed in the middle of the polymer part.
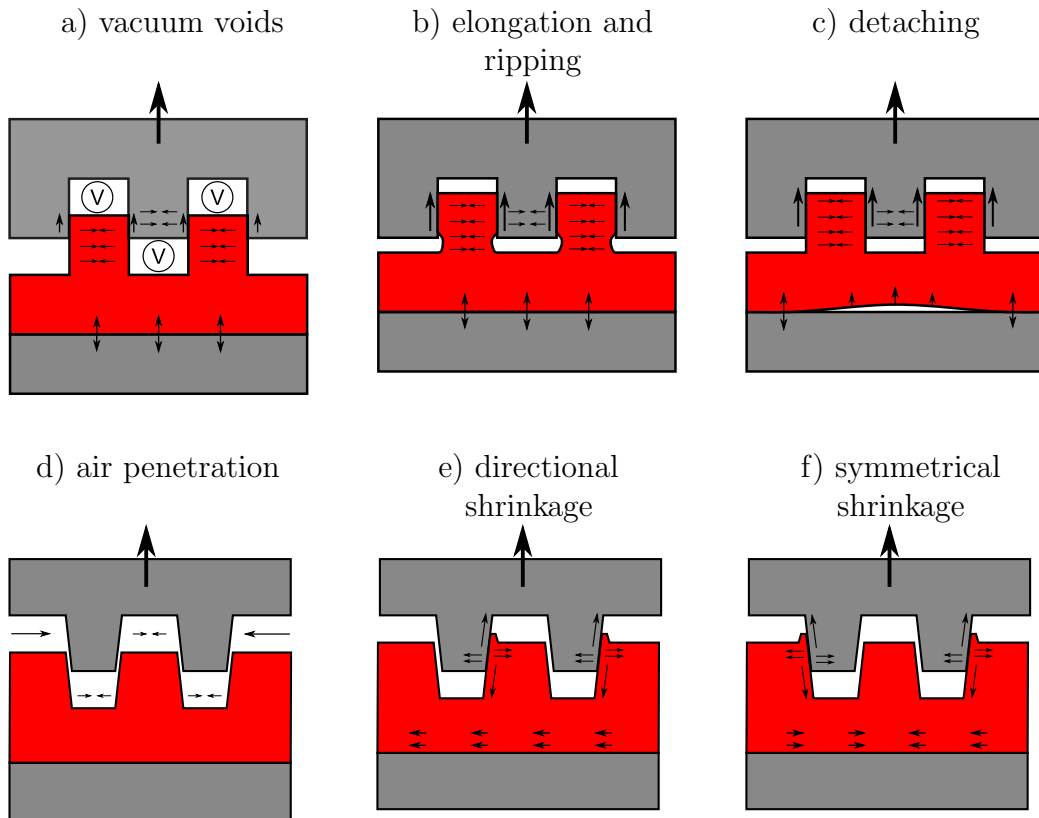

Figure 3.1. Demolding mechanisms for micro-structured polymer parts in injection molding based on Schift [78].

Figure 3.1 shows the previously described mechanisms that are responsible for hindered release, inhibited release or damaging of the micro-structure during the demolding process. These effects are best described for the hot embossing process but in injection molding these effects are similar. The main difference due to the unique filling of the polymer and the shorter cycle times are polymer orientations and increased directional shrinking in the injection molding process. This can lead to higher strain on the polymer and an additional mechanism that is based on the effect of Figure 3.1 c) where the polymer detaches from the mold, as described in the previous section. Figure 3.2 is a good example for a possible improvement if one considers the effects previously shown. In this case Merino suggests an implementation of

a pneumatic system assisting the demolding [61]. It illustrates an extensive improvement of the micro-structure (a, b) demolded with the pneumatic adaptation compared to the regular process without additional aid (c, d).
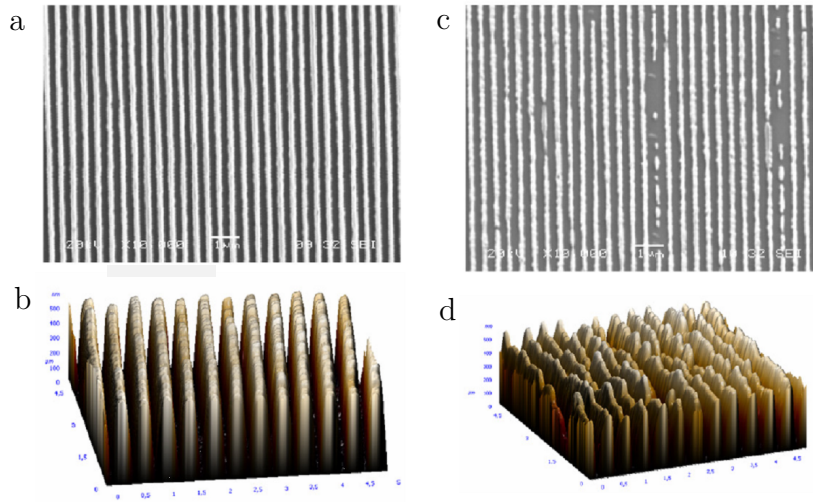

Figure 3.2. SEM picture of the demolded structure with a pneumatic demolding aid (a, b) and without an additional demolding aid (c, d) [61].

The pneumatic system injects air starting right before the polymer part is demolded. The air is injected from the side and will travel into the parting plane of the polymer and the mold. This aid reduces the generation of vacuum voids and lowers the stress exerted on the micro-structure. Additionally, the demolding force is not solely distributed among the few ejection pins. This reduces local stress and deformation of the whole stamper and produces a uniform, almost non-deformed micro-structure. For the unaided ejection process (c, d) a combination of effect a) and b) of Figure 3.1 leads to an inhomogeneously deformed and elongated micro-structure. These tests by Merino have been done for three different PMMA grades and a variation of different structures. The structures are line elements of six different widths ranging from 125 nm to 800 nm with constant depth of 500 nm. All of them are placed on one silicon wafer and replicated in one step in a hot embossing process. This allows studying the effect of the pneumatic demolding aid for different polymers and aspect ratios. While aspect ratios up to 2.5 are demolded perfectly using the pneumatic system, greater aspect ratios will still be damaged. This corresponds to the general assumption that the aspect ratio is a critical parameter for demoldability [3]. Still aspect ratio alone

is not enough to predict demoldability as aspect ratios up to 20 have been reportedly demolded [3, 56]. The pneumatic system may even have more impact when the structural size is getting bigger, e.g. 100 µm. The airflow can more easily enter the micro-structures even at higher aspect ratios. Merino disregards the effects among micro-structures since all of them are placed adjacent to each other. This is especially true for micro-structures in the injection molding process as the shrinking becomes a bigger issue. This understanding of the occurring mechanisms can help to design appropriate demolding-aids for certain applications to increase the production yield and reduce the number of defective parts.

3.2 Terminology for micro-structures

Before further discussing more detailed aspects of micro-structure demolding the commonly used terminology has to be introduced. This ensures that there are no misunderstandings when micro-structures are described. Figure 3.3 shows the geometric key parameters to describe micro-structures. This includes:

- The *pitch* (Figure 3.3 a) is a way to describe the pattern of the micro-structure, it describes the repeating interval of a *complete* unit. This includes the micro-structure and the gap to the next one. Similar used terms are interspacing or distance.
- The *width* (Figure 3.3 b) describes the size (projected on a flat surface) of a micro-structure on the polymer chip.
- The *height* (Figure 3.3 c) describes the feature size normal to the chip's dimensions. Depending on the application the features can protrude out of (height) or into (depth) the surface.
- The *aspect ratio* of micro-structures is defined as the ratio of height to width.
- The *draft angle* (Figure 3.3 d) describes the inclination of the micro-structure.
- The term *structure density* or *complexity* of a structured polymer part is used to describe the ratio of the structured area to the unstructured area. The terminology is often used casually to distinguish between heavily structured areas and and sparsely structured areas, as exact numbers often cannot be calculated.

The pitch correlates to the structural density which means that a lower pitch leads to a higher structural density on the same chip. In comparison a higher width will decrease the number of micro-structures that can be placed

on the same area, with the structured area remaining the same. The height and ultimately a high aspect ratio means, that the same structural density on a surface area has a higher cross sectional area. This property is often used for miniaturization of medical devices (compare Chapter 2.2 Medical applications).

a
pitch
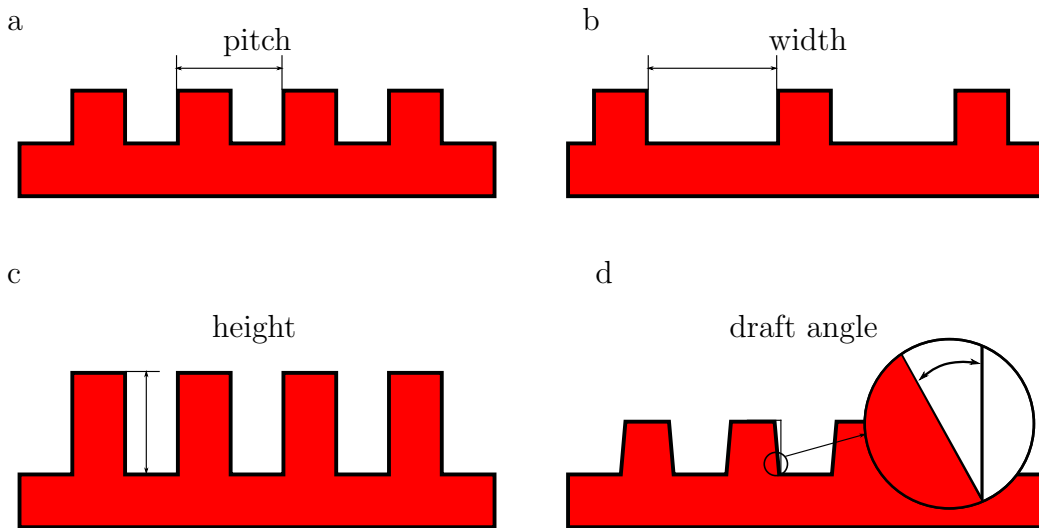
b
width

c
height

d
draft angle

Figure 3.3. Key parameters describing a micro-structure.

The magnitude of these key parameters greatly depends on the used micro-structures. There are two major categories, the patterns and micro-channels. Patterns are generally a lot smaller and aim at surface property manipulation while micro-channels are used for micro-fluidic application and are therefore a lot larger. Table 3.1 shows an overview of common structure sizes for patterns or channel structures. While patterns are generally made up from a small repeating unit, the pitch is generally low. Micro-channels are often placed on the polymer chip however best possible to connect all the working units, a pitch cannot be used to describe the channel placement in most cases. While the range of widths and heights is practically a magnitude apart, the aspect ratio is in exactly the same range, because higher aspect rations are very complicated to manufacture for all structure sizes (and low aspect ratios are undesirable). The draft angle as last parameter can vary greatly. Micro-channels use a draft angle only for demolding purposes as draft angles can influence the functionality of a micro-fluidic device. Therefore values around 4 ° are quite common. For patterned structures the draft angle becomes a tool to modify the surface properties even further. This means that pillars become cones for higher draft angles, while rectangular shaped structures become pyramids. The property of these shapes can be

altered even further with positive or negative orientation of the structure.

Table 3.1. Common structure sizes for different structure types [87].

Property	pattern	micro-channel
Pitch	<10 µm	-
Width	0.5-10 µm	20-500 µm
Height	0.5-10 µm	20-500 µm
Aspect ratio	0.5-5	0.5-5
Draft angle	0-45	0-10

3.3   Common demolding problems

The previous section shows that in the replication process different effects can occur. These may lead to different problems in the demolding step. The most critical outcome is the destruction of the structured area. This makes the polymer chip unusable and leaves the structured substrate (stamper) contaminated from the ripped off polymer structure. Figure 3.4 [84] shows that not only the polymer can rip (a), but that the demolding may also destroy the (silicon) stamp (b). In this particular case (a) shows a PMMA micro-structure that ripped after a thermal imprint process. But compared to defective polymer parts the damaging of the silicone stamper (b) is far worse. In this case not only one chip is defective but the negative cannot be used for further replications. These effects can occur to various extents leaving the product or even the stamper completely unusable. Especially dense and fragile structures like pillars with high aspect ratio tend to bad demoldability. This is why Song [84] emphasizes the necessity of research on demolding. He argues that this research is still lacking despite the fact that the demolding step, as the last processing step, determines the success of imprinting. This is often neglected as many research topics center around the moldability of micro-structures even when most structural damages occurs in the demolding step which can ruin any successfully molded structure.

Figure 3.5 shows a similar example of demolding defects. On the left is an overview of the molded part with the 5 mm x 5 mm structured zone in the middle. This study, performed by Fu et al. [29], was done with metal feedstock as molding material. This also explains the large ejection marks in
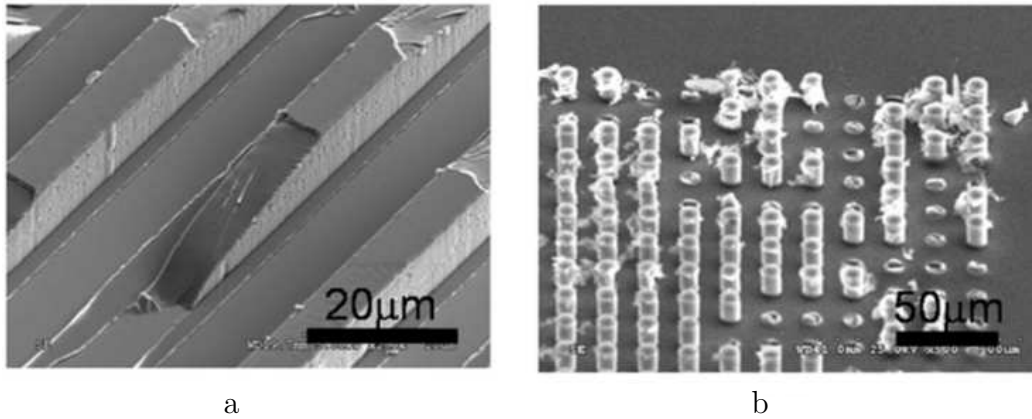
Figure 3.4. Scanning electron micrographs of damaged structures in (a) imprinted PMMA and (b) silicon stamp [84].

the left picture. The important information is that the whole area of pillars could only be partially demolded.

Solving, or at least understanding these problems is crucial for the improvement of future applications since the miniaturization and production of complex patterns (to achieve surface effects) are the main goals. These improvements are necessary especially to increase the density of small structures on a very small area. This combination is especially problematic because it is even more likely to exhibit these destructive effects. To do that and classify the problems different measurement concepts have been suggested and implemented with various drawbacks (see chapter 3.5).
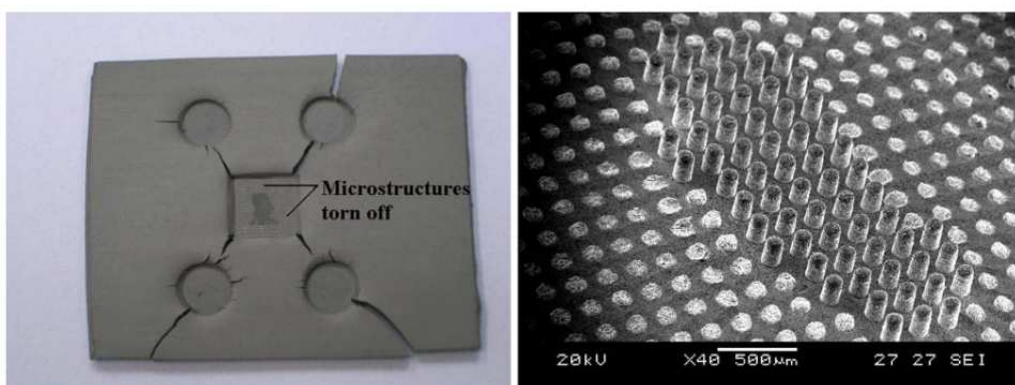

Figure 3.5. Demolding failure of a PIM hot embossed micro-structure [29].

3.4 Main Influencing Factors

The demolding of micro-structures depends on different influencing factors. They can be divided into the sections: *polymer material*, *design*, *mold* and *process* as shown in Figure 3.6. These factors will be discussed in detail and are also the main focus of this study.
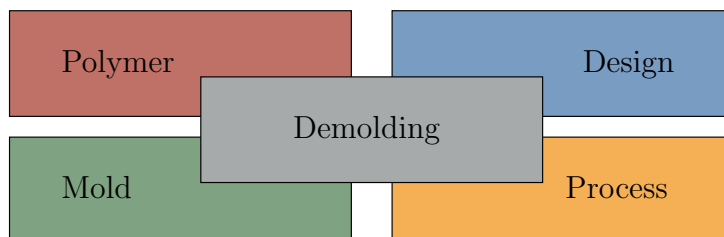

Figure 3.6. The four influencing factors for the demolding of micro-structures.

The determining effect that defines the actual demolding is the interaction of the interlocking surfaces. This interaction is comprised by all of the main influencing factors. The acting friction is the main result of these four influencing factors playing together.

The *polymer material* including any used additives is the first influencing factor. In most cases the polymer is defined by the application and the other parameters will be determined later. The polymer itself and all used additives will greatly influence the demolding-behavior. The effects can vary but many parameters like the flow ability, shrinkage potential, the friction coefficient between the polymer and the mold will have an effect on demoldability.

This leads to the *geometry* which defines the interacting surface of the mold and the polymer. The force necessary for demolding depends on the interlocking force and area. Therefore, the force will increases with higher structure density or structures which expose increased mutual surface (e.g. higher aspect ratio). Additionally, the placement of the structure and the type of structure, e.g. channels or pillars, will influence the friction due to different shrinking properties.

Choosing an appropriate coating material for the *mold* changes the friction between the mold and the polymer accordingly. In the mold, the friction can therefore be manipulated with the help of different coatings. These are applied to the mold (mostly just the structured insert) and can reduce the friction and therefore directly act on the demolding force. Any physical or chemical coatings change (ideally decreases) the static and dynamic friction, depending on its morphology roughness and material properties. The contact angle can be used to give a simple description of the coating properties.

The last parameter to act as a main influence is the replication *process* itself through the chosen process parameters. Mostly the acting temperatures (i.e. melt temperature and mold temperature) will play a tremendous role for the replication as well as the demolding of the manufactured part.

3.4.1 Polymer

The choice of the polymeric material is crucial. While some materials may induce sticking, others show almost no demolding problems. This means the material choice is important as it defines the core properties for further processing. Many additives can enhance the flow ability and therefore guarantee a better molding; lubricants can reduce friction and improve demolding. It is important to distinguish between properties that affect processing and properties that are relevant for the final application. The challenge is to find or create materials that combine all necessary properties for both. A polymer ideal for demolding would posses almost no shrinkage and thermal expansion/contraction at all, low surface energies and low friction with metal surfaces and low viscosity. Polymer properties that affect the manufacturing and demolding of micro-structures are (compare Figure 3.7):

Figure 3.7. A list of important parameters for the polymer that influence the demolding of micro-structures.

- *Thermal expansion/contraction*: Expansion or contraction is largely responsible for the stresses exerted on the structures that are replicated on the polymer surface. This expansion is described for each polymer by the thermal expansion coefficient.

- *Polymer shrinkage*: Shrinkage adds to the effect of thermal contraction, increasing the stresses even further especially for polymers with high shrinkage potential. The shrinkage unlike the thermal expansion is also influenced by the part geometry and the part orientation (prominent in the injection molding process):
- *Stiffness / Youngs modulus*: The mechanical properties of the polymer determine the forces that act at the contact surface of the polymer and the stamper. Higher stiffness leads to higher stresses for a similar strain (contraction or shrinkage) of the micro-structure.
- *Adhesion*: The type of polymer, amorphous or semi-crystalline, as well as the process temperatures define the surface adhesion. This means that variothermal temperatures as well as the general mold temperature will determine the acting adhesion and finally the demolding.
- Polymer melt *viscosity*: A lower viscosity not only reduces the necessary injection pressure, but also improves the filling of micro-structures.

These properties are important for any injection molding process. A good molding behavior is critical for micro-structured zones on the polymer part. Additionally, the particle size of fillers is important. Commonly used glass fibers enhancing mechanical properties can inhibit the molding of micro-structures. Especially particles that are larger than the micro features of the polymer part are problematic, e.g. a channel with a width of 50 µm is in the same size category as a glass fiber.

Material requirements for the application are completely different to the processing requirements. Depending on the field of application optical properties like transparency, transmittance or fluorescence are important. Even more, chemical stability or in life science bio compatibility are of great importance. Other applications like the one shown in figure 2.4 use electrical potential to enhance separation processes. This requires electrical insulation to suppress unwanted currents or electro-osmotic flow. The medical applications unfortunately restrict the choice even further, as the use of most additives is forbidden and only certain approved materials are allowed. Due to the above mentioned requirements the material property demands exceed that of regular injection molding applications. For that reason most micro injection molders have to use common injection molding grades. This happens only because of the lack of alternatives. The amount of polymer needed for medical applications is very low. That means that specific material design for medical applications is not feasible so far. Despite the improvements of the demoldability that are possible through the material choice, the current manufacturing approach has to be able to demold any material. This defines the approach for future polymer investigation. Standard materials have to

be screened, their demolding behavior analyzed and ideally custom tailored demolding improvements have to be investigated. Despite these restrictions the choice of material remains important and cannot be disregarded as main influence on the demolding.

Many designs for medical devices are based on present glass applications. The main goal is to supersede these glass applications by using better suited polymer materials. This is possible because depending on the application, polymers can provide properties specifically designed for the needed use. For many applications polymers additionally have to be medically approved (for example by the FDA) to ensure safe handling in the application field. Properties that make polymers unique for the field of medical applications include:

- Chemical stability: This is not only necessary as the final product might come in contact with different chemical substances, but also because many applications will utilize certain chemical substances to be able to operate according to the design specifications.
- Transparency: This is one of the key properties for most analytic chips (e.g. micro slide applications). Common analysis on polymer chips is done with optical means, using a broad area of the wavelengths. The polymer should ideally be transparent for the needed wavelengths and have no inherent luminescence or fluorescence that can effect the measurement.
- Electrical conductivity: Depending on the application no conductivity or only local conductivity is desired. In some special cases the whole polymer chip should conduct electricity. This property is for example used in electrophoresis applications.
- Heat conductivity: The heat conductivity is usually low for most polymers. In special cases, however, the conductivity should be increased for example to improve the efficiency of a PCR (polymerase chain reaction) device by improving the cooling rate when necessary.
- Sterilization: Medical components have to be sterilized in most cases before distribution. This is usually a property that polymers provide without further modification. Many different sterilization processes (e.g. radiation, ethylene oxide) can be used on polymers without affecting the final application.

This means that choosing a suitable polymer for an application consists of two parts. First all the necessary properties for the application have to be met, secondly the injection molding and demolding parameters should be regarded.

3.4.2 Design of the micro-structure

The design of the application, in this case the micro-structure, is the next one on the list of the four important influencing factors. Depending on the applications the structures may vary in size and shape. This is an overview over the main geometry parameters for a commonly used channel or pattern structure that influence the demoldability of the polymer part (compare Figure 3.8):

Figure 3.8. A list of important parameters for the geometry design that influence the demolding of micro-structures.

- The general *type of structure* will greatly define the surface interaction as pattern type structures will behave differently from structures based on a channel or pillar like shape.
- A high *aspect ratio* will almost always affect the demoldability in a negative way independent of the chosen structure.
- The introduction of a *draft angle* will help in the demolding process. Generally a higher draft angle is preferable for demoldability but often not for the application.
- The general structure *dimensions* (i.e. width or depth) will again determine the interacting surface area and therefore affect the demoldability.
- The structure *placement* interacts strongly with the shrinkage of the polymer, making placements in areas with little shrinkage preferable for the demolding step.
- A high *structural density* (often necessary for complex micro-fluidic applications) will again increase the contact surface for demolding.

While for some applications very small patterned structures play a huge role, most micro-fluidic applications utilize channel structures for their main functionality. While the patterned surfaces like a moth-eye structure (compare Figure 3.9 (a)) for optical applications the structure size often ranges in the area of a few nanometers, channel structures for lab-on-a-chip applications like figure 3.9 (b) are significantly larger. Channel sizes usually ranges from 50 µm to 500 µm. Furthermore, in most micro-fluidic applications there are only a few channels distributed on the whole chip, while a functional pattern covers large areas, sometimes even the entire surface. This means that micro-fluidic applications are often a lot less dense (structural density, high projected area). Figure 3.9 shows how different designs can define the overall surface properties.
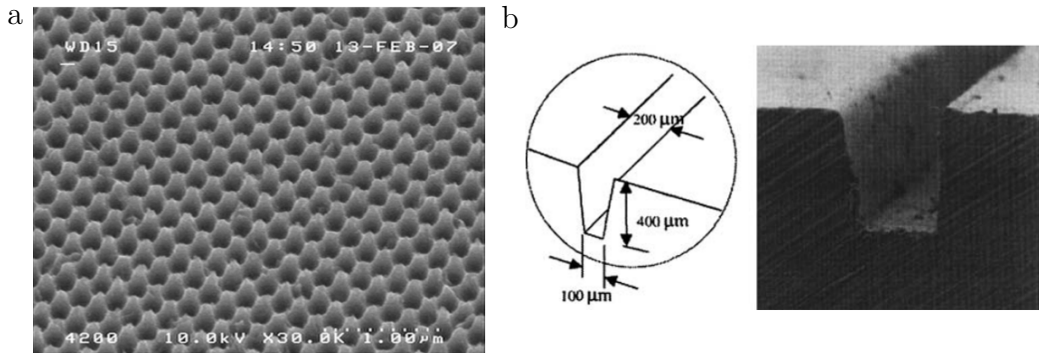
Figure 3.9. (a) SEM picture of a moth eye patterned structure [88]. (b) Micro channel with draft angle [98].

The overall micro-structure setup has a very large influences on the demoldability of the polymer part [3, 29]. Especially the draft angle of the micro-structure, especially for very low angles, can induce sticking of the polymer to the stamper (compare Figure 3.1). Furthermore, high aspect ratios (small channel widths compared to high channel depths) will likely induce strong deformation of the structure. These two effects can be easily understood and will play a large role especially for the channel structures for common applications. Still, the most complex interactions and demolding effects are determined by the chosen structure elements. Kawata et al. [48] have shown that it is reasonable to propose different channel geometries and vary several aspects. 3.10 shows the geometries they chose to test. To compare the geometries a demolding force measurement method based on the hot embossing process was used. The setup for this measurement and its implications are explained in Chapter 3.5.1 (page 55). With this structure choice Kawata [48] tried to compare orthogonal structures (a, c) and structures with

39

a draft angle (b, d). Additionally to the the difference in the draft angle, they tested the influence of a specific geometrical variation. In this case the choice was a leveled channel ground (c, d). The most important conclusion is that the measurements of this study confirm the obvious reduction of the demolding force when introducing a draft angle.
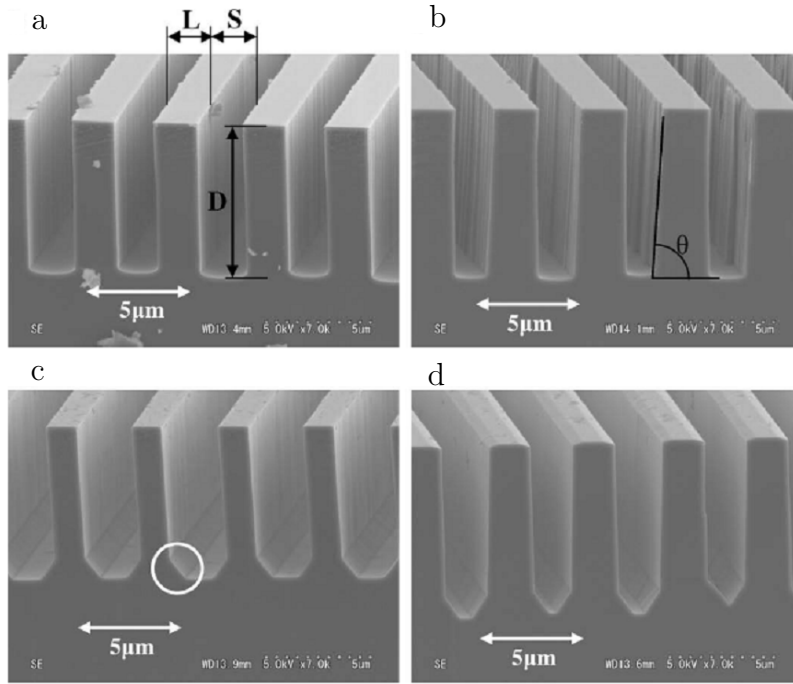

Figure 3.10. Different geometries to test the feature size and draft angle influence [48].

The draft angle has this positive impact due to several factors that vary with the introduction of the draft angle. The most influential and obvious ones as explained in 3.1 'Demolding mechanisms' are the venting of the vacuum voids, the reduced contact and shearing immediately after the initial detaching and the stress reduction in the micro-structure. Furthermore, since the draft angle reduces the stress level it is expected that other stress reducing optimizations will have a positive effect on the demoldability. The structures used in Kawatas tests prove this assumption, as the structure in (c) and (d) with an additional leveling induce even lower demolding forces than the structures in (a) and (b). Kawatas [48] experiments show that a reduction of over 50 % indeed is possible. The measurements show that with the introduction of a draft angle the force drops from approximately 0.7 MPa to 0.2 MPa. When introducing the leveled channel ground the force

40

drops from approximately 0.7 MPa to 0.4 MPa. The combination of both geometrical alterations yields a force close to 0 MPa.

Similar effects are shown by Song [83] for simulations of different geometries. He primarily focused on the influence of friction and stress as factors inducing the demolding force. His simulations show that the local shear stress can be up to 20 % lower for different friction coefficients (0 and 0.3) and the same polymer (PMMA) and geometry (micro channels). Changes in geometry, in particular the draft angle, can reduce the local shear stress by up to 25 %. Song suggests further that the influence of the micro geometry can most likely surpass the 25 % improvement measured for the local shear stress alone and is therefore of particular interest. All the forces for this comparison have been normalized with the total side wall area to ensure that influences from increased sidewall area are filtered out.

A similar study by Schmidt [81] shows the same results and makes additional effort to compare different geometry elements. Figure 3.11 shows the demolding force of concentric circles and square grids in comparison to a plain alignment structure. The draft angle is either 0° or 4° and the square grid is tested twice with a different aspect ratio. The lower aspect ratio grid is 400 µm deep while the other one has a depth of 800 µm. Additionally, the experiments with 400 µm depth and 0° draft angle have been done twice with another substrate to ensure reproducibility. The first and most important information the diagram shows, is that closed structures like concentric circles can produce an immense leap in the measured demolding force. This occurs due to the shrinking-offset of the structure. This means that a closed structure either shrinks symmetrically towards the shrinking center of the polymer part or asymmetrically due to an offset of the micro-structure. In both cases the micro-structure acts as a clamp and drastically increases the demolding force. Contrary to the common belief, higher aspect ratio structures will not have a larger clamping force. This is explained because the demolding force is defined as the 'peak' (maximum force) of the measured force over time. Higher aspect ratios need more energy - total amount of force over the entire demolding distance - to be demolded and are more likely to be deformed, but this in turn reduces the stress level at the bottom of the structure - due to relaxation - which leads to a lower maximal force.

The assumed theory that the clamping force induced upon shrinking of a micro-structure on the mold also explains why a structure in form of a ray was introduced by Michaeli in early stages of research on this topic [63]. Michaeli even claimed rays in direction of shrinkage as ideal structure for demolding [62]. To illustrate, Figure 3.12 shows the vector field of a simplified polymer plate shrinking towards its own center. The length of each arrow represents the displacement of the particular point. Concentric circles as
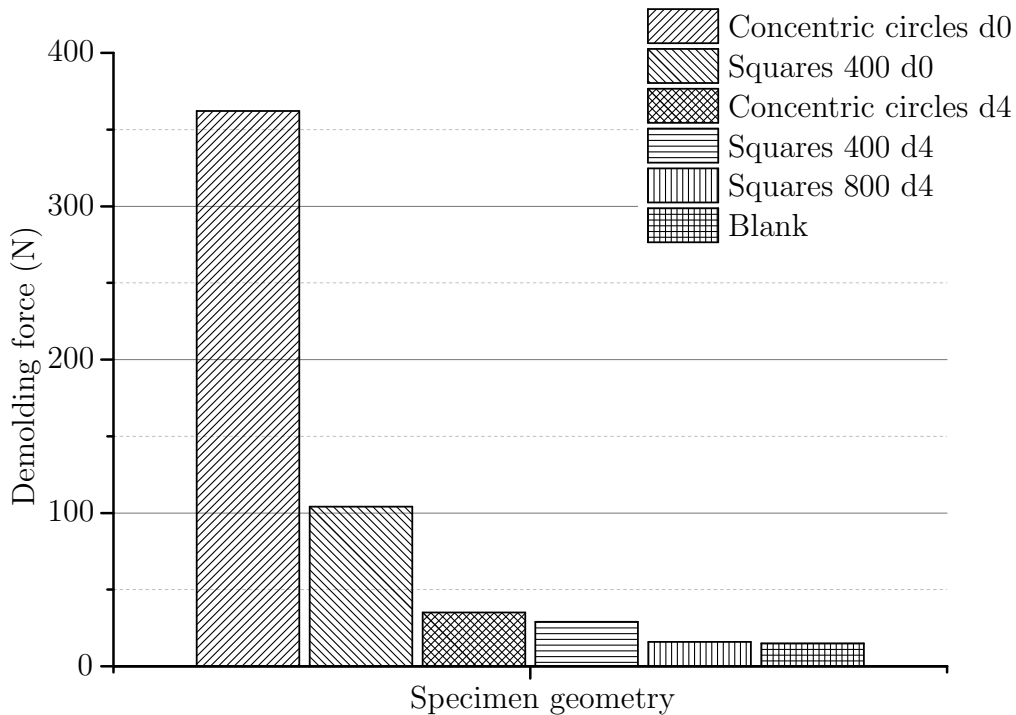
Figure 3.11. Demolding force of different structures [81]. d0, d4 = draft angle in degrees. 400, 800 = structure height in μm.

explained will shrink towards the center and exert a clamping force. Any structure that lies on a line intersecting the shrinkage center will produce the best demolding results, as the contact surface that is pressing against the mold is very small. An example would be the red structure with bound by the black outline. This structure is placed on the 'rays' of the vector field which would be ideally placed according to the shrinkage. The entire outline will remain inside the micro-structure after shrinking, unlike the placement of orthogonal channel structures, which is shown in figure 3.13.

This placement is particularly important for parts manufactured in injection molding. In the injection molding process the shrinking is not always homogeneous, especially not as symmetric as in the hot embossing process. This leads to an additional effect if the shrinking of the polymer part is anisotropic with the preferred shrinkage in flow direction. An example micro fluidic setup of orthogonal channels connecting the same two points can have a completely different demoldability. This happens for example if the setup is rotated by 180 degrees. Figure 3.13 shows these two setups (micro-structures), the shrinkage vector field, the red micro-structure in different placements and the shrinkage field that is acting as displacement
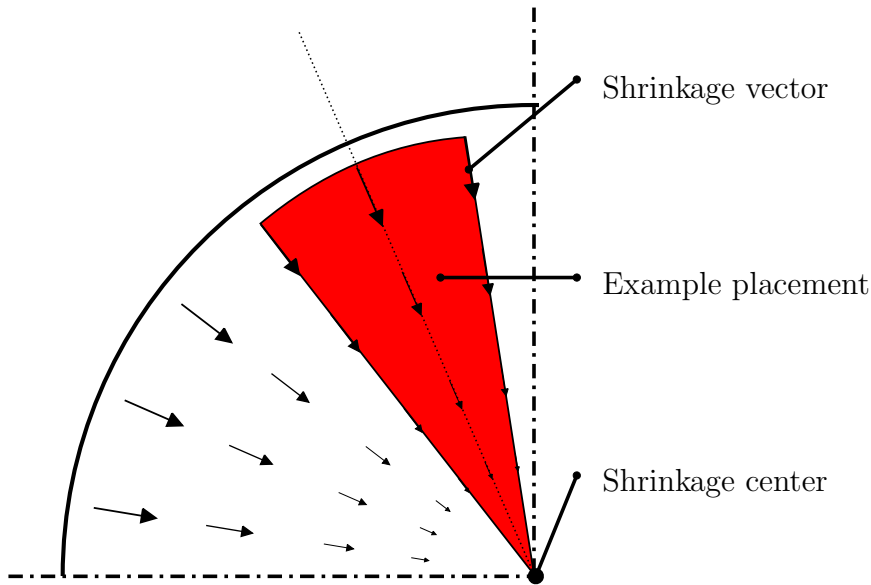
Figure 3.12. Exemplary shrinkage vector field of a symmetric concentric
polymer plate.

on the structure. The detailed view on the right side shows the stress area
in the channel as well as the area where the polymer might detach from the
substrate (stamper). The occurring stresses indicate that the setup (a) is
superior to setup (b). In case (a) the vertical channel is shrinking very little
towards the center and is therefore almost not affected by the resulting fric-
tion in the demolding step. The horizontal channel is shrinking towards the
middle line and has no contact area to shrink on. The friction critical for
the demolding therefore only acts on the width of the channel. In case (b)
the vertical channel is shrinking towards the shrinkage center in the middle
which results in a higher stress acting on the same area. Therefore, the nor-
mal force of the interacting surfaces resulting in the demolding friction is
significantly larger. The horizontal channel will shrink towards the middle
similar to the setup (a) with almost no interaction as well. This effect will
produce a far worse demolding result for structure (b) than for the setup of
structure (a).

The previous conclusion and assumptions led to further investigations
and to the simulation done by Guo et al. [37]. As previously mentioned,
closed structures will produce a unique state of stress. This seemingly dis-
advantageous property is not necessary always a disadvantage. In special
cases this effect can be put to good use. As shown in figure 3.14 the place-
ment of a so called stress barrier, i.e. essentially a large concentric circle, in
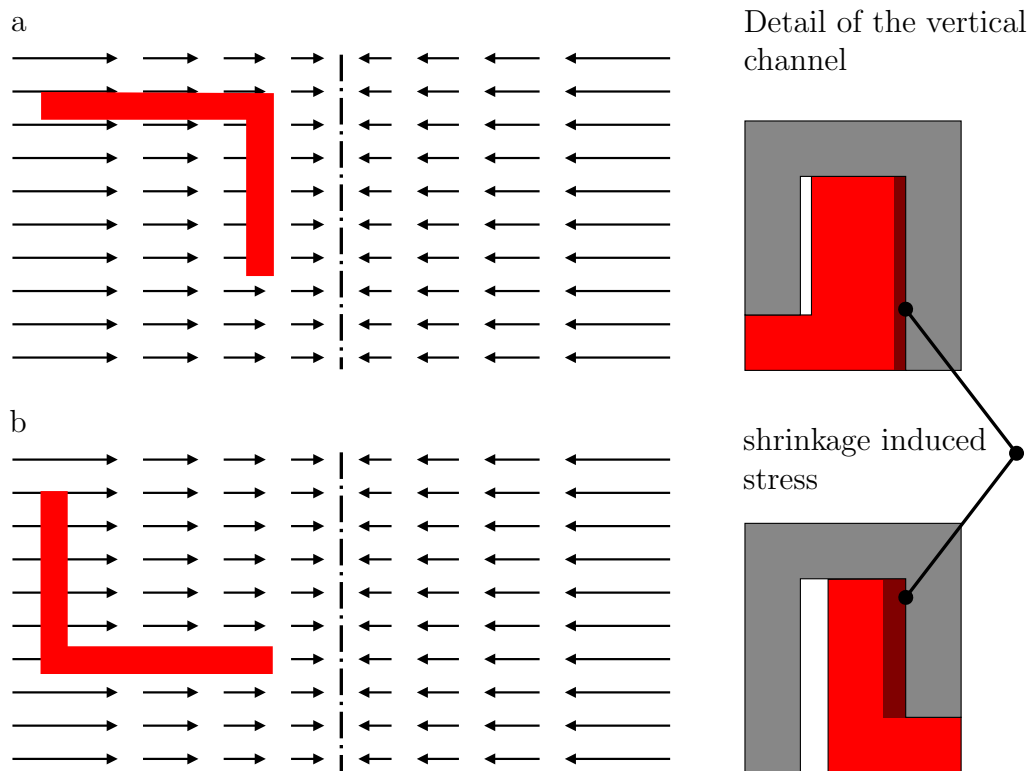
43

Figure 3.13. Micro fluidic channels with the same purpose but different placement (a, b) resulting in different shrinking and demoldability.

the hot embossing simulation will affect the local stress distribution. In this case it shifts the acting stresses in the PMMA polymer part from the microstructure to the stress barrier at the beginning of the demolding. Using the knowledge of the shrinkage vector field the occurrences can be visualized as follows. The stress barrier, which is placed on the outside of the required micro-structure is strongly exposed to the acting contraction (shrinkage). It shows that the clever placement of an, otherwise unneeded, stress barrier builds up high stresses and therefore figuratively 'absorbs' the stress that occurs due to shrinkage. This prevents a stress build up in the relevant micro-structure, which is placed inside the auxiliary structure. The maximum stress of the adjacent micro-structure could be reduced from 165.5 MPa to 67.4 MPa [37]. Thus, the stress barrier protects the micro-structure against high contact stress. The 'protected' micro-structure has therefore a reduced risk for damage due to the stress exposure. It also agrees with previous studies by Song [83] and Worgull [94] that suggests that the critical stress is at the bottom of the micro-structure acting at the beginning of the demolding process.
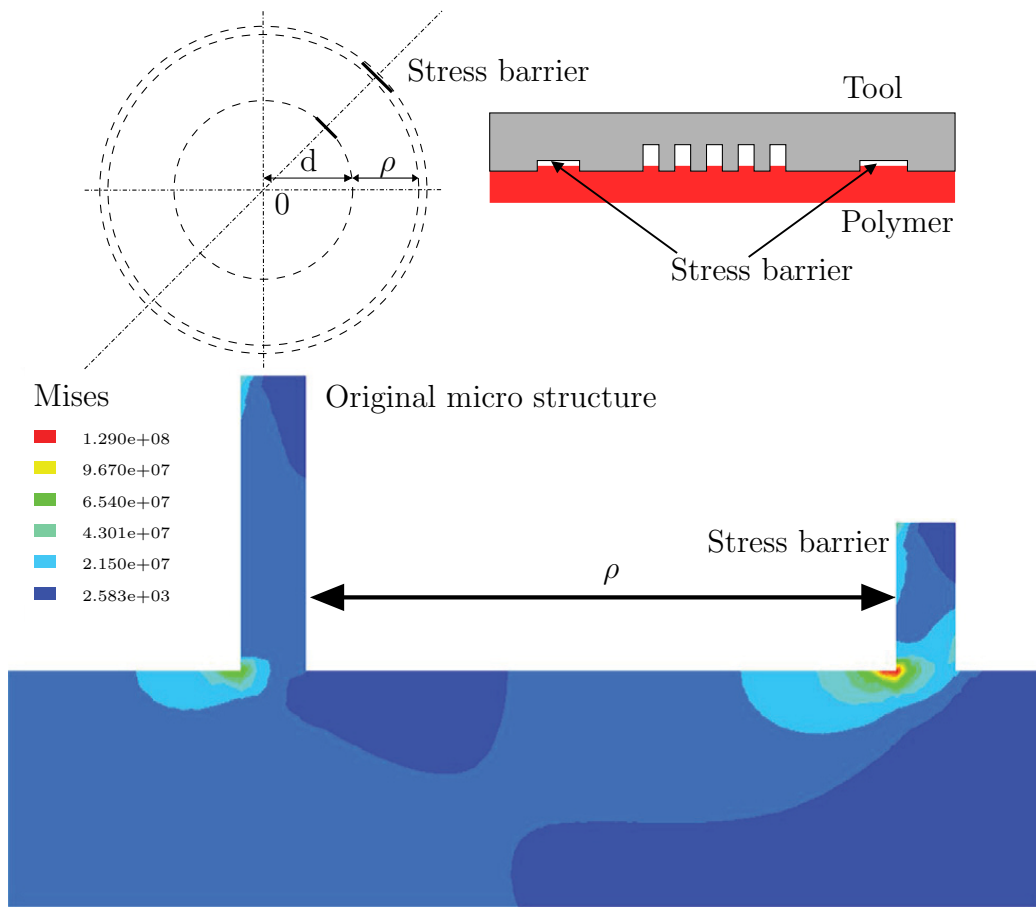
Figure 3.14. Stress distribution in a hot embossing simulation of a micro-structure with an auxiliary structure acting as stress barrier [37].

3.4.3 Mold

The mold or the stamper that is placed in the mold is the part that interacts with the polymer. The fact that the final polymer part can be manufactured with different setups leading to (almost) the same outcome allows many possibilities for different applications. Furthermore, unlike the restricted polymer choice these changes and possible improvements can be done with very little constraints. This makes it a good starting point to investigate the demolding behavior by altering the mold environment. This means particularly the mold material, especially the material of the mold or stamper carrying the micro-structure. In most cases the mold is steel and the stamper is either steel or nickel. First of all the stiffness of the chosen material will influence the part dimensions as steel will be more resistant against deformation in the injection process. On the other hand, surface properties will vary with

45

different morphologies due to the chosen material. This effect can be used by changing the morphology and surface properties by coating the stamper. Since it is known that the surface energy and therefore adhesion and friction can vary greatly among different (coating) materials, a great influence of coatings regarding the demoldability is expected. This is an overview of the main mold factors that influence the demoldability of the polymer part (compare Figure 3.15):
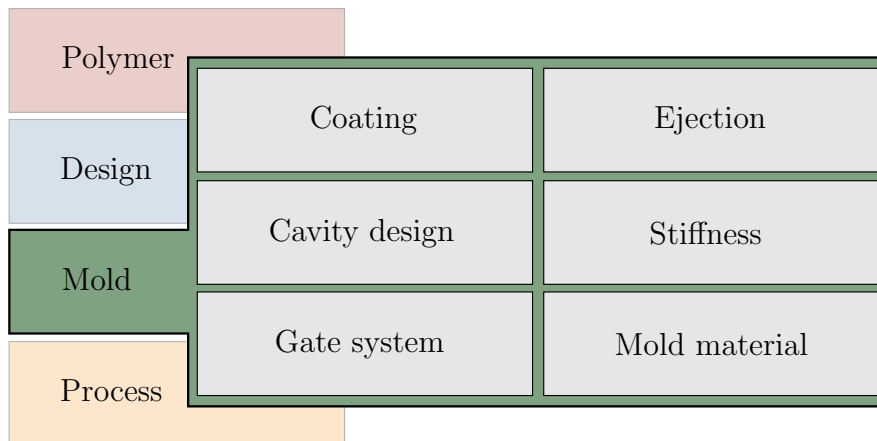
Figure 3.15. A list of important parameters for the injection mold that influence the demolding of micro-structures.

- The *coating* of the mold cavity or more specifically the structured insert directly influences the surface energy and the interaction properties to the respective polymers therefore directly influencing the demoldability of the part.
- The *cavity design* (i.e. the part macro geometry) influences the shrinkage behavior (due to orientations) and the demolding step depending on the part geometry (flat surfaces have a different demolding behavior than complex 3D free-form surfaces).
- The *gate system* (e.g. film gate or point gate) generates different orientations and influences packing pressure efficiency which in turn affects part shrinkage.
- The setup of the *ejection* system determines how the demolding is performed. Placement and number of ejector pins can thereby change the demolding behavior by introducing part bending for a poorly designed ejection system.
- The *mold material* and *stiffness* are partly responsible for the developing stresses right before the demolding which is a key factor in the demolding step.

Coating in this case is defined as the layer deposition of a material on the stamper. Table 3.2 shows how the demolding force varies with coatings of the interacting area in the mold [96]. In this example the demolding force was 340 N for an uncoated pin with PMMA. The mold was then coated with a fluorine carbon based coating. The coating was checked if it had properly formed, was then washed and prepared for the injection process. After an unstable starting phase - approximately 10 injection shots - the coated mold yielded a force of only 140 - 170 N. However, there was a loss of effectiveness after a certain number of molding cycles. This can be seen in the rise of the demolding force after 13,000 shots to 280 N. After rewashing the force dropped again to the initial 140 - 170 N. Finally after 20,000 shots the demolding resistance went back to the starting value of 340 N. This leads to three conclusions:

- The demolding force is a result of the interacting surfaces and therefore depends on the coating of the mold. This simple finding means that the interaction and subsequently the demoldability can be improved by using coatings in the mold (on the structured area).
- The coating may not be stable in the chosen process. This will lead to a diminishing effect or in some cases even the destruction of the coating. Either way the demoldability enhancement can lose effectiveness.
- The destruction of the coating or simply the interaction will cause a certain mixing of the final polymer part with debris of the disintegrating coating, causing undesired contamination.

In the study performed by Yamamoto [96] no degradation of the coating was observed, since the washing of the die restored the positive coating effects almost to the initial level. The first 10 injection shots are necessary to form a stable process. In these steps the coating becomes contaminated until the coating / contamination becomes stable. The polymer contamination of the coating lasts throughout the several thousand performed shots which explains why a direct correlation of the contact angles is not possible. This can be seen as different contact angles yield different almost contradicting results for the measured demolding forces (80° at 340 N, 85° at 270 N, 90° at 340 N).

Although many coatings have already been tested for different applications which may allow conclusions for the use in micro-structured applications, most knowledge is in the area of friction and wear resistance. Heinze [43] shows the application of different coatings in injection units. Titanium and chrome based coatings are in these cases very promising regarding their wear resistance. Chuna [20] also suggests the use of chrome based coatings and points out that it can lower the friction coefficient as well. Miikku-

Table 3.2. The relationship between the demolding resistance and the contact angle of water on a core pin at crucial times during the molding run [96].

Experimental state	Demolding resistance	Contact angle
Ejector operation load	4-7 N	-
Untreated pin after initial washing	340 N	80°
After corona discharge treatment	-	15°
Chemically absorbed film treatment	-	115°
After final die washing	140-170 N	120°
After 13.000 shots	280 N	85°
After rewashing the die	140-170 N	105°
After 20.000 shots	340 N	90°

lainen [65] shows that nitride coatings, tungsten and molybdenum provide a good protection of the stamper against abrasion or destruction. Furthermore, the adhesion to a nickel stamper was strong enough to endure over 10,000 shots with PC (Poylcarbonate) and PMP (Poylmethylpentene). He also points out that in his case all coatings were monolayers with a thickness less than 20 nm. The same properties are true for perfluorinated silane. They also reveal good protective properties while maintaining an extremely small layer thickness. Unfortunately, tribological tests show that the silane based coating is less stable than metal based ones, which can be detrimental for a stable use in the injection molding process. Still, Miikkulainen's study shows that some chemical coatings are sufficiently stable for the injection molding process.

Griffiths [35] tested the influence of two coatings (amorphous diamond like carbon (DLC) and SiOC) with two polymers (PC and ABS) and concluded that a great improvement through coating is possible. His parameter study shows, that process parameters need to be optimized for each material combination. Furthermore, the effects of the coatings are not consistent among different polymers. This means that predictions regarding the effect of a coating on the demoldability is almost impossible, as coatings can produce different results for different polymers.
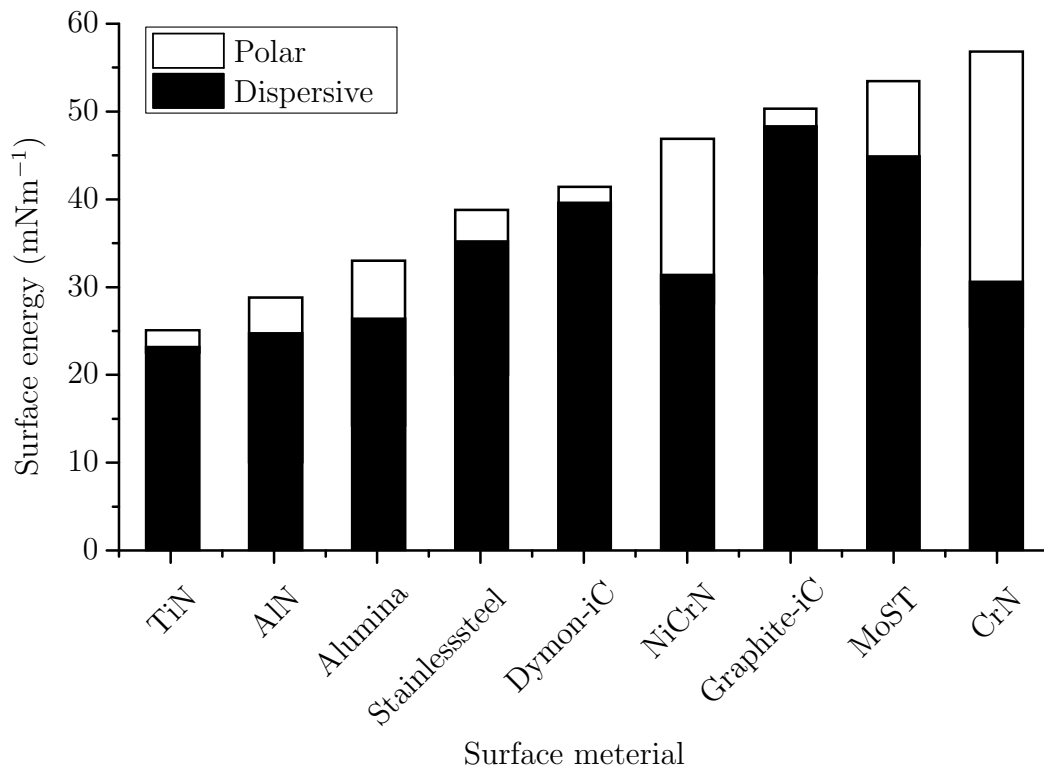
Figure 3.16. Surface energies of different materials calculated using the Owens and Wendt method [67].

Figure 3.16 shows the surface energy of different materials considering the polar and disperse component. The surface energy is measured via the contact angle (compare 2.4.2 'Adhesion and contact angle') using a polar and non-polar solvent. Using the Owens and Wendt method the contact angle values allow the calculation of the respective surface energy. Surface energy is a a very good indicator for the expected adhesion [8]. Adhesion plays a lead role for the demoldability of a micro-structured polymer part and can help to predict the influence of different coatings on the demolding force by considering their surface energy. This would suggest that titanium nitride, compared to a graphite based coating, will yield a lower demolding force. Further investigations should also consider the polar and dispersive part of the surface energy. This can lead to different view of this matter, as CrN will be ranged lower if only the polar or dispersive part is singled out. In fact the interaction will strongly depend on the polymer, polar versus non-polar, e.g. polypropylene has no polar parts. The applicability will therefore not only depend on the surface energy as a sole 'number' but on the resulting interaction (polar-polar, dispersive-dispersive). This again supports

the findings that polymers will interacts differently with the same surface coating.

3.4.4   Process

The last of the main influencing factors is the injection process itself. Several process parameters define the replication process. Suitable processing parameters are required to ensure the quality of the final part and desirable short cycle time. For economic efficiency the cooling time and therefore the cycle time is lowered to the least possible value with the help of complex and often expensive heating and cooling systems. This has to be done as temperatures are the most critical parameter for the manufacturing of micro-structures. Overall the most important parameters that can also be easily altered are temperatures and pressures. The melt and mold temperature profile will directly influence the filling behavior, the polymer shrinkage and the demolding. The pressure (injection and holding pressure) will counteract the shrinking and ensures the maintaining of the desired part dimensions. While the parameters like injection speed and vacuum are responsible for a good molding, demolding strongly depends on the demolding temperature and holding pressure (shrinking of the macroscopic part).

This is an overview of the main processing parameters that influence the demoldability of the polymer part (compare Figure 3.17):

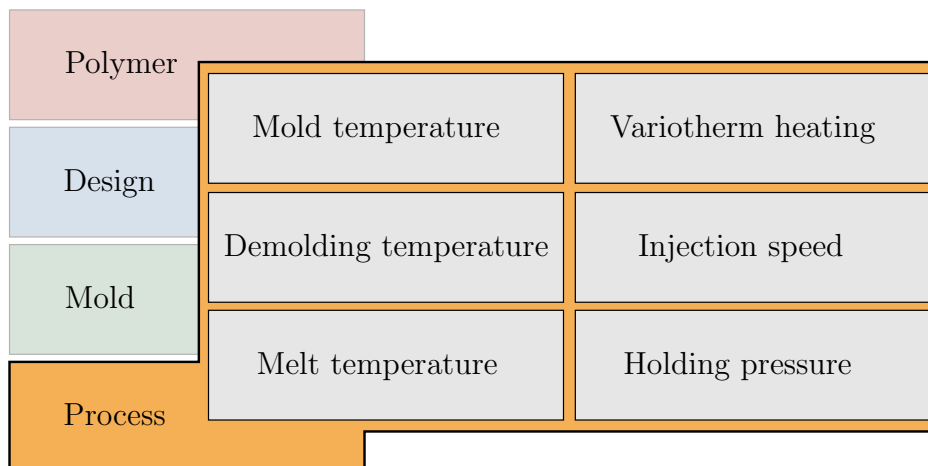| Polymer		
Design	Mold temperature	Variotherm heating
Mold	Demolding temperature	Injection speed
Process	Melt temperature	Holding pressure

Figure 3.17. A list of important parameters for the injection molding process that influence the demolding of micro-structures.

- The most important processing settings are *mold temperature*, which is the desired set temperature, and *demolding temperature*, which is

50

the actual contact temperature the polymer has reached right when the demolding starts. These are essentially the factors determining the polymer properties right at the demolding step. This includes the surface energy of the polymer, the stiffness, the shrinkage (and thermal contraction) and finally the stresses acting in the polymer.

- The *melt temperature* is mainly responsible for the polymer viscosity, the replication grade and therefore in the end also for the demoldability.
- The use of a *variotherm heating* affects the replication grade, the demolding temperature, the cooling, crystallization and shrinking of the polymer. All of these factors are relevant for the demolding step.
- The *injection speed* and *holding pressure* again affect the replication grade and the shrinkage behavior of the part.

A good example for the process effects is shown in Figure 3.18 for a hot embossing setup. The same line grating has been replicated in PMMA several times under different processing conditions. The outcome for different demolding temperatures varies greatly. These experiments done by Song [84] provide the same conclusions as the one done by Trabadelo [89]. Low demolding temperatures, in this case 25°C, will increase the stiffness of the polymer and wide areas will rip in the demolding process. In contrast at 100°C the polymer will be rather ductile. This will lead to local warpage and deformation of the micro-structure in the demolding process. 70 °C not only produces the most accurate reproduction of the grating but also the lowest demolding force of approximately 10 N compared to 80 N at 25°C and 50 N at 100°C. The measurements by Song [84] were done on an adapted mechanical tester from MTS functioning like a hot embossing machine.

Figure 3.19 shows again the importance of the demolding temperature in hot embossing. This study by Trabadelo [89] shows that the demolding force as a function of the demolding temperature is contrary to intuitive anticipation not a linear curve but exhibits a minimum at a certain optimal temperature. Even though the measurements consist only of four distinctive points a parabolic trend can be seen. The measurements of Trabadelo [89] point towards an optimal temperature, which is confirmed by Fu [30] in experiments and simulation and by Song [84] in simulation as well. The number of measurements in this case was deliberately kept low to ensure reproducible and comparable measurements. This was necessary because the silicon wafer containing the 500 nm pillars will accumulate damage after a certain amount of imprints. At that point the damaged wafer can no longer be used for actual measurements. Therefore, measurements at the required temperatures had to be performed in direct succession, and could not be repeated for confirmation of the findings.
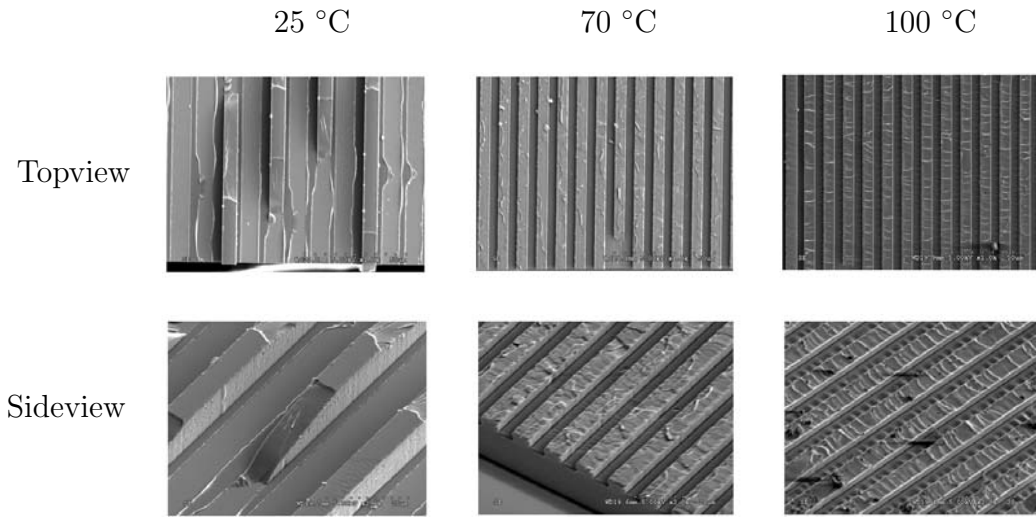
Figure 3.18. Side- and topview of imprinted PMMA patterns (line gratings) at different demolding temperatures [84].

This non-linear temperature dependence of the demolding force is caused by the overlapping of two different phenomena. Basically higher temperatures and higher holding pressure lead to the expansion of the polymer while lower temperatures and lower holding pressures lead to a contraction of the polymer. This will alter the occurring friction due to the changes in the stress levels of the micro-structure (compare Chapter 2.4.1 'Friction'). The expanding polymer will press against the mold [30]. This effect can be seen in Figure 3.20 when the diameter of the pillar structure gets bigger than its original 100 µm (positive Δd). This will increase the stresses and the friction which will lead to a poor demoldability. On the contrary a long cooling time or low cooling temperatures will cool down the polymer more necessary. This leads to the shrinking of the polymer onto the structured mold surface and additionally to an increased stiffness of the polymer. This effect with negative Δd is shown in figure 3.20 on the volumetric contraction side. This contraction has a similar effect as the expansion of the polymer and produces a higher stress level in the micro-structure.

The contraction exerts a force on one side of the stamper sidewall which increases the friction force. Both effects decrease demoldability or even inhibit demolding to a certain degree. This suggests that an optimal demolding temperature exists for the injection molding process as well. This point is found at the expansion and contraction equilibrium with the dimensional difference Δd equal to zero [30]. The polymer molding- and demolding-temperature can become a critical parameter for replication processes like
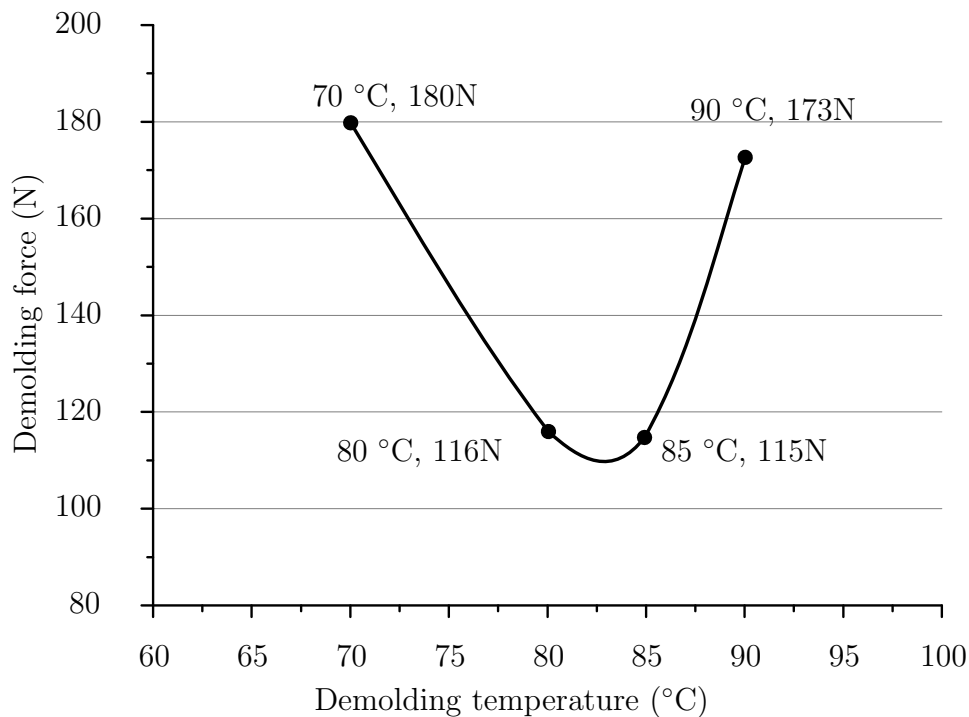
Figure 3.19. Influence of the demolding temperature on the demolding force in hot embossing [89].

injection molding or hot embossing. In the molding phase of the replication (molding window) the polymer needs to have the lowest possible viscosity, thus a high melt and mold temperature. After the molding ends and the demolding begins, if possible no deformation should occur. Therefore, the polymer has to have reached a certain temperature to ensure enough stiffness of the polymer part. A lower demolding temperature will subsequently increase the production cycle time (cooling time). Despite that, the melt temperature should not be chosen too low as this would unnecessarily increase the polymer viscosity and in the end will influence the molding results [55]. Furthermore, it has to be taken into account that these effects (e.g. shrinking) can be different for semi-crystalline and amorphous polymers due to their different morphology.
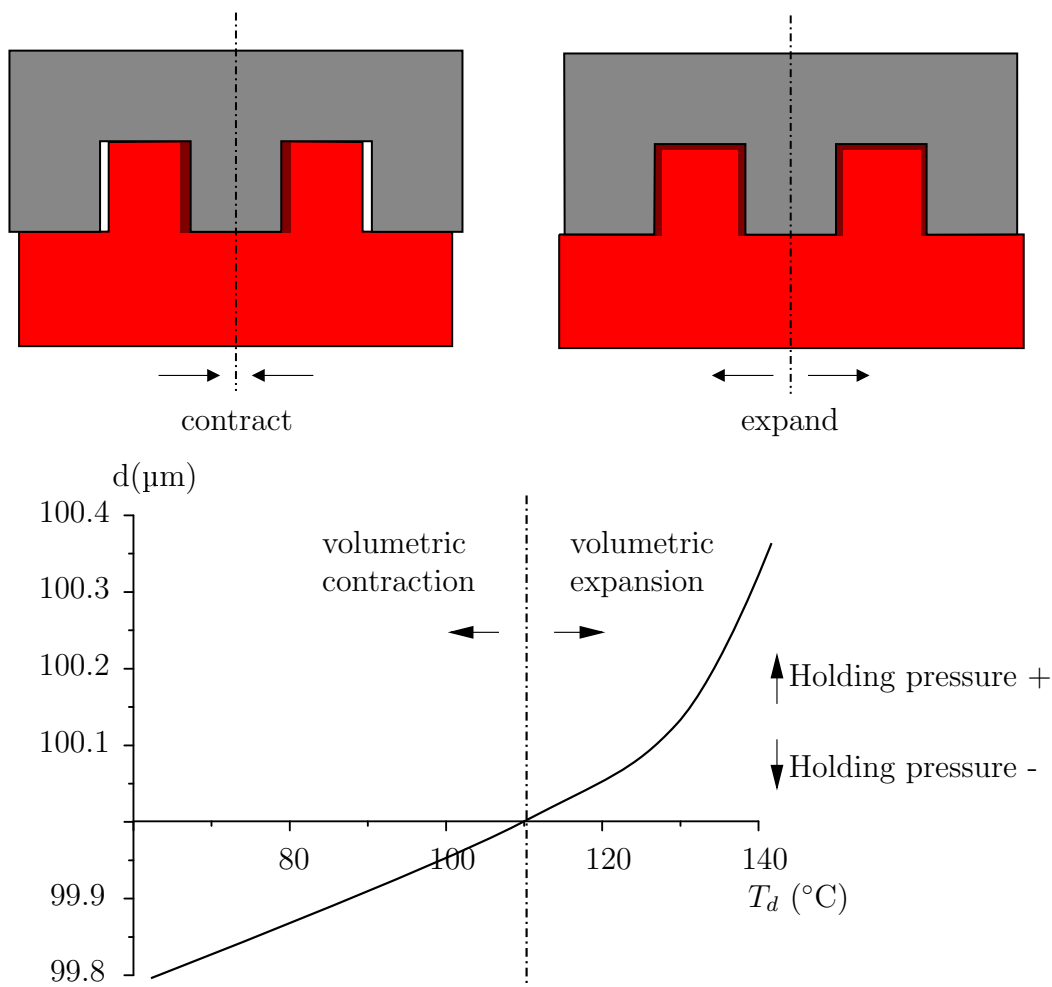
Figure 3.20. Thermal contraction and expansion of a micro-structured polymer based on Fu et al. [30].

3.5 Demolding force and measurement methods

Since many factors influence the demolding behavior, a measurable parameter needs to be defined in order to be able to evaluate this behavior quantitatively. As literature suggests [35, 89, 95] the demolding force acts as an indicator for the demoldability of the polymer part. Increasing forces suggest a worse demolding and a higher likelihood of damaging the microstructures. Figure 3.21 shows an example for the measured demolding forces in the hot embossing process [89]. The figure shows the force over time that is needed to move the stamper. In accordance to Chapter 2.1 'Replication of

micro-structured surfaces' the initial acting force is positive due to the applied embossing pressure. This positive embossing pressure (positive force) decreases after the embossing step is completed (in this case after around 15 s). The measured force then enters a negative range which represents the pulling against the acting vacuum pressure in addition to the motion separating both structured surfaces. The piston moves at a speed of 0.4 mm/min and the force signal is recorded every 20 ms. The peak (marked by pointers) that follows a disruption in the movement, is interpreted as the necessary force to demold the micro-structure. Despite the slow demolding speed, the measurement resolution is only 133 nm per measurement step, which limits the reproducibility. For the plain surface in (a), the induced force is 65 N, which is a lot less than the 111 N caused by the structured surface in (b). This is an obvious example that shows the strong relationship between the demolding force and replication parameters (in this case the structure) that may increase or decrease the demoldability. In this case a change in the surface topography of the molded part induces the rise of the demolding force. The same measurement setup was used to investigate the demolding temperature influence on the demoldability (compare Figure 3.19).
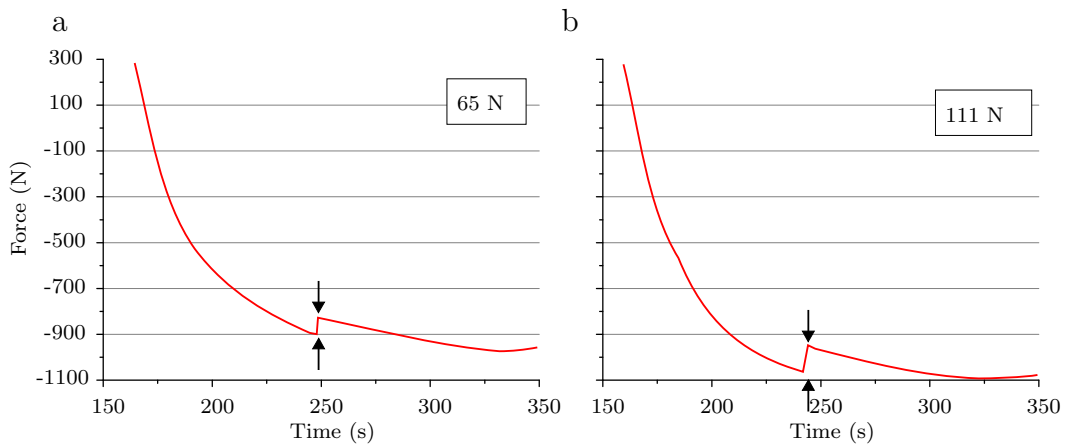
Figure 3.21. Comparison of the demolding force, (a) without surface structure, (b) with surface structure [89].

3.5.1 Measurement in hot embossing

A possible method to measure the demolding force in hot embossing was implemented by Kawata [47, 48] as shown in Figure 3.22. The device acts as a regular hot embossing process as described in the Chapter 2.1 'Replication' and similar to the setup for the measurements in Figure 3.21. The

replication of the structure happens as it usually would for any hot emboss-ing process under the acting embossing pressure. Right after the replication and the cooling is finished the support that holds the stamper starts moving upwards. In this case as seen in figure 3.22 the metal joint which is attached to a flexible coupling is introducing the movement. This induces the de-molding of the micro-structure. The pull-off force used to move the metal joint and ultimately the silicon stamp (Si mold) is measured in the process. The excitation in the positive direction during the demolding represents the force needed to separate the micro-structure on the PMMA/Si wafer from the polymer. This force is what is referred to as the demolding force. To measure the actual forces exhibited by the micro-structure a calibration with a plane surface is performed. This allows to record the forces acting in the demolding movement that are inherent to the system. The coupling adds an-other feature to the demolding setup as the apparatus can be implemented similar to a tensile strength measurement device. This allows for a precise velocity controlled demolding at very low movement speeds with accurate force measurement. Other measurements performed in the hot embossing process like done by Song [83] use the same method but exploit a tensile testing machine for a more precise pulling motion and force recording.
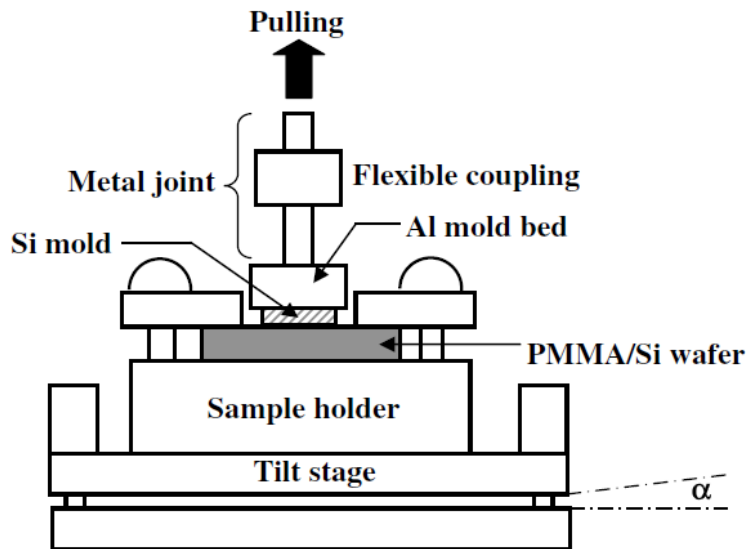

Figure 3.22. Schematic view of the tool for demolding force measurement in the hot embossing process [47].

3.5.2 Measurement in injection molding

Figure 3.23 shows the measurement device as used by Fu [30] in the injection molding process. A very similar system is used by Griffiths [34, 35].In this setup a load cell is attached to the ejection pins, measuring the force needed to push the polymer part out of the mold cavity. Just like for the hot embossing a calibration with a flat surface was performed. This was done to measure the demolding force that correlates to the micro-structure. In Figure 3.23 a plane surface (a) is measured in comparison to a structured surface (b). The difference between these two forces can be seen as the relative demolding force needed to demold a certain micro-structure. In this case the tests were done with a micro-structure array with round pillars arranged in a 24 times 24 (total of 576) set up. The size was set to a diameter of 100 µm and a depth of 200 µm produced using deep reactive ion etching. A schematic of the structured zone can be seen in the depiction of Figure 3.23 (b). The material for this experiment was a polymer metal feedstock. The conclusion by Fu [30] was that experimental measurements and simulation support the theory of a critical demolding temperature with certain limitations. This has been explained in the previous chapter 3.4.4 Process.
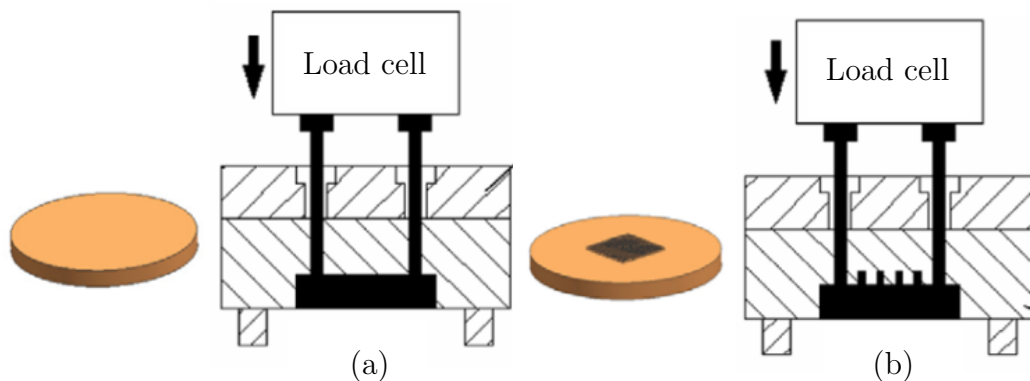
Figure 3.23. Schematic of a demolding force measurement device for an injection molding process. In case (a) for a plane surface and (b) a structured surface [30].

3.5.3 Drawbacks of current measurement approaches

Because of the fact that there are different studies on different subtopics, e.g. polymers, processing or geometry, there is no common denominator linking connecting the research. Attia [3] points out that due to the ongoing devel-

opment of micro-structured applications, specifications (e.g. used geometry dimensions) for these applications are hard to come by. What today cannot be manufactured, may tomorrow well be a production standard. This explains the non target oriented nature of the published research. Different research groups start from different points of interest investigating different aspects of the matter regarding what is currently needed. This leads to structural variety from pillars (Fu [30], Kawata [48]) or channels (Griffiths [35], Merino [61]) to rays ([49]) or other uncommon structures. Furthermore, the structural size is in some cases 100 nm and in other cases 500 µm. An additional influencing factor is the structural density. While some setups are tested with one single structure, others setups use patterns where structures are placed side by side leaving gaps in various sizes sometimes not much bigger than the structure itself. The in-depth descriptions are often lacking sometimes not even a summary that better describes the actual used micro-structure as well as its density (pattern), placement on the substrate or similar defining parameters.

This means, that the little information on the setup for the performed test makes it hard to compare different results. In all papers evaluated in this thesis most of the studies highlight different aspects. The same parameter is seldom investigated repeatedly or in combination with another parameter in the same setup. Still, findings of influences like demolding temperature or setup changes, e.g. measurement method, of the different studies that were performed, support each other. Unfortunately in many cases even if there are a similar conclusions, a comparison cannot be done accurately due to the missing information. This illustrates the need of transferability of the found conclusions to other setups, because of the big differences in evaluations performed in the different publications. The measurements are either done in hot embossing or an injection molding process using a completely different setup. The ejection pins in the injection molding system can bend the polymer specimen and additionally distribute the demolding force unevenly and poorly. In comparison the piston for the hot embossing process bends the polymer upwards which is completely contrary to the injection molding system. Apart from these influences like bending, the different shrinking behavior and the evaluation methodology even the definition of the demoldability (demolding force) varies as there is no standard for this kind of measurement. This allows only for proper comparison of different influencing parameters measured in the same setup. An approach for a suitable measurement device that allows for these comparisons in common injection molding processing conditions is discussed in Chapter 4.

Chapter 4

Design of a demolding force measurement device

The current situation clearly shows the need for a measurement device that is not only capable of showing differences in the demolding behavior but also operates in a production environment. The idea was to create an injection molding unit that fulfills all the standards for state of the art lab-on-a-chip manufacturing. Additionally, a measurement technique has to be devised that allows the measurement of the acting demolding forces in this process. This would be a considerable improvement over the previously described measurement tools (compare Chapter 3.5 Demolding force measurement and measurement methods). Using a production mold for the measurement unit as well therefore ensures actual and unaltered processing conditions for the measurement. This allows the system to make accurate predictions for the manufacturing of a certain micro-structure using injection molding instead of hot embossing. This will also point out different and new effects that are exclusive to injection molding process. An additional advantage of the injection molding process can be facilitated. Unlike the hot embossing process the injection molding process has cycle times that are a lot lower (by a factor of around 10). This helps to evaluate the reproducibility by increasing the number of measurements that are performed for one setup. Moreover, the process durability of the coatings for at least a few 100 shots can be evaluated. To reach this goal, several important steps had to be completed:

- Defining the general specifications for the injection mold that are necessary for manufacturing micro-structured polymer parts.
- Devise a comprehensive overview of possibilities to measure the demolding force in the injection molding process.
- Evaluate the feasibility of the concepts making sure the concepts can

be implemented.

- Preliminary testing of the most feasible concepts for further development.
- Final design and construction of the mold accompanied by fundamental simulations regarding temperature profile and injection step.
- Performing of initial tests to evaluate the functionality of the mold.

4.1   Demolding force measurement concepts

First of all a suitable measurement device has to be developed before the actual mold can be designed around it. This means that a way to record the movement and the acting forces in the demolding step has to be devised. For the basic demolding movement that leaves two options for the measurement device:

- Equipping the mold with an additional movement option (e.g. a motor inside the mold) to decouple the demolding movement from the machine movement,
- using an inherent machine movement (e.g. knee lever opening) to carry out the demolding movement,

Depending on the used application, the mold design (i.e. gate system) and most importantly the polymer, the injection pressures can reach up to 2000 bar. This is a critical point for the design of any movement or measurement system that is placed inside the mold. The forces acting on the measurement system (e.g. the load cell) or the movement system (e.g. wedge, spindel) will be very high. The final mold design has to account for these high pressure and find a way to prevent damage to the measurement system in the injection phase of the process. The in-mold movement systems that were evaluated need to be designed very robust to withstand the high injection pressures. This robust construction affects the movement accuracy leading to setups that cannot perform the required slow movement. Additionally, the size of a mold using an internal movement unit will increase drastically to accommodate the necessary adaptations. This will in some cases even prevent the mold from fitting into a regular sized injection molding machine. Therefore, the focus shifted towards the option of using the inherent machine movement. In this case the aim was to fit only the necessary measurement equipment into the mold, while the entire demolding movement is provided by the injection molding machine. Table 4.1 shows the movement options that were evaluated [14]. This list shows possible ways to implement the demolding force measurement.

Table 4.1. Possible ways to induce movement for the exact measurement of
the demolding step.

Movement in the mold	description
Wedge	make use of a movable wedge inside the injection mold
Spindel	use the rotation motion of the spindle to move the substrate backward
Cushion	using a pressured cushion as an actuator inside the mold
Hydraulic cylinder	using hydraulic pressure to move a piston inside the mold

Machine movement	description
Hydraulic mold opening	making use of the hydraulic mold opening motion of the injection molding machine
Electric mold opening	making use the electric mold opening motion (i.e. knee lever) of the injection molding machine
Hydraulic ejection	using the motion of the ejector pins provided by a hydraulic machine movement
Electric ejection	using the electrically induced motion of the ejector pins

4.2   Pretesting of the available equipment

Macro geometries in injection molding produce quite large demolding forces
in the demolding processes. Micro-structures on the other hand exhibit comparably small forces in the demolding step. Compared to a large polymer part
with a complex surface that interacts with the mold, the micro-structures
only have a small surface that is in contact with the mold. Usually the polymer parts with micro-structures are planar (simple chip applications) with
structures in the direction of demolding. This means after a small movement matching the micro-structure height of around 1 - 100 µm the part is
essentially demolded. For comparison a regular injection molded cup is in
contact with the mold for a long period during the demolding step. There-

fore, the dominating forces for micro-structure demolding (compare Equation 2.2 Chapter 2.4.1 Friction) are on a different level than for common injection molding parts. Any measurement concept needs to deal with these restrictions and be designed appropriately. Using the machine's inherent actuators the two available choices (i.e. the mold opening movement and the ejection pin movement) were evaluated. Additionally, it has to be taken into account that the common injection molding machines fall in two major categories regarding their movement framework. The machine movement can be either performed by an electric movement unit or an hydraulic aggregate depending on the setup.

The two machines used for this evaluation were an electric and hydraulic injection molding machine with a respective clamp force of 1000 kN and 1300 kN. To show the main differences of these two concepts thorough displacement measurements for the four available movement options were made. This will ensure that future measurements with the chosen movement option are reliable. To test these necessary parameters a highly accurate position sensor from Micro-Epsilon Messtechnik GmbH (Austria) was used to perform displacement (movement) measurements for all the movement options. The goal was to test the following properties to finally be able to select the appropriate movement option.

- *R:* Reproducibility of the the set movement option. Several measurements over an arbitrary number of repetitions (at least 5 times) have to yield the same measurement.
- *C:* Controllability of the machine mainly capabilities regarding the possible settings (i.e. the possible set values for the movement speeds) for the machine movement.
- *MS:* The actual movement speed that can be achieved measured as displacement over time. Generally a slow movement is better for the measurement.
- *EI:* External influences that act on the movement (e.g. inertia or friction). These influences can be shown in the the measured curve through deviations from the set uniform movement speed. No or little influences are desirable.

Figure 4.1 shows the measured curves for the investigated movement options. The four movement setups of the machine behaved as follows:

- The *electric mold* movement shows that the movement begins after a delay of around 7 seconds. This late onset of the mold opening motion is due to the high clamping forces acting on the mold. Therefore, it
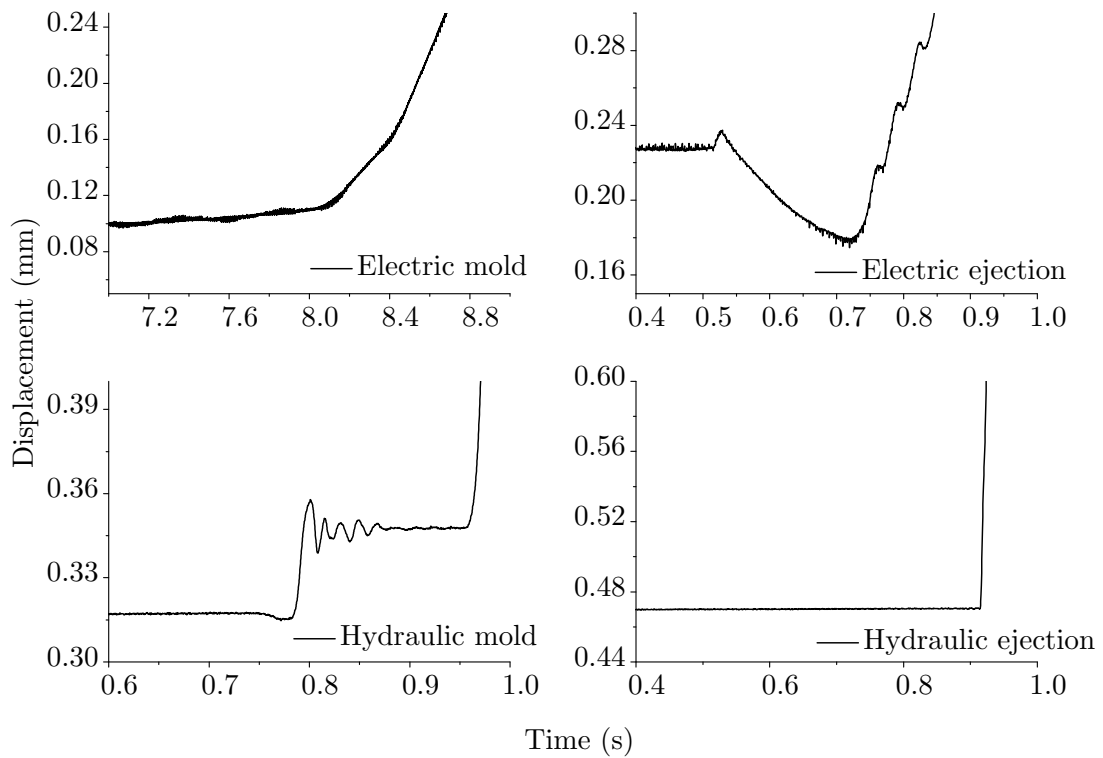
Figure 4.1. Displacement measurements over time with a movement speed of 1 mm/s for all four possible movement options.

is necessary to reduce the clamping force first until finally the opening motion starts. After this step the movement starts without any apparent influences.

- The *electric* movement of the *ejection* pins shows slip-stick effects while the motion occurs. This slip-stick effect can be seen in the movement curve as oscillation in the measured displacement. This movement inhibition (slip-stick) occurs due to the friction of the ejector pins. Additionally, the measurement of the movement was mounted on the ejection plate which moves several ejector pins at the same time. This will add to the overall measurement error. Moreover, the ejection pins appear to move backwards before the actual demolding movement.

- The *hydraulic mold* movement shows slip-stick effects during the movement similar to the electric ejection. In this setup the opening movement oscillation appears most likely due to two different reasons. First would be the friction of the entire system that leads to slip-stick. Second are disruptions due to the valves controlling the hydraulic pressure for the movement. The switching of the valves and the fact that

63

hydraulic oil is not incompressible can lead to a slight pulsing in the movement.

- The *hydraulic ejection* pins could not be adjusted slowly enough to measure anything but a steep flank in this setup. This means that in this case the demolding movement was over before any viable measurement could be performed.

Table 4.2 shows an assessment of the different movement options and how they performed in the previously defined categories. It can be seen that the fully electric mold opening movement is the only movement option satisfying all set criteria.

Table 4.2. Comparison of the different movement options of the fully electric and hydraulic machine concept.
R=Reproducibility, C=Controlability, MS=Movement speed, EI=External influences
+ = good, 0 = neutral, - = bad

Movement	R	C	MS	EI
Fully electric, mold	+	+	+	+
Fully electric, ejection	-	+	+	-
Hydraulic, mold	0	+	+	-
Hydraulic, ejection	-	-	-	0

4.3 Mold unit design

Based on the information gained in the pretesting, the mold design was executed. Figure 4.2 shows the concept for the injection mold incorporating the main design elements. The basic mold consist of the hot-runner, the gate system and the cavity (polymer part). As for any other mold a cooling system ensures that the part is solidified before demolding, which is done by the ejector pins (compare injection molding cycle in Chapter 2.1 'Replication of micro-structured surfaces').

In addition to the basic components that make up a common mold this mold includes the measurement equipment for the demolding force measurement, a special frame system that enables the fixing of the structured

substrates in the mold. Furthermore, a variotherm heating as well as a vacuum supply for the mold cavity is used to improve the replication quality. The variotherm heating and the vacuum are necessary key points for a proper replication of the desired micro-structures on a polymer (compare Chapter 3 'Demolding of micro-structures'). The frame that holds the micro-structure is directly connected to the load cell which is positioned behind it. This makes it possible to measure the acting forces for any chosen micro-structure that is placed in the frame system. The other part of the measurement system is the displacement sensor, located in the parting plane of the injection mold to record the mold opening motion. Meeting all these requirements in addition to the basic specifications for an injection mold, the design was finished in cooperation with a tool making company. The mentioned key parts that deviate from the standard mold design will be elaborated in the following chapters.
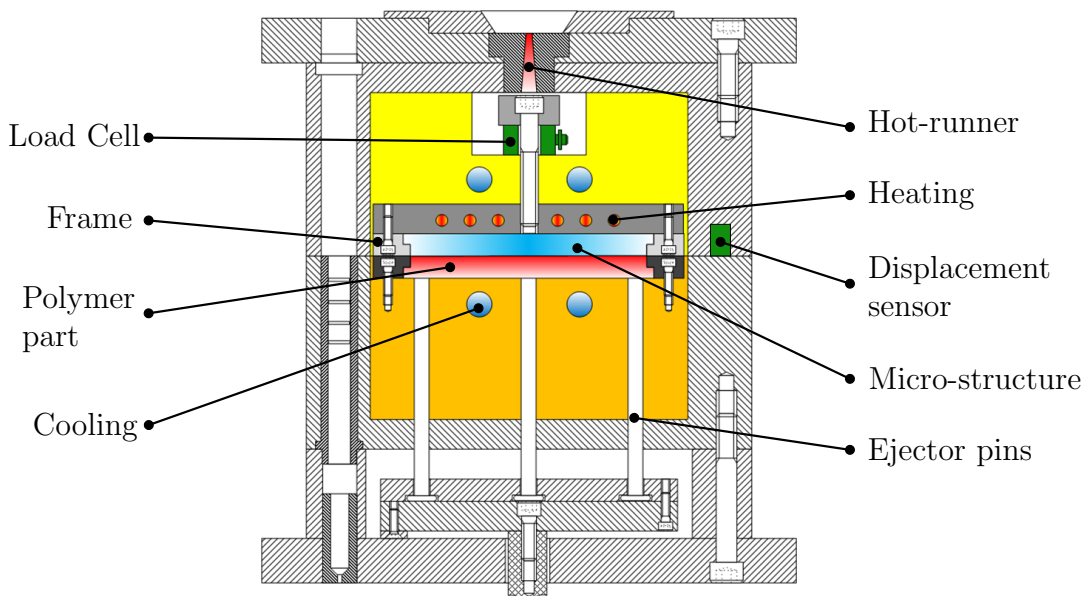
Figure 4.2. Schematic overview (rotated by 90°)of the necessary parts that make up the instrumented injection mold [15].

4.3.1 Force and displacement measurement

To ensure a reliable measurement of the demolding force a sensor with adequate resolution is necessary. As forces of around 200 N were expected, a sensor in the range of 0 N - 750 N was chosen. The most important part is the synchronization of this force signal to the corresponding demolding mo-
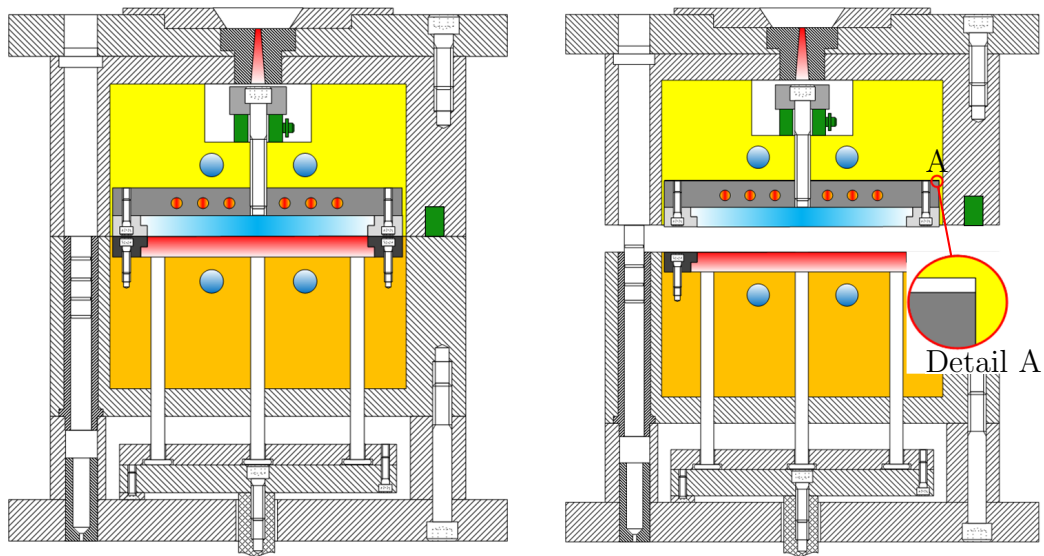
Figure 4.3. Opening motion of the mold and the effect on the movable mounting and the load cell behind it. Detail A shows the lift off of the frame system pulling on the load cell [15].

tion. The machine movement can be tracked but the provided resolution of 0.01 mm is larger than the micro-structures that will be tested. An additional displacement sensor in the parting plane of the injection mold provides the necessary distance information. This allows to assign the demolding force to the specific demolding position. The resolution in this case is below 40 nm. Table 4.3 shows the key parameters for the Micro-Epsilon displacement sensor (CSH1-CAm1.4) and the Kistler load cell (9001A). Using this equipment the mold opening can be recorded with sufficient accuracy for later evaluation. Figure 4.3 shows the mold operation during the measurement (in the demolding step). 'Detail A' indicates the area where the demolding force, that acts on the stamper, is 'lifting off' the micro-structure and the frame system from rest of the mold. The movement is prevented by the screw that connects the frame to the load cell. The resulting force of this pulling motion correlates to the demolding force. The clamping is done using a preloading force on the load cell according to the manufacturer specifications. This shifts the measurement range that measurements in both directions (pushing and pulling) are possible. This prevents unnecessary burden due to the injection pressure on the load cell.

Table 4.3. Specifications of the sensors used for the demolding force measurements [51, 64].

Load cell		Displacement sensor	
Range	0 – 750 N	Range	0 – 1 mm
Resolution	1 N	Resolution	0.38 nm
Linearity	0.5 %	Linearity	0.05 %
Calibrated range 10 %	0 – 600 N	Temperature stability	-12 ppm/K
Max. temperature	+200 °C	Max. temperature	+200 °C

4.3.2 Frame system

One of the aims for the demolding force measurements, besides making the demolding process visible, is flexibility. In this case that means being able to test different inserts, which can be different micro-structures, different coatings (surface treatments of the substrate) and a combination of both. This can be easily done using the frame system that is included in the mold. The macro geometry is a micro slide (MS) format with the standard rectangular dimensions of 25 mm x 75 mm (W x H). This macro geometry is fixed and cannot be changed. This format was selected because it is one of the most common formats for medical or laboratory devices. To achieve the desired flexibility for the structured surface it should be easily exchangeable. Therefore, the cavity (MS geometry) is placed on the ejection side of the mold. That leaves the die side flat and perfectly prepared to use a flat rectangular frame for carrying different inserts. With this frame the structured area, the insert, can be easily changed. To make this changing step as fast as possible, the frame can be opened up with the mold mounted in the injection molding machine, with the mold in an open position. Using this system, DOEs using different substrates (e.g. different structures, different orientations) can be easily performed. Figure 4.2 and Figure 4.3 show the frame setup holding the substrate in the opening step of the mold.

4.3.3 Variotherm heating

As mentioned in variotherm processing in Chapter 2.1 'Replication of micro-structured surfaces' a variotherm process handling can be crucial for the manufacturing of micro-structures. Certain designs cannot be replicated without variotherm heating at all. To ensure that the mold is a state of the art

device, a variotherm system has been incorporated. This will not only allow a better replication of complex micro-structures, but will also show the influence of the variotherm system on the demolding force. Among the different possibilities for heating up the cavity a ceramic heating was chosen. These ceramic elements provide a local heating right below the structured area and have a high power output of over 1000 W (compare Table 4.4) as well. Additionally, the heating area is almost exactly that of the micro slide (25 x 75 mm) making it as efficient as possible. This perfectly matching area helps as no unnecessary heat is introduced into the injection mold. This keeps the cooling time low because not much extra energy is added through the variotherm heating. To increase the efficiency even further and reduce the temperature right after the injection, the mold cooling is fitted as closely to the ceramic heating as possible. The only drawback of the ceramic heating is the brittleness of the component. To safely situate the heating unit in the mold the fixation of the heating element was carefully chosen. To make sure no flexural stress is exerted on the heating component it should always be under compression. To achieve that, each substrate has to come with the right thickness or a suitable distance plate. It is to note that the variotherm heating is controlled separately from the injection molding machine. Therefore the the injection start signal has to govern the control system for the heating unit. This means that the control cycle for the variotherm heating is controlled by a signal provided by the injection molding machine, thus integrating it in the injection molding cycle.

Table 4.4. Specifications of the AlN ceramic heating element by Watlow [91].

Ceramic heating element	
Voltage	240 V
Power	1455 W
Resistance	39.6 ± 9.9 Ohm
Max. heating temperature	400 °C
Temperature sensor type	Type K thermocouple

4.3.4 Vacuum

Vacuum just like variotherm heating is a crucial for the replication quality of micro-structures. A regular injection molding process can lead to air inside

the cavity that is sealed inside the micro-structures when the polymer is flowing over it. This will have immediate repercussions on the replication grade of the micro-structure. Since it is not possible to vent the micro-structure, the air inside the cavitiy has to be removed before the injection starts. To achieve the desired processing conditions a certain air pressure inside the cavity has to be ensured before the injection starts. A recommended value for the air pressure of 600 mbar was obtained from previous molding experience [46]. For process control the pressure drop is measured right outside the mold in the pipe connecting the vacuum pump and the mold. The pressure sensor is connected to the injection molding machine and used as a trigger for the injection step once a set pressure has been reached. To ensure the desired pressures propagates in the cavity as well as the micro-structure, the mold and injection process have to be adapted. The entire mold is sealed air tight back to the ejector moving plate. The vacuum is directed into a specifically milled channel next to the cavity in the parting plane. This channel aids the remaining air with flowing out of the cavity even with the clamping force acting on the mold. A gap of 4 µm [46] in the parting plane connects the cavity and the milled vacuum channel and is sufficient for a proper evacuation. The gap is also small enough to prevent the polymer from getting into these channels even with the injection pressure acting. A sealing ring in the parting plane prevents any air from getting inside once the mold is sufficiently closed. The process is adapted to this sealing ring and will not close entirely but only to make contact with the sealing ring. Only after the pressure has dropped below the set limit, the mold closes completely. Additionally, the vacuum is maintained over the whole injection step.

4.4   Finished mold design

This concept is based on the demolding movement of the injection molding machine. Any arbitrary micro-structure on an insert with the right dimensions can be placed on the fixed side (nozzle side) of the injection mold. Opening the mold will thereby demold the micro-structure. In the same step the displacement and the acting force of the micro-structure on the substrate is analyzed. This is possible due to the design of the frame system that is only connected to the mold via the load cell. All forces acting on the insert can therefore be recorded. Additional steps to improve the measurements have been implemented. To ensure as little friction as possible the fitting of the frame system was carefully undersized. To ensure a satisfactory molding of the polymer the mold was constructed to apply vacuum to the cavity. A specific heating device was incorporated to make use of a variotherm injection

molding cycle. To accurately measure demolding forces in injection molding compared to the hot embossing process additional boundary conditions have to be met, especially the fact that the injection molding machine plays an important part in the demolding measurement step. The demolding movement as described is completely different from an embossing machine. Using all this information a mold was designed based on the schematics described in Figure 4.2. The final 3D CAD design is shown in Figure 4.4 illustrating a rendering of the finished mold incorporating all the described specifications. According to all these specifications and design guidelines the mold has been commissioned and constructed.
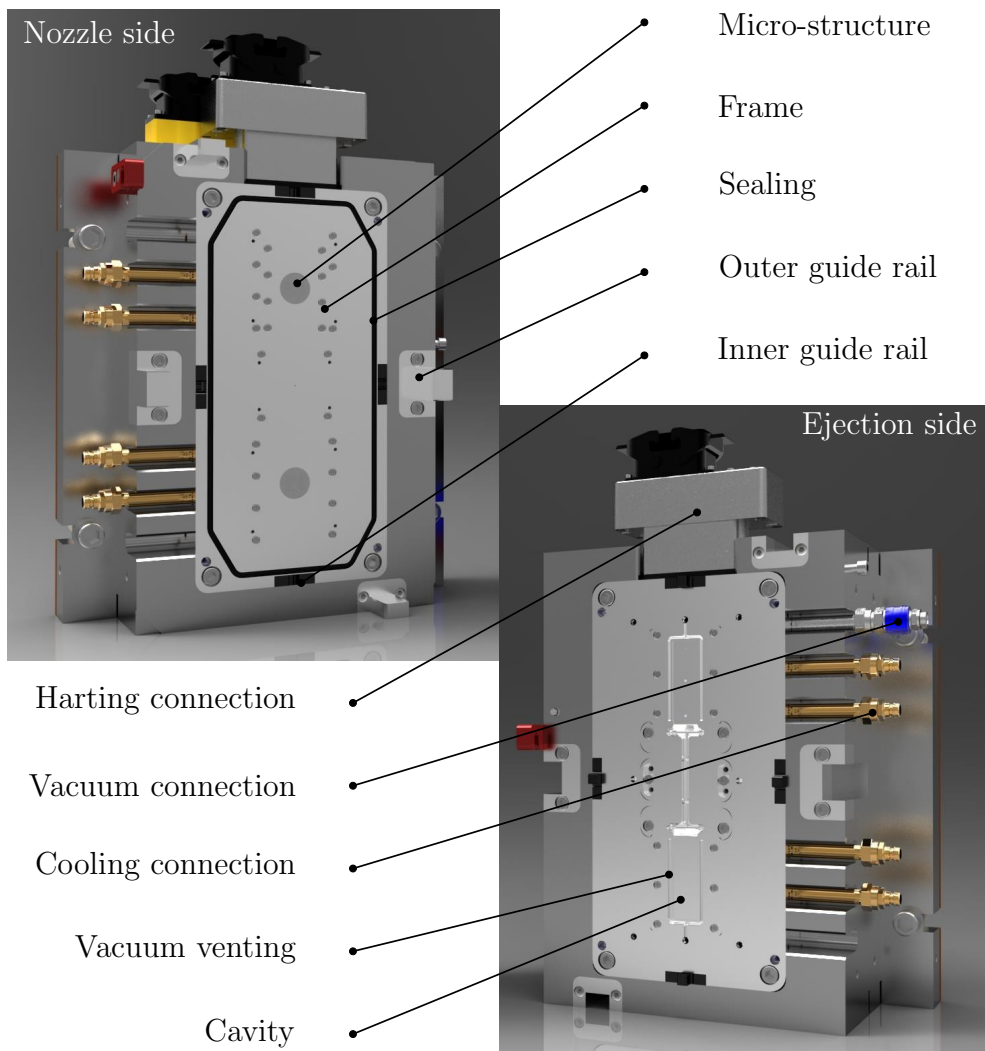

Figure 4.4. 3D-Rendering of the CAD files of final mold design before being commissioned [13].

70

The figure shows the essential components for this injection mold. This includes the the already explained components like the micro-structure, the frame and the cavity. It is to note that the mold is equipped with two identical cavities for MS-slide polymer parts. The reason for this is that due to the hot runner the cavity can not be placed at the center. Therefore, an off-center placement of one cavity a second cavity was added to balance the filling in the mold. The second cavity (the lower cavity) is not used for the demolding measurement. The measurement components (e.g. load cell) are all situated in the upper cavity, which is used to replicates the desired micro-structure. Additionally, the figure shows the sealing ring (black) that runs around the inner mold (light gray) keeping air from creeping in to the cavity through the parting plane. Moreover, each mold side is made up from two parts, the outer (dark gray) and the inner mold (light gray) section. This adds flexibility to the mold as the inner mold can be switched if necessary. Additionally, the manufacturing precision of the macro-geometry is increased in the inner setup. This is shown by the two separate guide rail systems. The outer one is only used for the centering of the mold opening and closing. The inner rail system is for the precise centering of the cavity to ensure the necessary part tolerances. Besides that the rendering shows the connections for the cooling and vacuum supply for both mold halves at the side. Finally, at the top of both mold sides standardized harting connections are located. These are used to lead out all the cables for the unique measurement system as well as the connection for the variotherm heating, the heating for the hot runner and the common pressure and temperature sensors.

Chapter 5

Experiments

5.1 Machine setup

To ensure that the measurement is working as intended, the pretesting has been performed according to chapter 4.2 'Pretesting of the available equipment'. The machine used for the demolding experiments was an fully electric Arburg 470A 1000-400 injection molding machine. To ensure the quality of the measurement two aspects for the machine setup have been verified. First how stable the machine performs consecutive injection shots and secondly how fast the machine can reach this stable process as well as how the machine reacts to changes of injection settings. Table 5.1 shows the actual values of critical injection parameters over 100 shots. For a constant part quality monitoring the acting pressure during the injection phase is a reliable value for observation. A good indicator for a stable process is the melt cushion at the end of the injection step. This value indicates that after the part is filled, the polymer remaining in the barrel is the same. This means little to no leakage in the screw occurs and the injected volume and switchover point are constant. The fact that all the critical parameters show values with low deviation supports the assumption of a stable process.

This electrical machine not only performs very stably over many successive shots, but also reaches a stable process very fast after a machine parameter change. Only two injection molding shots after a machine parameter change (e.g. injection speed, injection pressure or holding pressure) and the process is at a stable value again. This makes process changes very robust with the exception of temperature changes. Temperature changes take time until a homogeneous temperature field is reached. Temperature stability was reached as soon as as the monitored parameters showed the initial deviation between different cycles. This time was recorded and used for temperature

changes as minimum requirement to a stable process once again. After the temperature is in a steady state, the process is again robust and will not fluctuate for more than the two recommended injection shots after parameter changes.

Table 5.1. Several critical injection process parameters and their deviation during the injection molding process over approximately 100 injection cycles.

Parameter	Average value	Standard deviation	
		Absolute	%
Injection time (s)	0.237	0.0047	1.98
Change over volume (cm^3)	15.47	0.0919	0.59
Change over pressure (bar)	577.6	2.7226	0.47
max. Injection pressure (bar)	577.8	2.6961	0.47
Melt cushion (cm^3)	13.82	0.0873	0.63
Dosing time (s)	3.584	0.1390	3.8

5.2 Polymer

Different polymers are used depending on the application (compare Chapter 3.4.1 'Demolding of micro-structures'). Therefore different kinds of polymers were tested. Since the main research focus was on applications in the medical sector the used polymers were selected from this area. The primary focus for injection molding was therefore on thermoplastic polymers with the addition of a thermoplastic elastomers. Polypropylene (PP) was used as one of the most common polymers as representative for semi-crystalline polymers. The amorphous polymers which are commonly used for optical analytic chips are Poly(methyl methacrylate) (PMMA) and Cyclic Olefin Polymer (COP). While PMMA is often used for its superior properties for the final application (e.g. optical properties, interaction with tissue) [41], COP comes close in many areas (especially optical properties) while exhibiting 'better' processing qualities (e.g. lower viscosity compare Table 5.3). Finally, a thermoplastic elastomer (TPE) that is compatible with the used COP was chosen. This way it was possible to test the TPE in various concentrations. This led to the following list of polymers (shown in Table 5.2) used for the demolding

experiments.

Table 5.2. List of the polymers that were used in the experiments.

Polymer family	Polymer grade	Classification
PP	C7069-100NA	semi-crystalline
PMMA	Delpet 70NH	amorphous
COP	Zeonor 1060R	amorphous
TPE	Topas E-140	thermoplastic elastomer

Table 5.3 shows some polymer properties relevant for the demolding step. Most notably for processing is the viscosity, which is a lot higher for PMMA than for the other polymers. Additionally, it is expected that thermal expansion and contraction is dependent on the coefficient of linear thermal expansion and the current temperature which is influenced by the polymer's thermal conductivity. For the demolding step, the stresses acting in the micro-structures will be crucial for successful demolding. This is one of the main reasons TPE was introduced into the experimental design. The extremely low Young's modulus is expected to impact the demolding behavior for all of the prepared blends with TPE.

Table 5.3. List of polymer properties relevant for the demolding step measured at room temperature. The viscosity is the zero viscosity at the processing temperatures used for the polymers.

Polymer	Thermal conduction (W/mK)	Viscosity (Pas)	Young's modulus (MPa)	Coefficient of linear thermal expansion (1/K)
PP	0.29	160	1500	$9.3 \cdot 10^{-5}$
PMMA	0.19	2000	3500	$6.7 \cdot 10^{-5}$
COP	0.15	420	3000	$5.9 \cdot 10^{-5}$
TPE	–	–	50	–

For all the used polymers a suitable process was setup. For the replication of the micro-structure the main focus was the polymer viscosity. A

low viscosity in the classical process means less injection pressure as well as faster and better filling. A low viscosity becomes even more relevant for the filling of the micro-structures. Therefore, the melt temperature was chosen as high as possible to ensure a good replication quality. This parameter was selected for each polymer specifically at the upper end of the recommended processing temperatures. Table 5.4 shows the used polymer processing temperatures for all the demolding experiments. Moreover, the temperature ramp in the cylinder was set untypically even. This means that the desired melt temperature is reach sooner (by Zone 5) and not only at the die (Zone 6).

Table 5.4. Overview of the cylinder heating zone temperatures (in °C) for the used polymers (Zone 1 is the feed setion, Zone 6 is the die).

Polymer	Zone 1	Zone 2	Zone 3	Zone 4	Zone 5	Zone 6
PP	40	190	220	235	240	240
PMMA	40	220	260	265	270	270
COP	40	200	240	255	260	260
TPE	40	200	240	255	260	260

The TPE polymer was added to the investigation of polymers for different reasons. Most interesting is the fact, that the stiffness of the TPE is lower than of all the other polymers by a factor of around 100. This means that all the demolding effects that relate to normal forces (friction forces) are expected to be different because the acting forces are lower for TPE. Additionally, the TPE was selected to be compatible with the COP. This means that blends of COP and TPE are possible. Using this material compatibility, material dependent effects could be investigated. While polymers usually behave completely different in the demolding step using blended polymers the properties of one polymer can be slowly introduced to another. This means that changes in demoldability based on polymer inherent characteristics can be investigated. For this purpose two blends were prepared. One was COP with 10 wt% of TPE and the other was COP with 40 wt% TPE. These weight percentages were chosen based on previous experience of successfully blending TPE to other polymers in the extrusion process [31].

5.3   Design of the micro-structure

The design of the micro-structure has to regard a few important aspects. The chosen structure dimensions should range in the area of commonly used structures for medical applications. They also should be simple enough to allow conclusions regarding the influence of the micro-structure in the demolding process. A single structure has very little effect on the overall demolding and might not even produce demolding forces that are high enough to be measured. This means that no insight can be gained using such a configuration. Therefore, a set of different structures was used and the basic attributes were selected in a range that agrees with literature and common medical devices (for common structure sizes compare Chapter 3.2 'Terminology for micro-structures'). This means that the structural depth and width is in the range of 10 µm - 500 µm and an aspect ratio around 1. Simple channel structures as used in micro-fluidic applications were chosen. To measure a broad range of different effects several different micro-structures with these specifications were chosen for the investigations. As mentioned the complexity of the structures was kept to a minimum with one exception. On chip was chosen with a high complexity based on an established application. This chip was added not only to validate the findings for higher structural density but also verify the transferability of the gained insights onto an actual application. Figure 5.1 shows the four different structure designs that were used for the experiments. The schematic representation shows the whole micro-slide setup and parts of the gate system. This is important to understand the injection situation as well as the shrinkage direction. The exact definitions for the structures are as follows:

- The *Normal* chip refers to the basic micro-structure used for all the basic coating tests and reference tests for comparison with the all the other structures. The structure consists of channels with aspect ratio 1 and a width and depth of 50 µm. Additionally, there is a slight draft angle of approximately 4° to help with the demolding. The channels are oriented vertically on the side of the chip and horizontally in the center. The entire structured area is placed in the center of the micro-slide as shown in Figure 5.1 'Normal'.
- The *Perflow* chip contains only horizontally placed channels. This means that all the channels are arranged perpendicular to the polymer flow. The channel has an aspect ratio of 0.5, a width of 100 µm and a depth of 50 µm and a pitch of 300 µm. Just like the Normal chip all the channels have a draft angle of around 4°. The whole structured area is a square with 20 x 20 mm. The structured area is placed at the

flow end of the chip.

- The *Inflow* chip has exactly the same channel dimensions as the Perflow chip. The difference is that the structured field is rotated by 90 °. This means that the channels are oriented in the direction of polymer flow. The position and size of the structured field remains the same.
- The *MedAp* medical application chip consists mostly of micro fluidic channels in the range of 25 - 500 µm. Additionally, there are some structures that are used for filtering that are smaller than 25 µm. A few structures act as wells, which are larger than 500 µm. Overall this chip has the highest structural density as the whole are is covered with structures. Furthermore, this chip is an exact replica of a medical application that is already commercially sold.
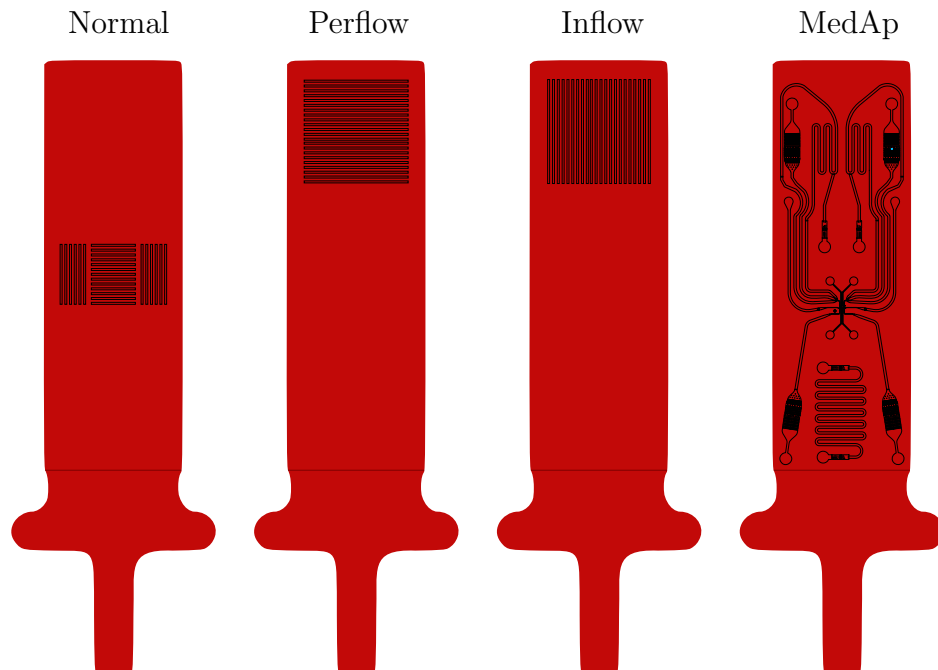

Figure 5.1. Schematic representation of the different used micro-structure and the placement on the polymer part.

The *Perflow* and the *Inflow* structures can be used for two different aspects. Due to the structure orientation the effects on the demolding of the channel orientation in regard to the flow front can be measured. Moreover, differences in the demolding behavior due to the structure placement (close and far to the gate) can be revealed. To achieve that, both structures the *Perflow* and *Inflow* insert can be rotated by 180 ° placing the structured area

either close to or far from the film gate. With this option effects due to the polymer shrinkage can be investigated. It was expected that effects inherent to the injection molding process can be studied. This includes foremost the shrinkage towards the film gate, where the part is locked in place. Therefore higher demolding energies are expected for the structure placement far from the gate. The *MedAp* is an application used to validate the results from the simple test structures for a more complex setup as used in lab-on-a-chip productions.

5.4 Mold

The mold and mold materials, mainly of the structured substrate, provide a very promising method to improve the demoldability. This can be done by changing the material of the cavity that is in contact with the polymer. The contact material directly influences the friction and adhesion which are the dominant factors defining the demoldability. The easiest way to alter the surface properties is to use coatings on the micro-structured insert. Using coatings the interaction of the polymer and the mold can be changed. Since the polymer is often defined by the application an easy modification like the coating of the mold is desirable. The most important property of coatings is that they can be applied without altering the manufacturing process of the mold or the used materials (i.e. steel) because the coating is only applied after the entire setup is already functional. This works especially well for the nickle substrates that carry the designed micro-structures because the insert is designed to be an easily changeable part. The only drawback when using a coating on the insert is that the deposited material layer on the micro-structure changes the dimension by up to 2 µm. This value depends on the coating method and the used coating parameters. To investigate the effect of different coatings the 'Normal' micro-structure was prepared several times with the exact same structures. Afterwards, these inserts were coated with different coatings.

These coatings do not only change the surface properties based on the coating material but also based on the morphology of the coating. The roughness or general surface topology depends on the coating process (e.g. physical vapor deposition) and the used process settings, used voltages, time and temperatures. To better understand how similar coatings may vary, the chrome based coating was selected as a reference coating. Therefore, CrN coatings were provided from two different contractors and with different processing properties. The main idea was to understand how small variations in processing or the supplier can affect an otherwise identical coatings. One

CrN coating from Oerlikon Balzers Coating AG (Lichtenstein) was ordered twice to ensure reproducible measurements for supposedly identical coatings. Additionally, the influence of different coatings had to be investigated. This was necessary to better understand how completely different coatings (and therefore different friction and adhesion) act on the demolding. Therefore, different coatings were evaluated additionally to the already chosen CrN. These were selected in collaboration with partners that also provide these coating as well as a company that has experience manufacturing medical devices. Table 5.5 shows an overview of the coatings selected for testing. This includes the vapor deposited coatings (TiN, CrN and DLC) as well as an in-house manufactured coating (silane). The silane coating is a wet chemical deposition coating based on fluorine silane chains to achieve a low surface energy.

Table 5.5. List of all the 'Normal' inserts that were prepared and coated for testing. *LZL* = Laserzentrum Leoben; *MUL* = Montanuniversitaet Leoben; *Oerlikon* = Oerlikon Balzers.

Coating	Contractor	Additional information
Nickel	None	uncoated
TiN	Oerlikon	normal setup
CrN1	Oerlikon	normal setup
CrN2	Oerlikon	same setup as CrN1
CrN3	LZL	normal setup
CrN4	LZL	extra thin
DLC	Oerlikon	normal setup
Silan	MUL	chemical deposition

Figure 5.2 shows the measured contact angle for all the coatings with water and diiodo methane. Silane with the highest contact angle provides the mold surface with the lowest surface energy, while the uncoated nickel ranges in the mid to low range of all the measured values. The two coatings CrN1 and CrN2 manufactured by Oerlikon show contact angles similar enough to support assumption that both of these coatings can be regarded as practically identical. The CrN coatings provided by the LZL both show lower contact angles then the one from Oerlikon, indicating that the manufacturing process can and will influence the surface properties. Moreover, CrN4 shows a lower contact angle than CrN3, due to the different requirements for both of these

coatings (CrN4 was coated with a lower thickness than CrN3).

Setting up the experiment to test all of the coatings with no change in the processing settings revealed if the surface properties affect the demolding behavior. These measurements were performed for all selected polymers to also reveal polymer characteristic behavior. This was particularly important as the polar and dispers composition of the polymers is different and was expected to change the interaction with the respective coating.
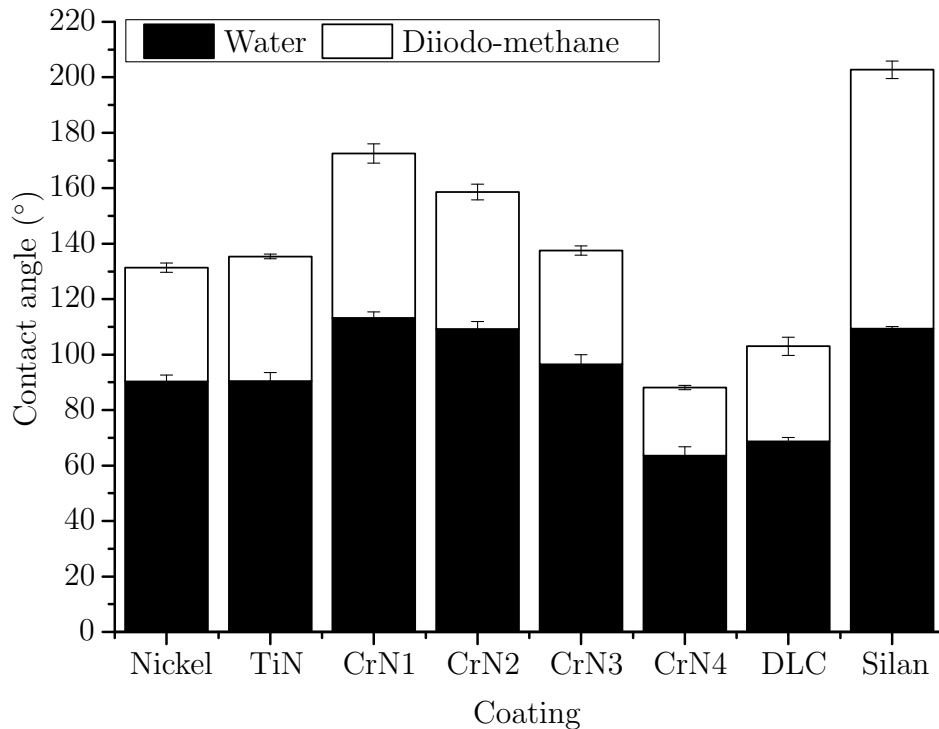

Figure 5.2. Contact angle measurements of the different coatings that have been applied on the 'Normal' insert.

Finally, the experiment was extended towards actual applications. Therefore a case study on the MedAp application was performed. The MedAp structure just like the Normal structure was prepared several times. Furthermore, the list of tested coatings has been modified for this setup. The main goal was to test new coatings in the demolding process. Since the new structure might bring additional influences that change the demolding process a particular coating for comparison was selected. Table 5.6 shows a list of all the used coatings. An uncoated version of the chip as well as a basic TiN coating was used as reference. The uncoated chip served as a reference for the process to date while the TiN was used as a coating that performed well in previous tests. For the new coatings zirconium carbo-nitride (ZrCN) [52],

tungsten carbide/carbon (WC/C) [10] and molybdenum disulfide (MoS$_2$) [90] were chosen as more exotic coatings based on literature that either investigated the demolding properties directly, claims good friction properties or mentions a certain degree of utilization in polymer processing.

Table 5.6. List of the MedAp inserts that were prepared and coated for testing. *Eifeler* = Eifeler Swiss AG.

Coating	Contractor	Coating material
Nickel	None	uncoated
TiN	Eifeler	Titanium nitride
WC/C	Eifeler	Tungsten carbide/carbon
MoS$_2$	Eifeler	Molybdenum disulfide
ZrN	Eifeler	Zirconium carbo-nitride

5.5 Process

While a lot of processing parameters influence the moldability and the replication grade of the micro-structure, the main parameters for the demolding step are the acting temperatures (e.g. melt and mold temperature). Therefore, any study regarding the demoldability of a part must not affect the micro-structure replication. Otherwise measured effects may result from the differently molded structure rather than the demolding properties. To ensure a constant replication a reliable process for the molding has to be setup. Table 5.7 shows the most important parameters used for the specific polymers that allowed a good replication (compare Chapter 5.6).

The holding pressure profile was setup after the optimal filling conditions were found. The best values for the polymers are shown in Table 5.8. These values were carefully selected to ensure a homogenous part thickness. This resulted in very short holding pressure time steps. Holding pressure at the beginning will propagate towards the end of the part. The more time passes the worse the transmission of the holding pressure becomes. This means holding pressures at later stages affects the part less and less. Additionally, the extremely thin film gate (0.4 mm) led to a sealing point that was around 4 seconds of holding time. At this point no additional material could get into part. Therefore, small stepwise reductions in the holding pressure were necessary to ensure a homogeneous part thickness. These steps were determined

Table 5.7. Overview of the default injection molding process parameters for the used polymers.

Set parameter	PP	PMMA	COP	TPE
Mold temperature (°C)	50	90	80	80
Variotherm set temperature (°C)	200	200	200	200
Variotherm actual temperature (°C)	110	110	110	110
Injection speed (cm^3/s)	35	35	50	50
Cooling time (s)	25	10	10	10
Back pressure (bar)	60	100	100	130
Dosing volume (cm^3)	25	25	25	25
Changeover point (cm^3)	14.7	14.7	14	11.6
Decompression (cm^3)	0.75	0.5	0.5	0.5

experimentally until the part thickness could not be improved any further. The first holding pressure interval shows 0 seconds because it represents the switchover point. This means that the switchover from the higher injection pressure to lower holding pressures is decelerated (if it is not set the pressure drops faster). This is important to prevent material back-flow due to pressure drop, before stabilizing at the set holding pressure.

Table 5.8. Overview of the holding pressure profile for the polymers.

Polymer	Duration (s)				
Holding pressure (bar)	0	0.25	0.2	4	0.1
PP	370	300	200	100	100
PMMA	750	400	200	200	100
COP	600	300	200	200	100
TPE	600	300	200	200	100

Despite the fact that many of the process parameters can influence the demolding the focus was limited to the mold temperature and the variotherm process control. The main reason is, that the demolding temperature has already been identified as a critical parameter in literature (compare

Chapter 3.4.4 'Process'). Moreover, the process range where parts can be manufactured is very slim, especially for PMMA, therefore many parameters cannot be varied freely. Since the goal was not only to produce parts, but produce parts of the same quality, the process window got reduced even further. Table 5.9 shows the possible ranges for the mold temperature (which is the set value for the demolding temperature) for the used materials. Among these all the mold temperatures in 10 K steps were tested.

Table 5.9. Mold temperature range as selected for the respective polymers.

Mold temperature (°C)	PP	PMMA	COP	TPE
low	30	70	60	40
	-	-	-	-
high	70	90	90	90

Furthermore, all settings were tested with and without the use of the variotherm system. To ensure the same process for both configurations a 10 s time window at the beginning of the injection molding cycle was used as a place holder. In case the variotherm system was used, these 10 s were used for the heating. The 10 s were determined so that the structured surface reached the desired temperature of 110 °C. This temperature is in the range of the the glass transition temperature of PMMA and COP. Moreover, it is close enough to the melting temperature of PP as well to ensure a good replication. The long process cycle, due to the very slow mold opening, ensures that the mold temperature at the end of the cycle is always the same. This was especially important when comparing the variotherm processing with the process without variotherm.

5.6 Measurements of the replication grade

As mentioned this study focuses on the demoldability and not the moldability of different micro-structures. To ensure consistent and comparable results a constant replication grade has to be maintained for all the performed experiments. Therefore, extensive measurements of the channel depths accompanied the manufacturing of the polymer parts. These measurements were done with a standard FRT Surface Measuring Systems. The depth value used for evaluation of the replication is the average value of several measurements. One measurement contains several channels per measured line as shown in

Figure 5.3. Additionally, this line measurement was repeated on several positions on each molded part. The channel width, which is also an important parameter for the replication grade could not be measured reliably due to the draft angle of the channels. The draft angle of the micro-structure blurred the FRT measurement over the the measured side wall area and made it impossible to derive a width value from these measurements.
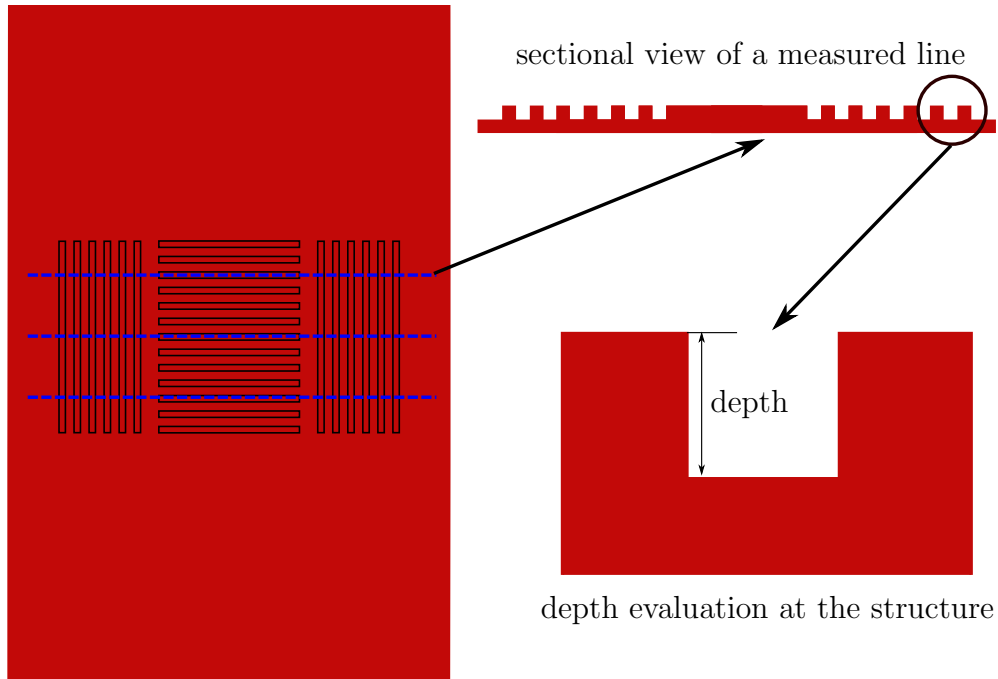

Figure 5.3. Illustration of the measurement positions for the depth analysis for the polymer part molded from the 'Normal' insert.

The carefully chosen process settings revealed almost no deviation in the replication from the structure dimensions of the insert. Table 5.10 shows a selection of measured channel depths for a variety of different parameters (i.e. insert, coating, polymer, melt temperature and mold temperature) and the measurement deviation. These measurements show, that the channel depth for the given setups vary only within the accuracy of the available measurement method (1 µm. They also show that none of the varied parameters like the polymer or the process settings had any measurable influence on the replication grade of the micro-structure (channel depth). A large number of additional measurements for all the the used temperatures and stampers confirmed these findings. This constant replication independent from the tested parameters made it possible to correlate the demolding forces to the demolding behavior and not to geometries that were replicated differently [85].

Table 5.10. Measured channel depth for different polymers, the respective processing settings as well as different coatings for the 'Normal' insert.

Stamper	Material	T_{melt} (°C)	T_{mold} (°C)	Depth (µm)
Ni	PP	240	40	54.76 ± 0.86
TiN	PP	240	40	54.56 ± 0.69
Ni	COP	260	70	54.85 ± 0.72
TiN	COP	260	70	54.82 ± 0.71
Ni	PMMA	270	80	54.66 ± 0.43
TiN	PMMA	270	80	54.42 ± 0.90

5.7 Signal evaluation

To interpret the measurements and compare results from different measurements a robust signal processing had to be used. The steps to a quantifiable value are explained in this chapter starting with the original signal. The goal is to get from the recorded displacement and force information to a value that describes the demoldability of the polymer part. It will be shown that the discrete demolding peak in the force measurement that is often described in literature could not be detected for most setups. To still be able to evaluate and compare the used setups the demolding energy calculated from the demolding force was used to describe the demolding step.

5.7.1 Signal recording

The force and displacement signal were both recorded with 1400 Hz which is the maximum for the used configuration. The A-D (analog-digital) converter supports higher frequencies which could not be implemented for these signals, because both charge amplifiers for the displacement sensors and the load cell only support 1400 Hz. Using the necessary data recording with 1400 Hz introduced two problems that needed to be addressed. The first difficulty was the inherent noise that was present in any measurement which usually gets worse with higher frequency measurement. The second problem was the generation of redundant data, duplicate data points, due to the high recording frequency. These data points did not only slow down calculations (e.g. integration) but also produced signals of different length for each measure-

ment. This as undesireable as the signals from different measurements had to be compared. Especially in combination with the very low mold opening speed at 1400 Hz a fluctuation in the cycle time of around 1 s would produce measurement vectors that are 1400 elements longer. Additionally, for the slow movement a lot of indistinguishable data was produced (same displacement information for several measurement points). This is the reason why signal processing after completing the recording was necessary.

Figure 5.4 shows the two relevant signals that were recorded during the injection molding cycle (over time). The displacement sensor was calibrated very accurately to the range from 0 - 1 mm. Therefore, anything over 1 mm is regarded as an open mold. Additionally, the sensor never showed the value 0 mm even for the closed mold. This is due to the fact that the sensor has an assembly offset inside the mold of approximately 0.16 mm. This offset is for safety reasons to prevent the mold opening/closing from damaging the sensor. The offset was corrected mathematically in the signal processing for easier readability and interpretation of the data. The mold closing can bee seen in Figure 5.4 as the measured displacement drops from 1 mm to the sensor offset of 0.16 mm.

Additionally, the measured force on the load cell drops below the initial 0 N because the mold closing exerts pressure onto the frame. This drop is rather small compared to the 600 kN clamping force acting on the entire mold. This is in accordance with the design, as most of the force is directed through the main body of the mold outside of the frame system. The forces are negative due to the assembly of the load cell with clamping force. This leads to a negative amplitude for a 'pushing' onto the load cell and a positive excitation for a 'pulling'. The large drop in force signal right after the mold closing indicates the injection of the polymer. This high kink in the force signal matches the expected impact from the polymer melt as it flows right over the measurement cavity. Furthermore, the displacement sensor also shows a small deviation to positive values at the same time. This is a result of elastic deformation of the mold from the acting injection pressure in the cavity. Afterwards, the cooling period starts immediately with no change in the measured signals. This period is followed by the demolding which starts with the mold opening movement. This mold opening was set as slowly as possible to record as much of the demolding of the micro-structures as possible. The set value was 0.1 mm/s which is the lower machine restriction for the mold opening speed. The mold opening step therefore took a little over 30 seconds. To achieve this low speed without unintended acceleration at the beginning of the motion the machine automatically reduced the clamping force of 600 kN very slowly to 0 N before the actual opening motion was beginning. This had no effect on the measurement other than extending the

cooling time, which was taken into consideration (same cooling time for each polymer). These two signals (force and displacement) were recorded for each injection molding cycle simultaneously and are considered one measurement.
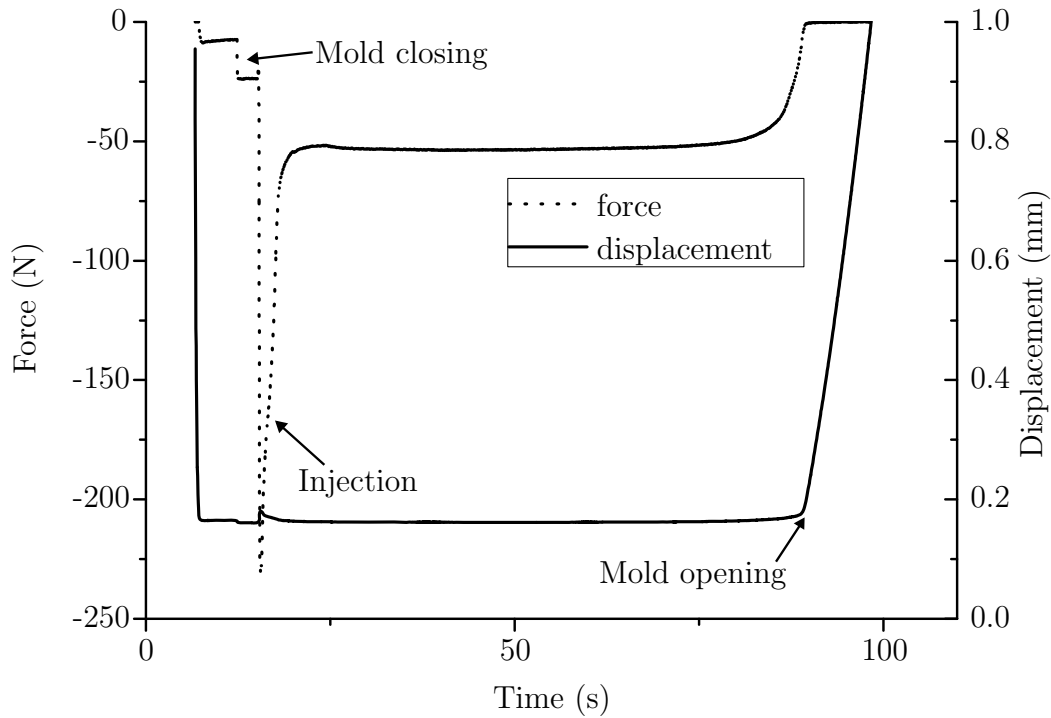

Figure 5.4. Force and displacement signal for one injection molding cycle before modification.

5.7.2 Signal processing

The signal processing is a signal modification that is done exactly the same way for every measurement. This is the preparation of the measured data for further processing. To be able to evaluate either the demolding forces or the demolding energies the signals had to be cut, smoothed and interpolated to achieve that. First the mold opening section of the data was cropped out of the entire signal, discarding the rest of the recorded injection molding cycle. This was the relevant section for evaluation, so extracting it as early as possible sped up all the succeeding calculations on the remaining signal. The data was in this step reduced from the original around 200.000 data points per sensor and measurement to approximately 20.000 points. Subsequently

a smoothing function was used to reduce the noise. A smoothing was chosen as it performed better than the low pass filters it was compared to. The criteria for comparison to low pass filters was the x-position of the signal and a possible shift of the signal. The quality of the noise reduction was only secondary. This was important for the force displacement curves that were integrated later. Both signals were synchronized using the time measurement. This means that even small shifts in the signal could and would influence the calculation of the demolding energy. High pass filters or common averaging functions shift the signal along the x-axis, if only by a little. The small noise that remained after the smoothing was further reduced in the interpolation step that was performed next and ultimately averaged out in the integration step. The applied smoothing is based on Savitzky Golai base polynomials and was used in accordance with similar research done in this area [69]. Using second degree polynomials over a span of 200 points produced sufficiently good results without distorting the original signal. After this noise reduction step the measurements were normalized/standardized for further comparison. This means that the measurements that all had a different number of measurement points had to be tailored to the same length and aligned properly. To achieve that, a custom displacement vector of approximately the length ranging from 0 mm to 0.9 mm with the measurement resolution of 0.001 mm was created. All signals were then interpolated on this displacement vector. This ensured all signals had the same length, the same step size and no redundant information. Figure 5.5 illustrates this mapping process of the measured displacement on the designated displacement vector. For this step the measurement data is interpolated linearly for all data points. After this step the data points are selected from the interpolated signal for each predefined grid point of the custom displacement vector. This step made it possible to make the data handling and presentation time-free. This means that finally the measured force at the same displacement can be compared for all the performed measurements.
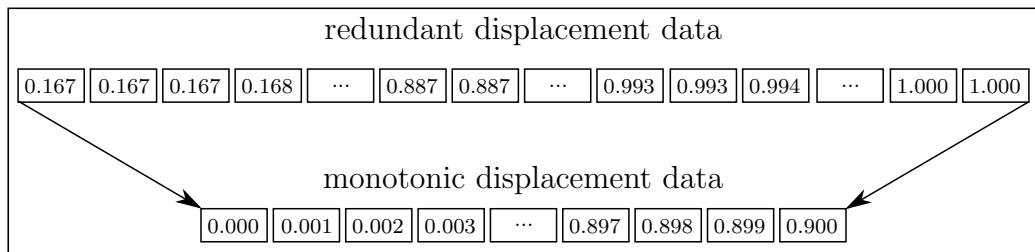

Figure 5.5. Definition for the interpolation vector as a fixed strictly monotonic equally spaced vector.

Figure 5.6 shows a diagram of several measurements for the same setup after the signal processing has been performed. This means the signals have been filtered to reduce the noise, they have been normalized and finally have been synchronized and aligned to start at 0 mm displacement. To zoom in on the relevant section for the measurements this diagram is reduced to the first 0.3 mm of the mold opening. This detailed section was chosen because the measured force reached 0 N approximately after the initial 0.2 mm of mold movement and did not change anymore later on. This means that the demolding is essentially over at this point when the load cell shows the initial load of 0 N - acting force when the mold is open with no strain exerted on the load cell - and there is no more measurable contact of the polymer part and the insert. Figure 5.6 additionally shows 5 repeated measurements with the the same settings. The close up shows that there are indeed sevreal curves that are almost identical (i.e. good reproducibility).
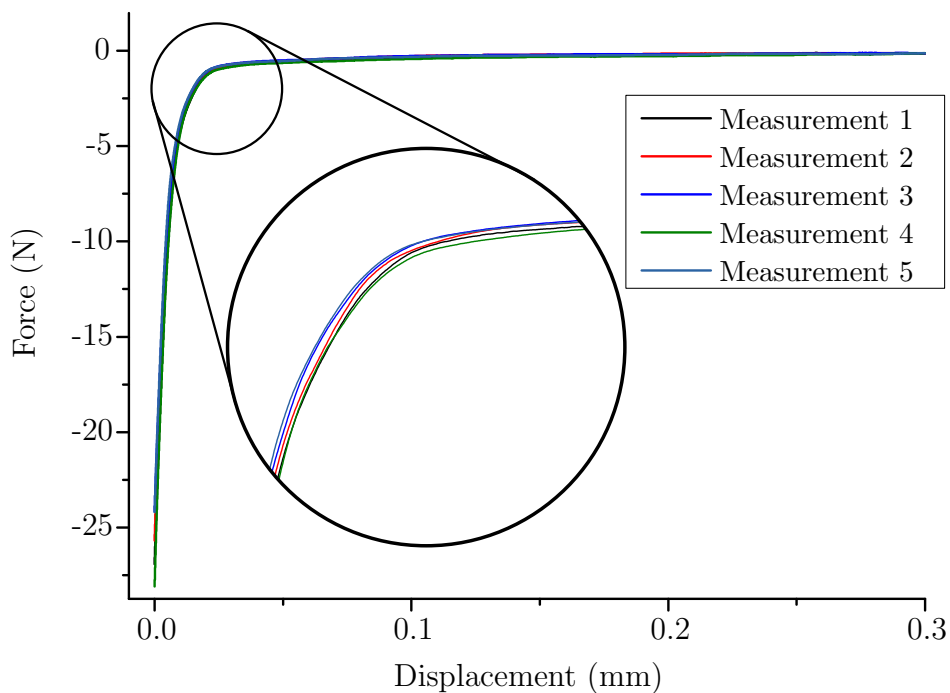

Figure 5.6. Several measurements of the force and displacement signal after smoothing of the data.

5.7.3 Demolding energy

Just as mentioned in literature (compare chapter 3.5 'Demolding force measurement and methods') the initial aim was to use the force-displacement

measurements for evaluation of the polymer part demolding properties. As shown in the previous chapter a force peak indicated the demolding step in several publications. For most of our performed measurements a distinct peak in the demolding force could not be detected. Reasons for this are probably the used polymer materials as well as the micro-structures. Therefore, the evaluation of the demoldability was done with an additional integration step. To make a comparison of the different measurements possible the demolding energy was calculated. The demolding energy in this work is defined as the energy needed to separate the two surfaces, as shown in Equation 5.1, the integral of the force over the displacement.

$$\int_0^E \mathrm{d}E = \int_0^1 F\,\mathrm{d}s, \tag{5.1}$$

Where:

E: Demolding energy.

F: Acting demolding force.

s: Displacement while demolding from 0 mm to 1 mm.

For numerical evaluation the integral becomes a sum leading to Equation 5.2. Making use of the evenly spaced points from the normalized signal after the interpolation makes the integration step straight forward.The implementation was done using the trapezoidal rule for integration as shown in equation 5.3.

$$E = \sum_{s=0}^{1} F\Delta s \tag{5.2}$$

$$\int_a^b f(x)dx = \frac{b-a}{2(N-1)} \sum_{n=1}^{N-1} (f(x_{n-1}) + f(x_n)) \tag{5.3}$$
$$= \frac{b-a}{2(N-1)}[f(x_1) + 2f(x_2) + \cdots + 2f(x_{N-1}) + f(x_N)]$$

Where:

$f(x)$:   represents the function to be integrated.

a, b: Integration boundaries.
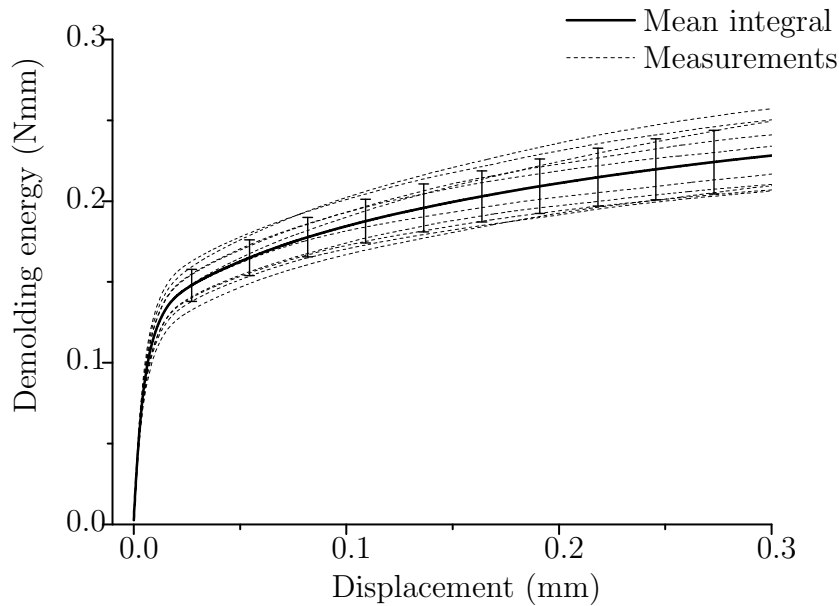
N: Number of measured points.

Figure 5.7. Demolding energy calculated for ten measurements including mean and standard deviation.

Figure 5.7 shows the integration result for one arbitrarily selected setting with repeated measurements. Usually 10 measurements were performed for each tested configuration. Each signal was then evaluated as explained in this chapter to get the demolding energy. Finally a mean curve and its standard deviation was calculated for these 10 curves per setup. This mean integral is then used for further evaluation and comparison of different configurations. After reducing 10 measurements to one energy curve one value on this curve had to be selected as a representing energy value. This is necessary because the comparison of different curves is nearly unmanageable. To easier see the differences between the measurements the energy was evaluated at 0.1 mm displacement. This is an empirical point that shows the differences in energy best for the tested setups. Additionally, the value was chosen high enough to ensure that the demolding step has already finished. Figure 5.8 illustrates this evaluation at 0.1 mm for some example measurements. In this example it portrays the resulting integral curves and the standard deviation for some randomly chosen setups. The resulting bar diagram for the single values shows the respective demolding energy at the evaluation point. This diagram makes a comparison of the demoldability for a large number of parameters possible. Therefore, these diagrams will be used for comparison of the demolding measurements for all the investigated areas.
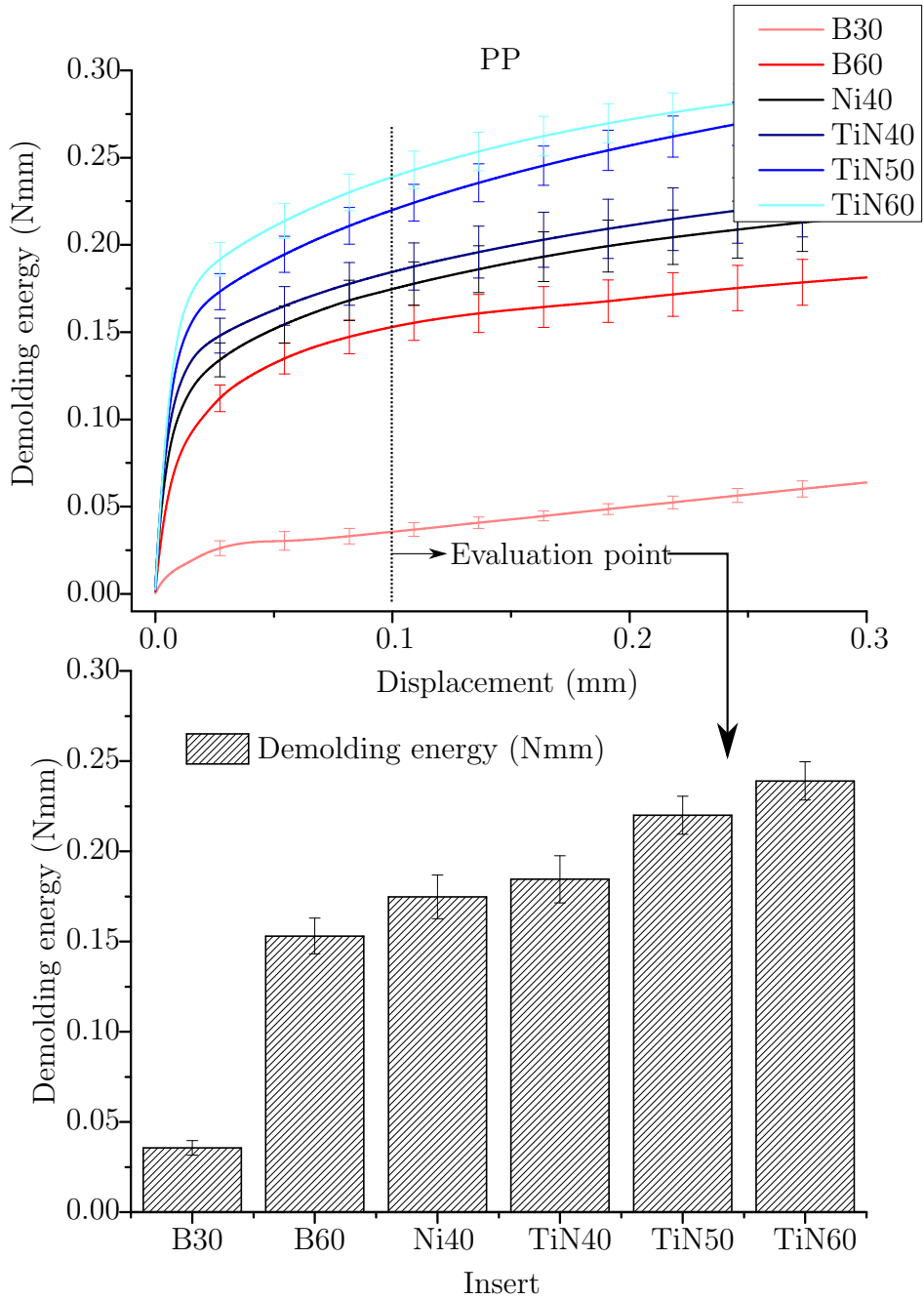
Figure 5.8. Top: Integral mean curves for different micro-structures, temperatures and coatings.
Bottom: The resulting bar charts and the demolding energy with the standard deviation at the evaluation point.

5.8 Overview over the experiments

All of the planned experiments were focused around the investigation of the four influencing factors. Therefore, several of the experiments include more than one influencing factor. For the evaluation of the results and a clear attribution to these defined factors, the experiments were summarized into four studies for better understanding. Table 5.11 shows four the studies and the parameter that were varied in it. The first study targets the material where all the used polymers for selected micro-structures and constant processing parameters are summarized. The second study, the design, focuses exclusively on two different structure types (i.e. Perflow and Inflow) and their respective placement. The third study, the mold, is an investigation that sums up all the used coatings for the Normal and the MedAp stamper. Finally, the different processing conditions are illuminated for COP, TPE and both of their blends for the fourth study.

Table 5.11. Summary of the performed studies to display all the influencing factors efficiently.

Study	Investigated influencing factor	Variable setting
Study 1	Polymer	PP, PMMA, COP, TPE and two COP-TPE blends
Study 2	Design of the micro-structure	Perflow and Inflow chip in two configurations: Close to the injection gate and far from the injection gate
Study 3	Mold unit	Different coatings for the Normal and the MedAp chip
Study 4	Processing conditions	Different mold temperatures for each material and the variothermal processing

For these four studies the following hypotheses were formed:

- *Study 1*: Confirmation of different polymer demolding behaviors. This includes the influence of the polymer stiffness: higher stiffness should lead to a higher demolding energy which means a worse demoldability. Blending TPE to COP is therefore expected to reduce the demolding energy just by lowering the polymer stiffness. Special attention here

is on different friction and adhesion behaviors that are completely un-known so far (sticking of TPE).

- *Study 2*: It is expected that structures perpendicular to the flow direction are harder to demold than structures in flow direction. Furthermore, placement close to the gate is expected to produce lower demolding energies than placement far from the gate. Additionally, this effect should be independent of the selected polymer.

- *Study 3*: The coating materials with lower surface energy are expected to improve the demoldability. Additionally, it is expected that polymers depending on their polar and disperse makeup will behave differently with the same coating. This relation is also expected to be temperature dependent as adhesion properties change especially with the polymer temperature.

- *Study 4*: For this study at first the influence of the variotherm system has to be confirmed. For the use of the variotherm system a higher demolding energy and a worse demoldability is expected. The other important parameter in this study is the mold temperature as it changes several parameters like shrinkage or the polymer stiffness. Therefore clear predictions are nearly impossible. Nevertheless, a similar behavior as for hot embossing, a parabolic dependance with an optimal demolding temperature, is expected.

Chapter 6

Results

6.1 Polymer

The processing parameters for this comparison were selected polymer specifically. This section will not go into the process effects as further influences of the process are discussed in section 6.4 'Process'. The selected processing parameters for the result comparison is shown in Table 6.1.

Table 6.1. The selected melt and mold temperature for the result comparison of the polymers.

	PP	PMMA	COP	TPE	Blends
Melt temperature (°C)	240	270	260	260	260
Mold temperature (°C)	40	80	70	60	60

The polymer plays a major role for the demolding behavior and changes the interactions of all the succeeding factors. This is the main reason it is investigated first. Additionally, the polymer will be discussed again to some degree in each of the following chapters to point out the different natures of the selected polymers for the other investigated settings.

Before specific effects can be discussed further, the general impact of the polymer is illustrated by using a cross section of the results for illustrative purposes. This cross section was chosen to give a broad overview over a variety of different influencing factors. This includes first and foremost the results for all the different tested polymers and polymer blends that where used for the experiments. Additionally, this cross section is comprised of three stampers that have been selected to improve clarity. Two stampers with

the normal structure were selected: One uncoated stamper and one coated with TiN. The third stamper included is the MedAp application stamper.

This cross section contains a lot of different information and is therefore split into three parts. The first is a close up of the used polymers, the second part focuses on the change in demolding behavior of the blends. The last part is a general overview of these settings focusing on some additional interactions. Figure 6.1 shows the polymer behavior for the three selected stampers. The left most illustration for Nickel (a) shows that the differences between the polymers are less then expected. Especially the fact that PMMA (the material with the most demolding problems) is on the same level as PP is surprising. Another surprise is that COP shows a very low demolding energy. This behavior is exactly the same for the TiN with only a slight difference for PMMA, which is lower in this case (b). This shows that PMMA is the only polymer that is affected by this parameter change. This would indicate that the differences between polymers are not that large and only occur for special combinations (PMMA and TiN). Configuration (c) shows how important the polymer selection is after all. With the MedAp stamper PP becomes the material with the lowest demolding energy while COP and TPE increase drastically compared to the two previous settings. The reason for this change is most likely caused by two different factors. First is the fact that the Normal and the TiN setup only cover a small portion of the surfaces leaving a large portion of steel as contact area. This is an explanation why there is almost no change between (a) and (b). The second factor is the different nature of the MedAp surface. This explains why the behavior of COP and TPE changes so drastically when in contact with the MedAp stamper. Both materials show different adhesion when in contact with a polished Nickel surfaces.
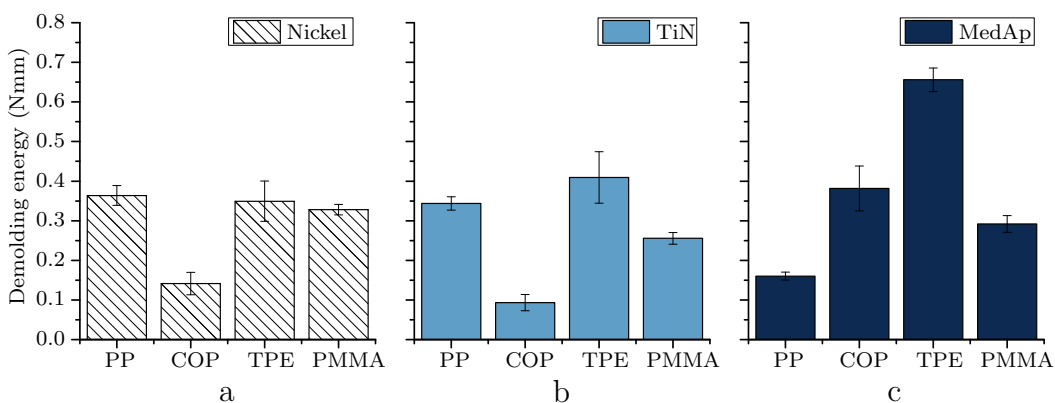

Figure 6.1. Comparison of the demolding energy of the different used standard polymers.

For a better investigation of the interaction behavior (e.g. adhesion) the focus in Figure 6.2 is on the transition from COP to TPE. The expectation is that there is a trend with higher TPE concentration coming from the COP with the lower demolding energy to TPE with the higher demolding energy. If adhesion is the only factor affecting the demolding energy a linear correlation should be observed. In Figure 6.2 (a) the big influence of the added TPE, but no linear content specific behavior can be seen. Adding 10 % or 40 % TPE does not produce a measurable change in this setup. It is still surprising that only a small TPE concentration can effect the behavior in this way. Figure 6.2 (b) shows an even more interesting behavior and gives a possible explanation for this behavior. Adding TPE increases the demolding energy as expected, but adding 40 % TPE to COP produces higher demolding energies than TPE alone. This can be explained by a combination of the adhesive property change of the material (in this case TiN) with a simultaneous stiffness change. Adding TPE changes the adhesive properties increasing stiction to the surface (higher for TiN than for Nickel). At the same time the stiffness of the polymer blend decreases with increasing TPE content. With low TPE (i.e. 10 %) concentrations the influence of the additional adhesion is higher than the drop in the polymer stiffness in Figure 6.2 (b). This could not only explain the high demolding energy for COP40 but also the interaction seen in Figure 6.2 (a) and (c). In the right most diagram (c, MedAp) a similar behavior as with the Nickel stamper can be observed. In this case it is most likely that the adhesion behavior for these two surfaces (Nickel and MedAp) and TPE are different, yielding generally lower demolding energies for COP-TPE blends.
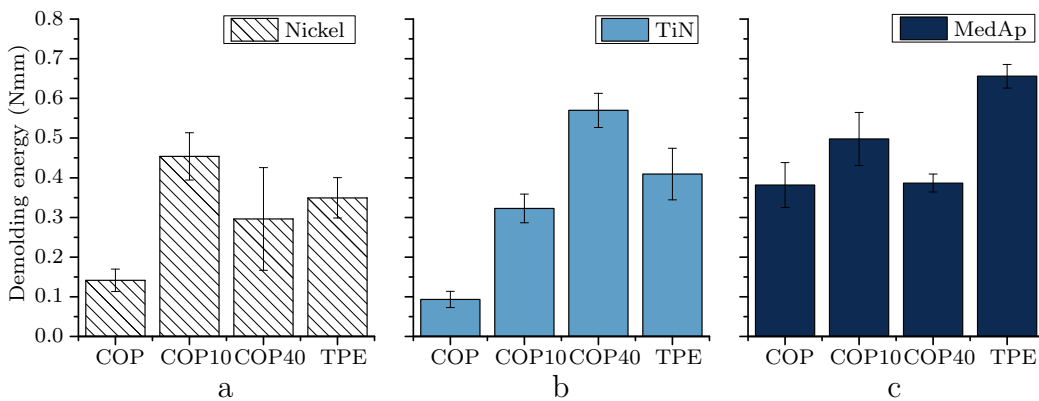

Figure 6.2. Comparison of the demolding energy for COP, TPE and the two blended materials.

To summarize the polymer behavior all of the previously discussed demolding energies are shown in one diagram to point out some additional effects. This can be seen in Figure 6.3 that shows the demolding energy for the four discussed polymers and two blends (COP10 and COP40). In this diagram it is even more clear that no polymer significantly exceeds the others in regard to the demolding energy. This was unexpected as polymers like PMMA that generally have a worse demoldability were expected to yield higher values for the demolding energy. PMMA is a special case that exhibits a unique (stiff) demolding behavior resulting in a systematic underestimation of the demolding energy. This effect will be discussed in a separate chapter especially targeting PMMA (compare Chapter 6.5 'Demolding behavior of PMMA'). The second assumption was that independent from the polymer the structural density or complexity will show similar trends. This means that a more complex geometry should yield higher demolding energies than less complex ones (complexity in this case refers to higher aspect ratios, more structures, a larger structured area and or smaller structures). This was not the case as measurements in Figure 6.3 show. For the most complex structure, the MedAp application, the measured demolding energies are very dependent on the polymer. For COP or TPE as expected the demolding energies are higher for the MedAp stamper than for the Nickel or TiN configuration. The same trend cannot be observed for PP, which shows very low demolding energies for MedAP compared to the Normal or TiN stamper. There are two effects that are most likely responsible for this behavior. First is the surface finish of the MedAp, and second is the adhesion and therefore interaction of PP with this surface. The surface of the MedAp is very smooth (polished) due to the manufacturing method. While the Inflow and Perflow stamper have the same surface, all the Normal structures (this includes the coated Normal structures) have a higher surface roughness. The reason is that the latter stampers have been manufactured with 3 mm thickness (and not 1 mm) which affected the surface roughness in the plating process. For PP the role of the surface finish seems to exceed the one of the structure. All other polymers show the expected correlation, i.e. higher demolding energies with a higher structure complexity.

The interaction of the different polymers with the stamper coatings could not be deduced from these measurements. The polymers were expected to influence the demolding step differently depending on the coating it was paired with, but neither the magnitude nor the interaction with different coatings was clear. Only an individual investigation of the surface coating / polymer combination can show how the process step is actually affected. Figure 6.3 shows perfectly why predictions regarding the polymer influence are almost impossible and have to be studied case by case. This can be
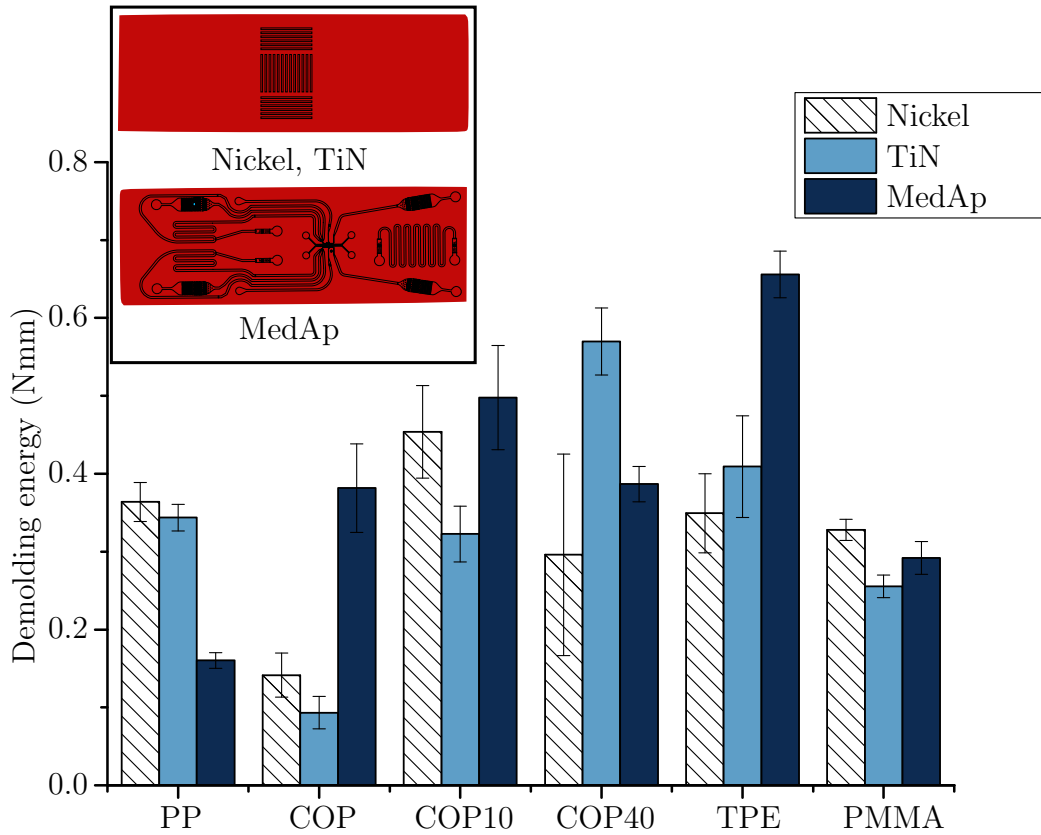
Figure 6.3. Comparison of different polymers and blends for three selected
stampers.

seen as the effect of the polymer varies greatly in combination with the
TiN coating. While PP and TPE do not seem to interact with TiN, the
demoldability improves for COP, COP10 and PMMA. The COP40 blend on
the other hand produces an even worse demolding energy in combination
with TiN.

The main insight is that different polymers depending on their properties
might exhibit a completely different demolding behavior. Different adhesion
properties might work with some structures and roughnesses but not others.
Going even further some coatings that work well for a given polymer might
have an adverse effect for another. Additionally, the polymer or polymer
blend will change the operating point. This means that blending polymers
or the use of additives can have unexpected influences (e.g. deformation of
the part due to the lower stiffness) on the demoldability of the part. The
extent of these effects will be discussed further in the following sections that
address these parameters in detail.

6.2 Design of the micro-structure

Right after the polymer choice the micro-structure itself is an important factor deciding the demolding force. The most obvious assumption that 'more' structures (higher complexity) will negatively affect the demolding energy already does not hold true for all polymers. Additionally, the structure can interact with the mold in different ways depending on its placement. The acting mechanisms have already been discussed (compare Chapter 3.1 Demolding mechanisms), the implications are further discussed in Chapter 3.4.2 'Design of a micro-structure'. Making these effects visible and looking into polymer specific behavior is the main goal of the micro-structure investigation. Figure 6.4 shows the key results of the measurements regarding the structure placement investigation. PP and COP were selected because they show important differences that can occur between polymers. PMMA will again be discussed in a separate section due to measurement difficulties.

PP behaves just as literature predicts. Channels in flow direction yield a lower demolding energy than structures perpendicular to the flow direction. This effect was shown in Figure 3.13 in chapter 3.4.2 Design of a micro-structure. The micro-structures shrink towards the injection gate. This leads to a higher stress level at the bottom of the micro-structure. Perpendicularly placed micro-structures will exert a force over the whole sidewall of the structure leading to higher friction forces. Structures in flow direction will not be affected by shrinkage in the same magnitude, resulting in a lower surface area that is under the influence of friction.

The next step is the placement of the structure relative to the injection gate. This changes the demolding behavior (especially for COP) and also the shrinkage potential. The higher shrinkage, that occurs far from the injection gate, will therefore lead to a worse demolding of the part. This behavior is reflected in Figure 6.4 for PP as the demolding energy rises for both types of structures when placed farther from the gate.

These mechanisms are different for COP. The Perflow structure behaves as expected yielding higher demolding energies when placed far from the gate. The Inflow stamper however behaves unexpectedly and not according to predictions. First, the demolding energy for the Inflow structure is higher than the one of the Perflow when placed near the injection gate. And secondly, the demolding energy of the Inflow stamper does not change or even decreases a little when the structure is placed far from the gate. The reason for this effect is most likely a different separation of the polymer part and the structured surface in the demolding step. Usually for evenly distributed structures or structures at the center of the chip, the separation takes places in one step, also referred to as parallel demolding. But as described in
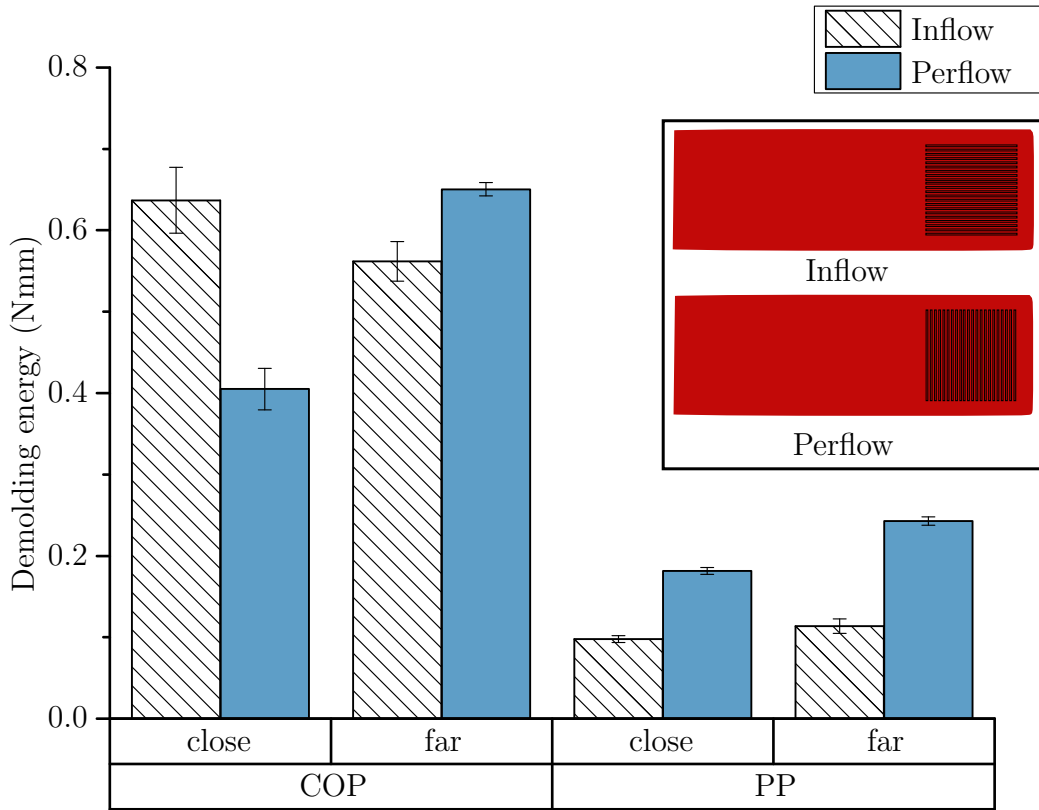
Figure 6.4. Demolding energy of COP and PP as a function of structure orientation (Inflow and Perflow) and placement (close and far from gate)

chapter 3.1 D'emolding mechanisms', mechanism c) detaching, segments of the polymer chip will stick to the structured surface while others will demold. This can lead to two different effects. Figure 6.5 shows what can happen for the placement of the structure close to the gate. Since the demolding is mainly guided through the sprue, as a design necessity in this setup, the demolding will start near the gate. If the structure is also placed close to the gate, it will demold immediately, slightly skewing the polymer part in the direction of the structure (Figure 6.5 from state 1 to state 2) . This effect will be reduced if the structures are placed in flow direction.

This effect changes drastically when the structure is placed far from the gate. Figure 6.6 shows what can happen in this setup. In this setup the structures demolds only after the rest of the polymer part has already detached from the mold. Depending on the micro structure this will lead to either deformation 2a or 2b as shown in Figure 6.6. If the structure is placed in flow direction it will peel off of the stamper along the micro channels lead-
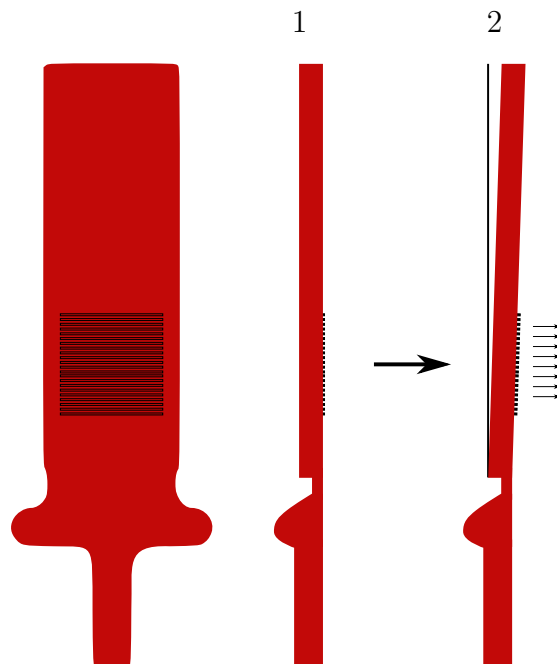
Figure 6.5. Part deformation for the 'close' structure placement.

ing to 2a, a slightly bent polymer part. In case of structures perpendicular to the flow direction the force needed to demold is higher. This delays the demolding of the micro-structures leading to an 'S-shape' deformation of the polymer part. This leads to the effects observed for COP but not for PP.

There are two criteria that have to be met for this effect to become relevant for the measurements. First the demolding energy has to be high enough, indicating that sticking is more likely to occur, and secondly the polymer stiffness which is counteracting this deformation. PP therefore does not show this deformation behavior due to the good demoldability. COP on the other hand yields generally higher demolding energies leading to the described demolding effects. In case of the COP the deformation is very small and can only be seen due to the fact that the demolding energy of the Inflow stamper is independent of the structure placement (i.e. far or close to the gate). The effect becomes more apparent for both CO-TPE blends due to the drop of the stiffness of the blend. This leads to visible deformations to a degree that the demolding energy measurement cannot be performed as the demolding occurs over a displacement of more than 1 mm which is outside the measurement range of this setup.
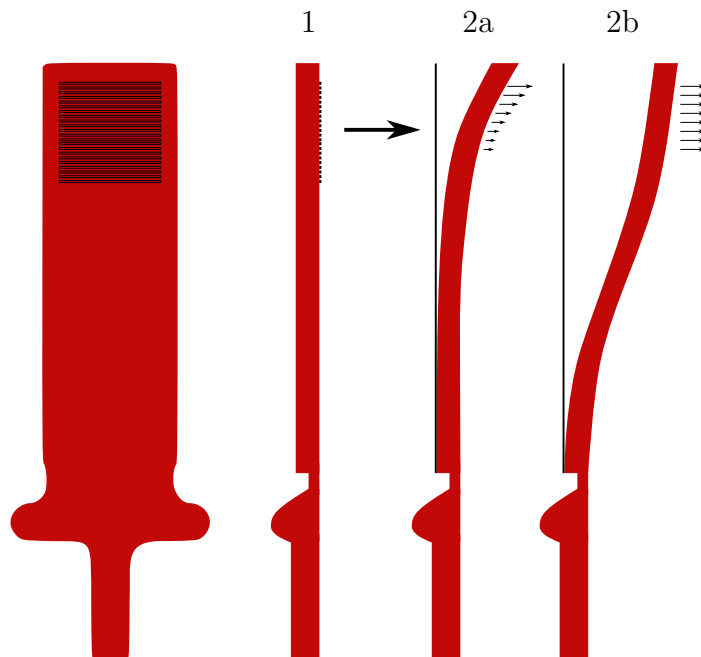
Figure 6.6. Part deformation for the 'far' structure placement.

6.3 Mold

The results of the mold investigation, i.e. the investigation of the mold coating, is divided into three parts. The first section addresses the initial coating tests performed on the Normal substrate. The second part focuses on the MedAp medical application and its performance using different coatings. The last section will outline the correlation of the measured contact angles and the demolding energy measurements.

6.3.1 Screening of different coatings on the Normal substrate

The first step was the general screening of different contractors, different coatings and different coating process settings. Secondly, these findings were transferred to the MedAp application for further investigation. Figure 6.7 shows the impact of the different coatings for three different polymers performed with the Normal test structure. It is to note that as expected for this setup the PMMA shows the highest demolding energy values, while PP shows the lowest. While COP is set between these two polymers the standard deviation for this measurements is abnormally high (over 20 %). After the evaluation for COP was completed and those deviations became obvious

the process setup was investigated. The reason was an error in the holding pressure settings after an obligatory fill study for the process setup. Despite the fact that those values cannot be distinguished reliably it revealed different information in the process. It shows that the holding pressure affects the reproducibility of the injection molding process (e.g. the part thickness) while the replication quality remains unchanged. This means that a process that can replicate the micro-structures is not necessarily a stable process.
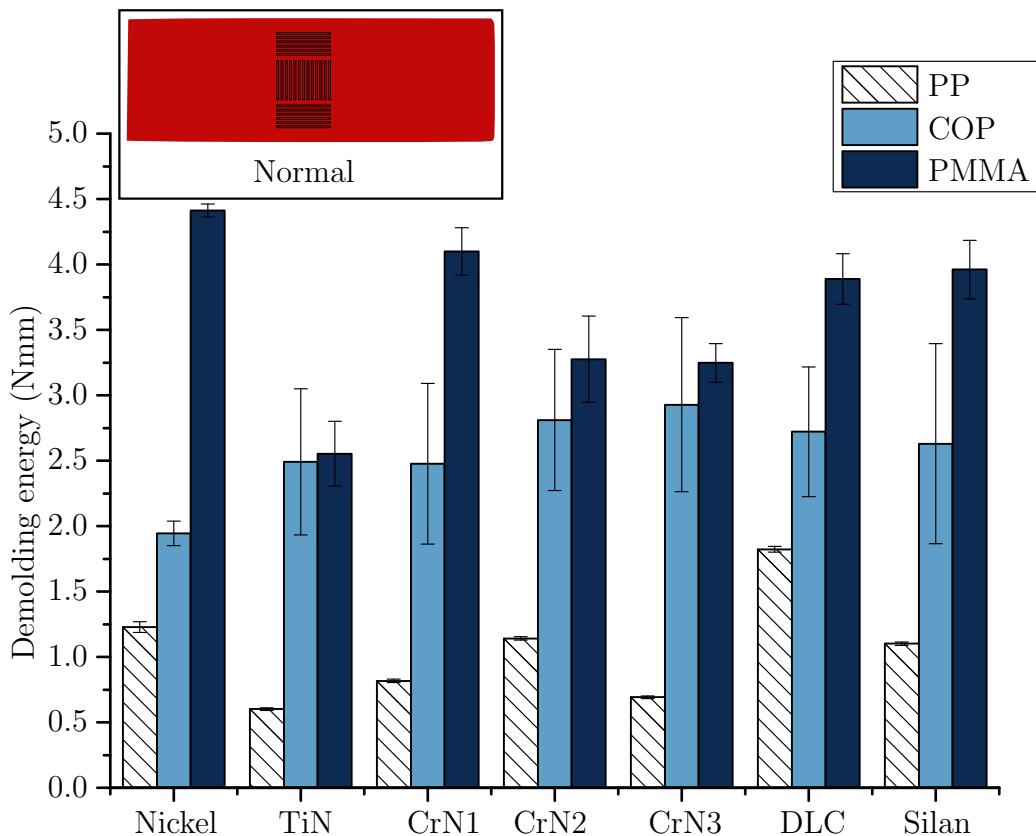

Figure 6.7. The impact of different coatings on the Normal stamper on the demolding energy for the used polymers.

The picture looks completely different for PP and PMMA. While PMMA also has a higher deviation than PP in the measurements it can still be evaluated. The figure shows that any coating for PMMA will at least perform as well as the nickel stamper, while most of them actually improve the demoldability. Especially the TiN coating shows very low demolding energies. For PP the distinctions of the demolding energy between the different used coatings are even clearer. For DLC the demoldabiliy clearly falls off, while the chrome based coatings and the TiN seem to improve it. Additionally, there

are not only differences between the CrN coatings but also in the behavior between the PMMA and the PP. For PP the demolding energy increases from CrN1 to CrN2 while it drops for PMMA. While the differences for the CrN coatings were unexpected, the difference between PP and PMMA is clearly related to the polymer properties. Finally the silane based coating shows little effect for any of the polymers. This was also unexpected because the low surface energy suggested a low demolding energy as well. This is probably a result of the low stability of the wet chemical silane based coating. This was confirmed later as contact angle measurements showed that the coating was spoiled after the few performed shots in the injection molding machine.

6.3.2   MedAp case study

After these initial tests the coatings for the second study were selected. Figure 6.8 shows the measurements for the MedAp with the selected coatings. PMMA is not included in this diagram because of several manufacturing issues (e.g. breaking of the part) but is discussed separately in chapter 6.5. The most interesting finding is that the uncoated stamper performs best for PP. This is unlike what was expected from previous measurements. The reason for this is most likely the significantly lower roughness of the MedAp compared to the Normal test chip as explained in the previous polymer result chapter (Chapter 6.1). The effect is the complete opposite for COP. The very smooth and uncoated nickel surface yields the highest demolding energies while all the coatings perform better. While part of the improvement has most likely to do with a change in surface roughness, the coatings themselves show differences as well. Most notably TiN shows a very low demolding energy.

Additionally, the durability of the coatings is an important issue. Just like the silane coating, the other coatings were also observed for deterioration over time. Especially on the smooth surface of the MedAp the stiction of the coating is limited. This could be observed very well for the WC/C and MoS$_2$ coating. WC/C showed some minor defects (i.e. cracks in the coating and visual spots) after the first 50 shots. MoS$_2$ on the other hand showed major delamination over large areas of the stamper after the first 50 shots making the coating useless. All the other coatings showed no sign of deterioration even after several 100 injection shots.
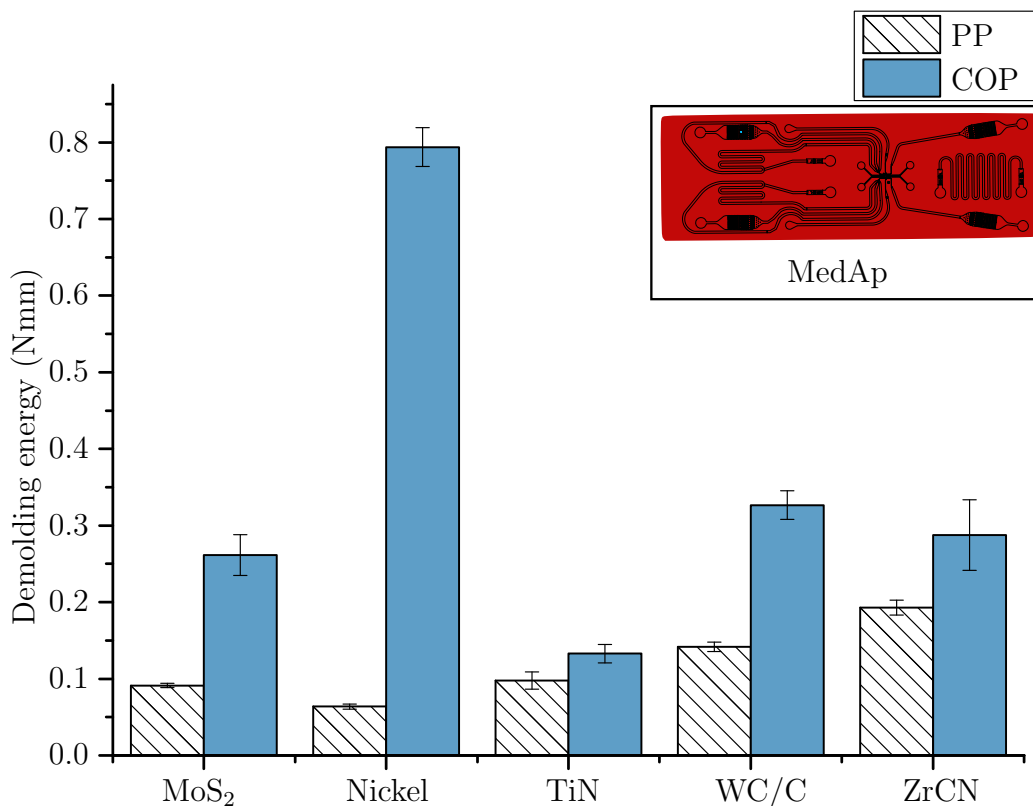
Figure 6.8. Coating influence on an established medical applications.

6.3.3 Contact angle correlation

The optimal outcome of the contact angle study would be a model that could predict the performance of a coating based on a contact angle measurement which would prevent expensive experimental effort. Coatings have many different properties that define the interaction with the polymer. Therefore, the first attempt was to correlate the performance of individual coatings to their contact angle. For this the measured contact angles (compare Figure 5.2) were used for a correlation test with the measured demolding energies. To test for a linear dependence a Pearson product - a moment correlation coefficient - was calculated. This correlation was calculated for PMMA and PP with the measured contact angles. The polar contact angle measured with water, the disperse contact angle measured with diiodo-methane and a virtual total contact angle to test for a correlation that depends on both the polar and the disperse component. The result is shown in Figure 6.9 and Figure 6.10 with the confidence ellipse for the calculation. The correlation coefficients are shown in Table 6.2.
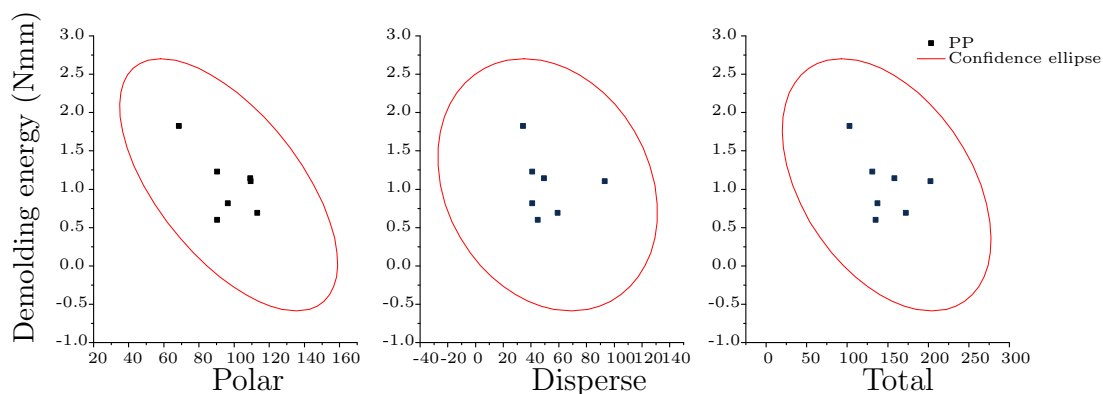
Figure 6.9. Pearson correlation of the demolding energy for PP with the contact angles of the respective coating.
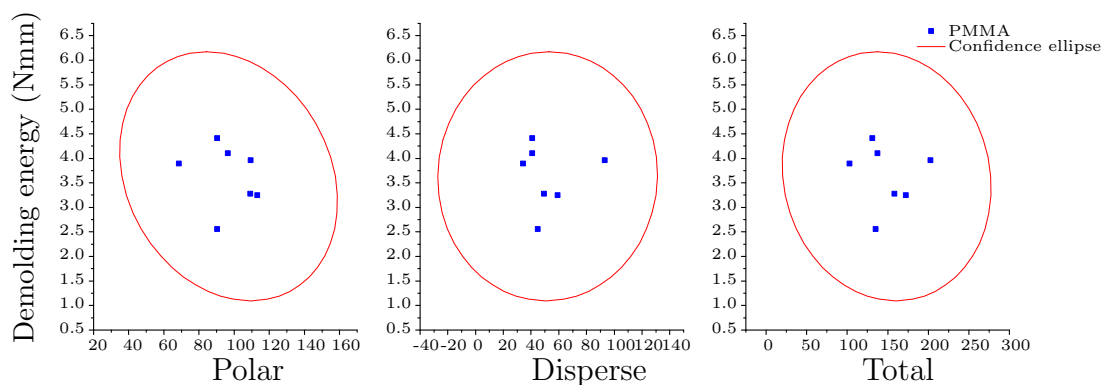

Figure 6.10. Pearson correlation of the demolding energiy for PMMA with the contact angles of the respective coating.

For PP the linear trends are negative indicating a declining linear trend. This could indicate that lower surface energies might improve the demolding energy for PP. Additionally, the trend is stronger for the polar contact angle than the others. PMMA shows a much lower correlation. For the disperse contact angles, the trend seems to reverse the direction, but the correlation is the lowest one that was calculated. Overall, correlations below ± 0.6 are ignored in all scientific areas. Other scientific areas are split into those with precise measurements (e.g. sensor measurements) and non-precise measurements (e.g. surveys). With precise measurements the calculated correlations should be at least over ± 0.8 for a statistically significant correlation [12,82]. This means, that for the tested combination no significant trend could be observed. Still the correlation shows, that there is a small likelihood that the

trend is negative (lower surface energies lead to lower demolding energy) if present at all.

Table 6.2. Pearson correlation coefficient between the different contact angles of the coatings and the demolding energies for PP and PMMA

	Polar	Disperse	Total
PP	-0.62249	-0.21608	-0.43252
PMMA	-0.20302	0.01288	-0.08983

6.4   Process

The last influencing factor to affect the demoldability of the polymer part is the injection molding process. The results are divided in the two different investigated parameters: First the analysis of the variotherm heating system and then the investigation of the mold temperature for different materials.

6.4.1   Influence of the variotherm system

All the measurements were executed with and without the use of the variotherm system. This was done for all possible setups with a few exceptions. In some cases the use of the variotherm system affected the demoldability to the degree where no demolding was possible at all (i.e. breaking of the part). This is in accordance with literature, as the use of higher temperatures for the molding of the micros-structures generally reduces the demoldability of the part. The trend in the demolding energy is the same for both process setups. This is not only true for different temperatures, but also for all the used polymers and the used coatings. This is the reason why the results are always shown for the injection molding setup without the variotherm system. This way all the tested configurations can be compared and investigated for the effect of the influencing parameter without the need to regard the in-mold heating specifically. It is important to note, that contrary to the expectation, demolding energies with the variotherm heating were lower than without using additional heating. This effect can be seen in Figure 6.11.

The reason why the demolding energy is underestimated for variothermal use can be seen in Figure 6.12. It shows a comparison of the force signal
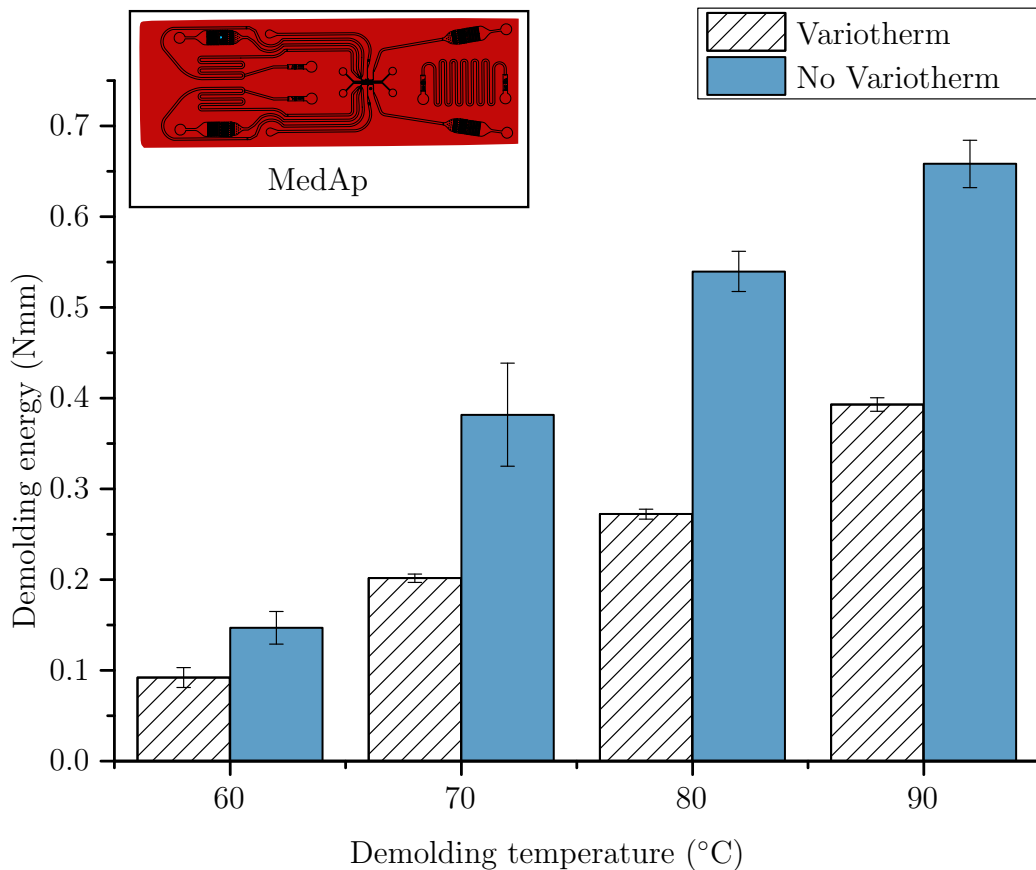
Figure 6.11. Influence of the demolding temperature on the demolding energy of COP with and without variotherm process.

over time for two identical processes, where one is making use of the variotherm system and the other is not. As explained in chapter 4.3 'Mold unit design', the load cell is preloaded to measure forces for tension and compression. Additionally, the load cell is placed directly behind the variotherm heating system. The heating in the injection molding cycle inadvertently led to the expansion of the heated steel parts of the mold. This additional stress was detected and can be seen in the force measurement as the temperature induced force. The process was designed to end at the same mold temperature after each cycle regardless whether variotherm was used or not. This can be seen as both force signals have the same level just before the demolding starts, indicating that the temperature stresses have vanished. Unfortunately, there is still a small draft in the recorded force signal leading to a small tilt and a slightly lower level after the demolding, when variotherm is on. This was corrected mathematically, to improve the evaluation of the

signal. This correction led to the lower calculated demolding energies when using the variotherm system.

Despite the fact that a direct comparison of the measurements with and without the variotherm system is not possible at all, the conclusions regarding the influencing factors are not affected by this systematic measurement error. This is the case because the overall trends are the same with and without the variotherm system.
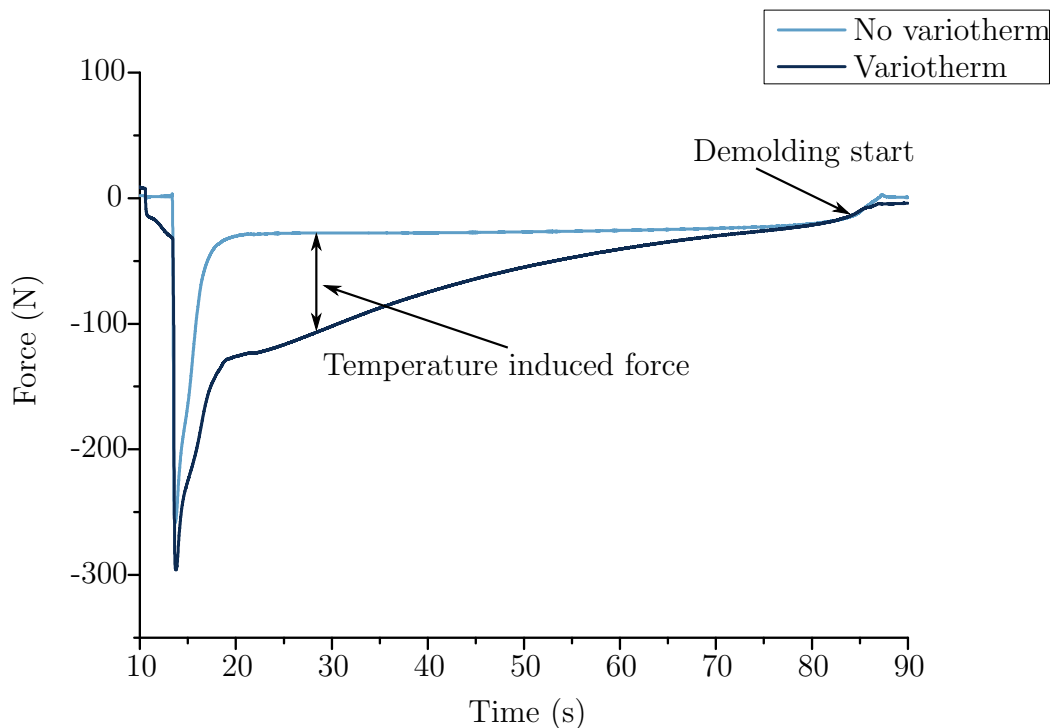

Figure 6.12. Influence of the variotherm system on the demolding force measurement.

6.4.2 Influence of the demolding temperature

The demolding parameters that is studied most is the demolding temperature. It not only influences the shrinkage, thermal expansion or contraction, but also the stiffness of the polymer right when it is demolded (compare Chapter 3.4.4). Since the demolding temperature cannot be controlled directly the mold temperature was varied instead for the investigation. To better illustrate the interaction of the material and the used temperatures a special focus is on the evaluation of the COP, the TPE and its blends. This ensures not only the best overlapping of the chosen demolding temperatures for all

configurations, but also discloses the influences of adhesion and elasticity due to the nature of the blends. Figure 6.13 shows the behavior of pure COP and TPE materials in the mold temperature range where the manufacturing of the polymer part was possible. TPE needs lower mold temperatures than COP for a successful manufacturing process. Despite the different processing ranges, the same effect can be observed for both polymers. As the mold temperature rises, the demolding energy rises accordingly.
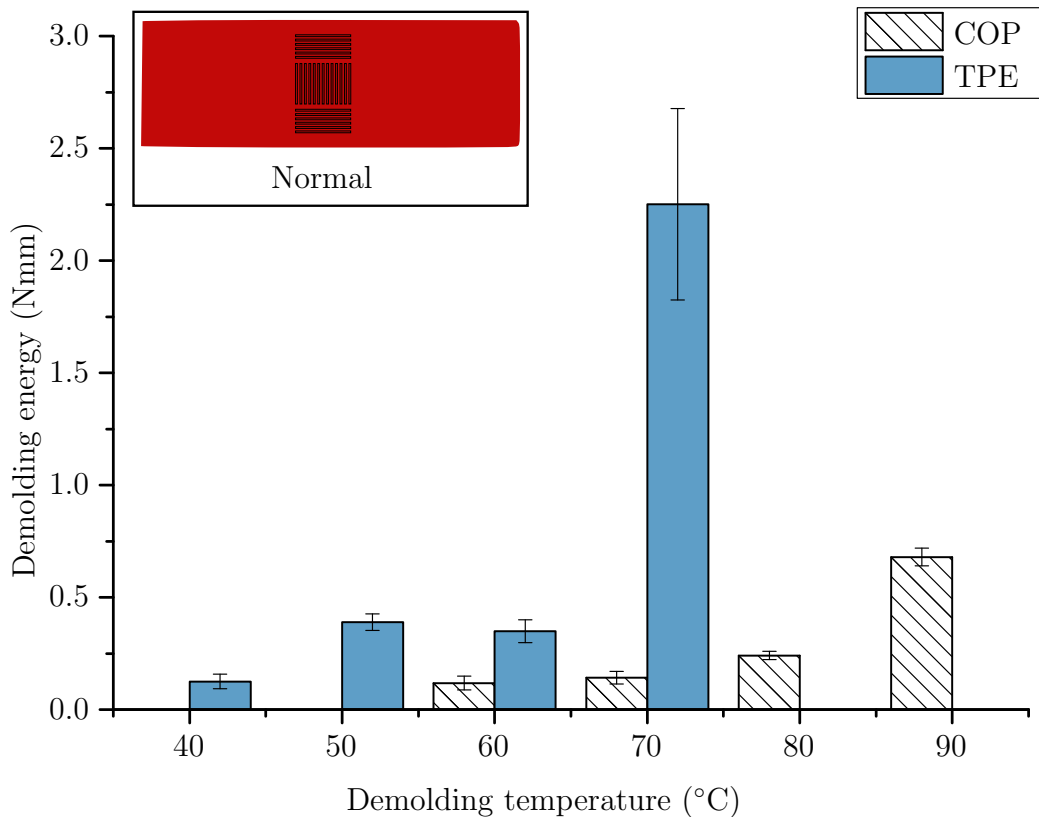
Figure 6.13. Demolding energies of COP and TPE at different mold temperatures.

The main difference in the material behavior is that the demolding energy for TPE rises in a steeper way. While the material stiffness changes little for TPE in this processing setup, the adhesion increases. This effect occurs until the demolding energy skyrockets as the 'sticky' TPE is peeled off of the stamper. This happened at temperatures above 70 °C where the measurement was not reproducible any longer. This can also be seen as the standard deviation goes up significantly for the measurement at 70 °C. This effect is different for COP. While the demolding energy also rises with

higher temperature the manufacturing was limited by the mold tempering to 90 °C. Generally higher temperatures support the peeling effect, which also increases the demolding energy. Lower temperatures on the other hand will lead to breaking of the part, as the stiffness of COP, as well as the stresses increase drastically in this area.

Figure 6.14 shows the behavior of the two blends. Both blends could be manufactured for the whole temperature range (i.e. COP and TPE temperature combined). The materials show some new properties depending on which polymer effects are dominant in the given temperature range.
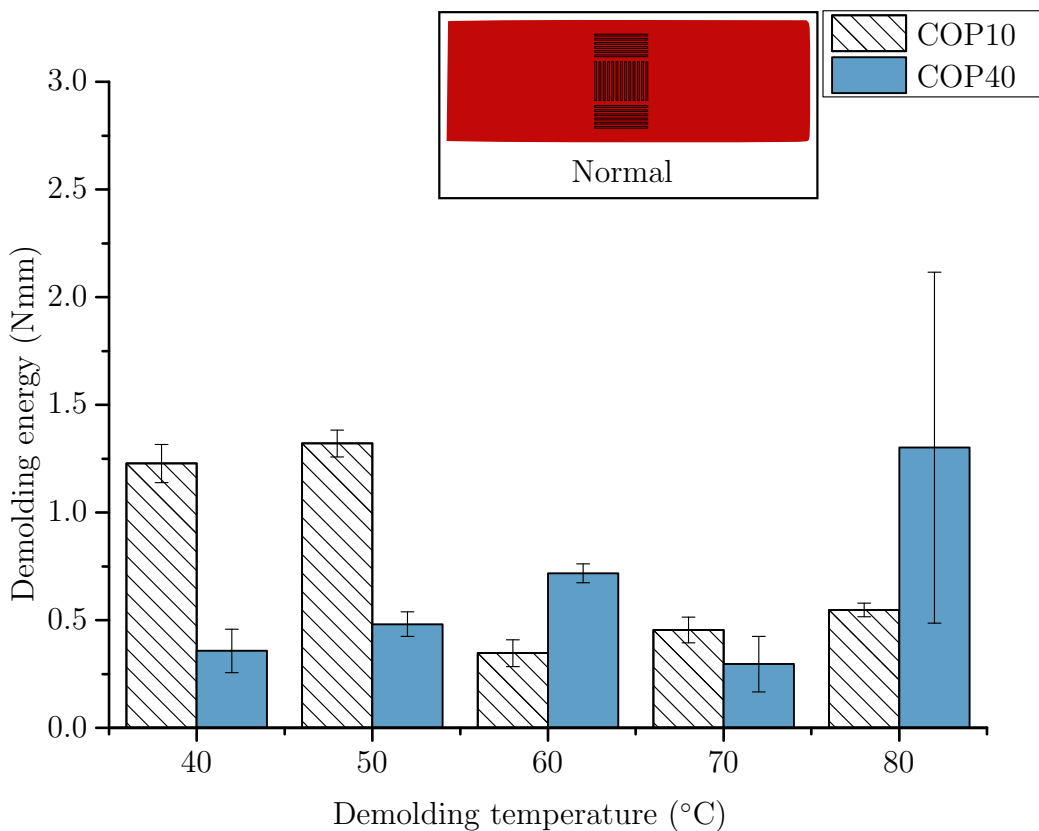
Figure 6.14. Demolding energies of the two blends, COP with 10 wt% and 40 wt% TPE, at different mold temperatures.

Despite that, both blends showed similar behavior. The most interesting aspect to note is that the demolding energy rises towards lower temperatures. Especially the material with 10 wt% shows a significant increase at 40 and 50 °C.The COP could not be manufactured at this temperature, but the addition of TPE with a very low stiffness made the manufacturing possible. The higher demolding energies are a result of the additional adhesion from

the TPE component and the effect is increased due to the high stiffness of COP. This hypothesis is strengthened by the behavior of the 40 wt% blend. Due to the high TPE concentration the increase of the demolding energy also takes place at higher temperatures (at 60 °C). Additionally, the material is softened up by the TPE to the degree where the overall level of the demolding energy drops in that temperature range. At higher temperatures the effect of TPE becomes dominant again. This can be seen for the blend with the higher TPE concentration, as the overall measured demolding energy as well as its standard deviation go up. This trend continues for a mold temperature of 90 °C, with even higher values and deviations that range outside of the normal demolding energy measurements.

6.5   Demolding behavior of PMMA

As mentioned in several of the previous chapters PMMA needs additional focus, as it does not always behave as the other materials. There are two issues that prevent a meaningful comparison of the PMMA values with the other polymers. The first is the restricted range in which PMMA could be measured. Being the most difficult material to demold many process settings could not be manufactured at all (compare Table 6.3). Therefore, only few measurements could be compared making conclusions about the influencing factors difficult. Additionally, the measurements for PMMA showed a different nature than the other polymers. Due to the increased stiffness and completely different sticking properties, PMMA was the only material that showed measurable demolding force peaks as suggested in literature (compare chapter 3.5 'Demolding force and measurement methods'). All investigated polymers other than PMMA had a comparably good demoldability and showed demolding force curves that approached 0 N as the demolding progressed (compare chapter 5.7 Signal evaluation). Figure 6.15 shows the force-displacement curves for PMMA instead of the otherwise used demolding energy curves. The curves clearly go above the 0 line as the demolding produces additional forces unlike the other materials. The visible force peak is an indicator for the demoldability of the given configuration. Despite the fact that the curves are similar to what is suggested in literature, the measured forces are a lot lower. This makes an evaluation of these measurements unreliable. Even more so for the demolding energy integrals, as the integral value gets distorted by the steep slope in the beginning and the overshoot above the x-axis. The only conclusion that is possible is that among these coatings MoS_2 and WC/C perform worst.

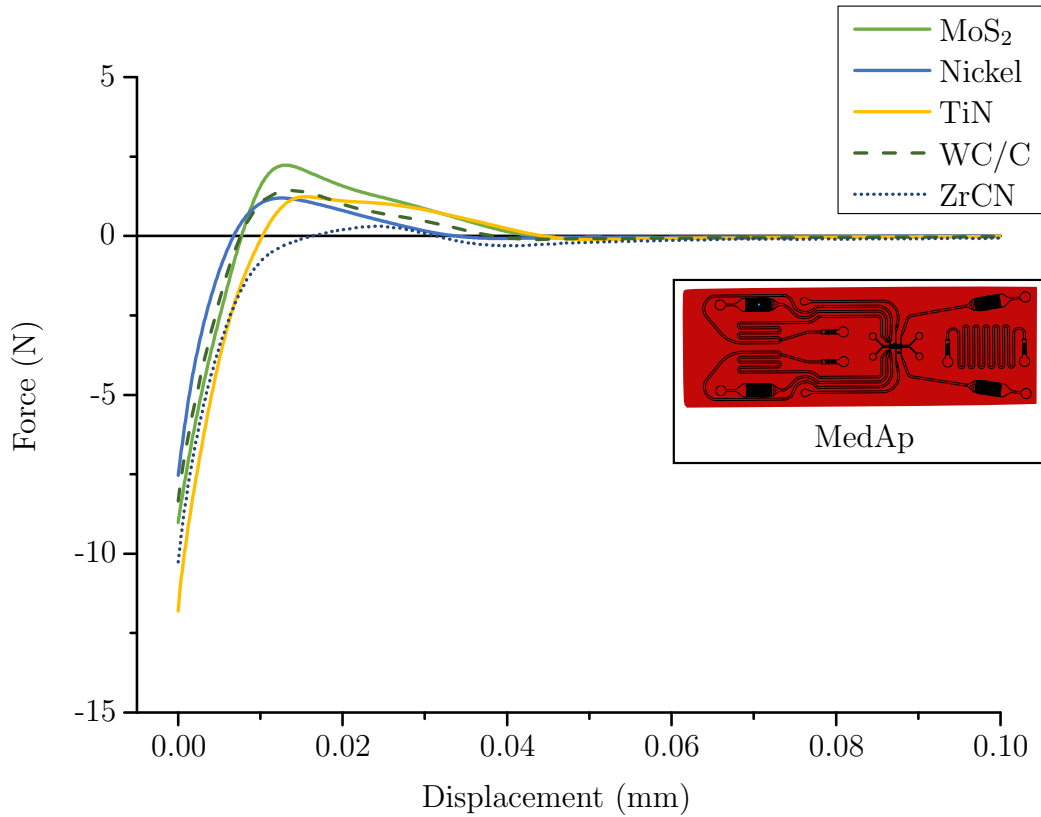This is validated further by the failed demolding attempts as shown in

Figure 6.15. Demolding force curves for PMMA and different coatings.

Table 6.3. This overview shows a short comprehensive overview of all the selected configurations for PMMA. The choice of color (i.e. red and green) indicates whether a specific configuration could be used to manufacture microstructured parts. Red means that the part broke when the mold opened while green denotes that a part could successfully be manufactured. The normal stamper could only be used without using the variotherm heating. Additionally, using the TiN coating on the Normal structure no parts could be manufactured. This is attributed to the coating properties based on the insert surface (compare chapter 6.1 Polymer results). This can also be seen as TiN performs well for the MedAp chip, even with the use of a variotherm system. MoS_2 and WC/C fail completely in this regard producing the worst part failure among all the process settings, i.e. the complete part sticked to the insert and could hardly be removed even with the use of external forces. The Inflow and Perflow insert showed that for PMMA structure placement is less important than structure design. While none of these two stampers could be manufactured with the variotherm system, the Inflow stamper could

114

be replicated disregarding the position of the micro-structure. The Perflow stamper could not be replicated in PMMA for any tested setup. This confirms again that PMMA is one of the most critical polymers for 'lab-on-a-chip' devices and makes TiN or ZrCN an interesting alternative to the base material (nickel) to improve demolding. This can be deduced as these are the only coatings that could be demolded (even with variotherm) and they the promising low demolding force peaks.

Table 6.3. Overview of PMMA and what configurations could be manufactured. *green* = can be manufactured, *red* = part breaks

Micro-structure	Configuration	No variotherm	Variotherm
Normal	Nickel	green	red
	TiN	red	red
MedAp	MoS$_2$	green	red
	WC/C		
	Nickel	green	green
	TiN		
	ZrCN		
Inflow	Nickel/Close	green	red
	Nickel/Far		
Perflow	Nickel/Close	red	red
	Nickel/Far		

6.6   Summary and injection molding guide

After the investigation of the influencing factors summarizing the main conclusions can provide a structured approach towards a functional injection molding process for micro-structured surfaces. Therefore, the four influencing factors are discussed resembling a stage gate process. This approach is necessary due to the many interactions among the influencing factors and the absence of clear trends that apply for all of them. Figure 6.16 shows the first

two steps towards the final polymer part. The first step therefore is the polymer choice. The polymer choice affects all subsequent parameters the most. If possible PMMA should be avoided due to its high stiffness and tendency for sticking. The modulus, the thermal properties, and adhesion and friction can generally be a good indicator to determine the demolding possibilities before any of the other influencing factors come into effect. Only after the polymer is selected or provided by the application the micro-structure design should be set. In many cases the structure is defined by the application. If not, simple design guidelines can change whether a part is demoldable or not. Placement of the structures near the shrinkage center (i.e. near the gate for the injection molding process) is favorable. The orientation of flow channels in relation to the melt flow direction can be critical as well. Channels that run perpendicular to the flow front are generally worse for the demoldability than channels in flow direction. In theory the first two influencing factors (polymer and design) are interchangeable, but COP shows a different behavior for structural placement than PP, thereby reinforcing the order of setting the influencing factors.

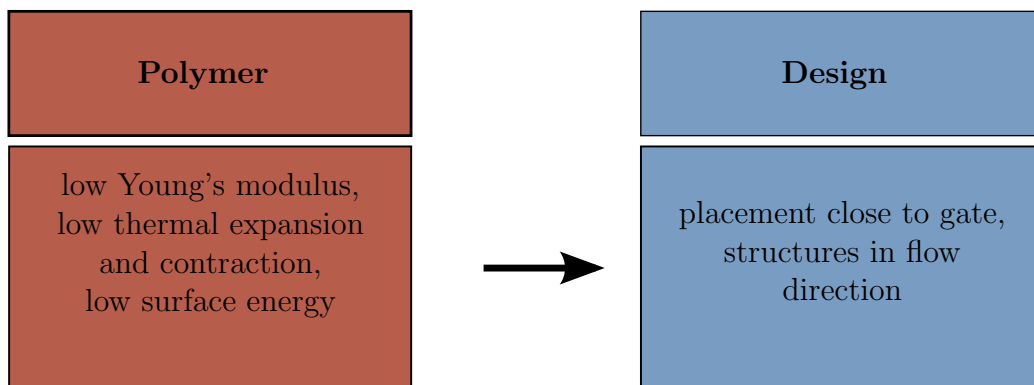| Polymer	Design
low Young's modulus, low thermal expansion and contraction, low surface energy	placement close to gate, structures in flow direction

Figure 6.16. Preferable polymer and micro-structure parameters for optimizing the demoldability in the injection molding process.

Figure 6.17 shows the last two steps towards the final polymer part. The mold, or more specifically the mold coating, can change the interaction (i.e. friction and adhesion) of the polymer and the structure drastically. This can help making previously impossible manufacturing setups possible. The most important aspect here is to choose the coating with regard to the polymer. For example PMMA performed very well for the MedAp chip with the TiN coating. Other coatings can affect the demoldability in an opposite way. This was shown when WC/C and MoS_2 made it impossible to demold the MedAp structure. Therefore, the selection should in any case be tested for the corresponding polymer material, because contact angles or surface energies are

no indicator for performance with a specific polymer. The last step is the injection molding process. This is the influencing factor that can counteract an unfavorable demolding behavior after all the parameters are set. Some setups like PMMA and the Perflow stamper could not be manufactured at all. For COP the processing parameters can counteract a unfavorable demoldability. While COP with the Perflow stamper also leads to part breakage for many setups, increasing the mold temperature makes manufacturing the polymer part possible. Additionally, there is an important difference to the observations documented in literature. Literature reports a critical demolding temperature for several investigations using a hot embossing machine. This critical demolding temperature could not be found for the injection molding process. Finally, the variotherm system will not change the demolding tendencies, but will generally worsen the demoldability of a given setup.

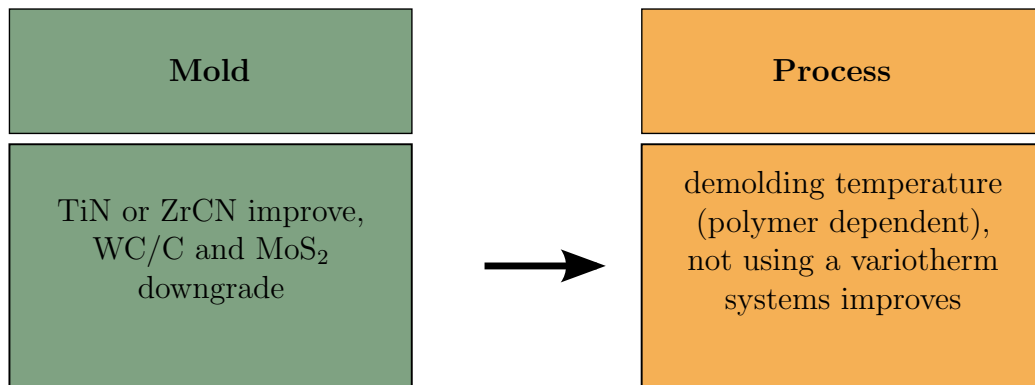Figure 6.17. Preferable mold and process parameters for optimizing the injection molding for micro-structured parts.

This means that an optimal product development procedure should choose the polymer first, optimize the micro-structure design to accommodate the respective manufacturing process (e.g. injection molding), select a suitable coating for the selected polymer and finalize by finding the appropriate operating point.

Chapter 7

Summary

7.1 Conclusion

Little research work is reported in the literature on the combination of the demolding step in injection molding and polymeric medical applications that are utilizing micro-structures. In this work, the critical process step of manufacturing micro-structures during the injection molding - the demolding step - was investigated. To investigate the demolding step, an injection mold was designed that allowed accurate measurements of this process step. First measurements showed that force peaks due to the demolding are not common in the injection molding unlike it was reported for the hot embossing process. Therefore a demolding energy was calculated for the comparison of the demolding results. This demolding energy was confirmed to be not only viable for describing the demolding step, but can also be measured with sufficient accuracy and reproducibility. Using this setup, four factors determining the demolding step were investigated. These factors were the polymer, the micro-structure design, the mold and the injection molding process. These factors interact with each other in a complex manner - no clear trends could be detected. However, the following observations for the influencing factors could be confirmed.

- The *polymer* is the deciding factor for the demolding quality. Several polymer properties will directly affect the demolding energy. This includes stiffness, thermal expansion as well as adhesion and friction. PMMA, which has an especially high stiffness, is therefore the material with the most demolding problems. PP on the other hand can always be demolded. COP is hard to demold for some configurations. The demolding of these COP configurations can be improved by blending with TPE, which lowers the polymer stiffness.

- The orientation and position of the *micro-structure* is another important aspect for the demolding step. The orientation of the micro-structures affects demoldability, leading to an increase in the demolding energy for a perpendicular structure orientation. The demolding energy can increase even further when affected by the polymer shrinkage. Placing the structure farther from the injection gate therefore results in higher demolding energies. For example PMMA in a far from gate configuration could not be manufactured at all. Additionally, structure placement can deform the macro geometry in the demolding process. This can lead to an 'S-shape' deformation of the part.
- The *mold*, or more specifically the mold coating, can change the interaction (i.e. friction and adhesion) drastically, making previously impossible manufacturing setups possible. The contact angles and thus the surface energies of the mold coatings are no criteria for the demolding energy. The polymer determines whether a coating will improve the demoldability or have a negative effect on it. PMMA will work well with the TiN coating, while TiN will not improve the demoldability of PP. WC/C works for COP but makes demolding PMMA impossible.
- The *processing* conditions, specifically the temperatures, affect the demolding step. The mold temperature determines the temperature of the polymer for the demolding step. This defines the stiffness, adhesion, and friction properties of the polymer. Despite the measurable influence of the demolding temperature, a critical demolding temperature, as was suggested in literature for hot embossing, could not be found for the injection molding process. The demolding energy shows the same trends with and without the use of the variotherm system. While the trends stay the same, the demolding gets worse with the variotherm system on. An example for this is PMMA which cannot be demolded for many settings when using the variotherm heating.

Even though no general trends could be derived in this work, it showed that it is possible to reliably measure the demolding energy and use it to assess the respective molding setup. Furthermore, it showed coatings that can improve the demolding drastically for some polymers. Especially the TiN coating performed better than expected for PMMA and several micro-structures.

7.2 Outlook

This in-depth investigation of a completely new measurement setup shows promise in analyzing the mechanisms that determine the demolding step in the injection molding process. The investigation of the parameters also reveals the complex interactions that exist between the important parameters. For better understanding of these interactions the four main influencing factors need further investigation. The following steps that connect perfectly to the performed research are suggested:

- The *polymer* investigation should focus on temperature dependent parameters that are often neglected (i.e. stiffness). An investigation here can lead to better understanding of the temperature related stresses in the demolding step.
- The *micro-structure* investigation should also include protective auxiliary structures. The influence on the replication quality has already been proven, but the effect on the overall part demoldability is still unclear.
- The *mold* especially the mold coatings showed promise in improving otherwise unchangeable setups in regard to the demoldability. To further improve these effects, a better understanding of the mechanisms that coatings have is required. To achieve that, surfaces with different roughness should be manufactured and tested. In this step an additional focus should be on the surface morphology to investigate the interaction to different polymers more closely. Complementary hot contact angle measurements with the respective polymers are of great interest for deeper understanding of the interactions.
- The injection molding *process* proves to be different to the hot embossing in many of the performed experiments (e.g. no critical demolding temperature). Therefore, several of the investigations already completed for hot embossing should be redone in injection molding.
- To complement the experimental research simulation experiments should be set up. These simulations should cover injection molding simulations to analyze the polymer and process side (e.g. thermal setup and material stiffness) as well as mechanical simulation to model the demolding step using the parameters provided from the injection molding simulation. The mechanical simulation can focus more closely on the interaction of the surfaces modeling the micro-structure and the coating (i.e. friction and adhesion) properties.

References

[1] E. Altendorf, D. Zebert, M. Holl, A. Vannelli, C. Wu, and T. Schulte. Results Obtained using A Prototype Microfluidics-Based Hematology Analyzer. In D. J. Harrison and van den Berg, A., editors, *Micro Total Analysis Systems '98*, pages 73–76. Springer Netherlands, 1998.

[2] A. Amirsadeghi, J. J. Lee, and S. Park. Surface adhesion and demolding force dependence on resist composition in ultraviolet nanoimprint lithography. *Applied Surface Science*, 258(3):1272–1278, 2011.

[3] U. M. Attia, S. Marson, and J. R. Alcock. Micro-injection moulding of polymer microfluidic devices. *Microfluidics and Nanofluidics*, 7(1):1–28, 2009.

[4] H. Becker and U. Heim. Hot embossing as a method for the fabrication of polymer high aspect ratio structures. *Sensors and Actuators A: Physical*, 83(1–3):130–135, 2000.

[5] H. Becker and L. E. Locassio. Polymer microfluidic devices. *Talanta*, 56(2):267–287, 2002.

[6] Ferdinand P. Beer. *Vector Mechanics for Engineers*. McGraw-Hill, sixth edition, 1996.

[7] G. Berger and W. Friesenbichler. Demolding forces and coefficients of friction in injection molding. A new practical measurement apparatus. *Proceedings of ANTEC 2009*, pages 1699–1703, 2009.

[8] B. Bhushan. Adhesion and stiction: Mechanisms, measurement techniques, and methods for reduction. *Journal of Vacuum Science & Technology B: Microelectronics and Nanometer Structures*, 21(6):2262, 2003.

[9] E. Bormashenko. Why does the Cassie–Baxter equation apply? *Colloids and Surfaces A: Physicochemical and Engineering Aspects*, 324(1-3):47–50, 2008.

[10] R. Brown. Mold release composition containing tungsten disulfide: US Patent 3915870.

[11] Bruzzone, A. A. G., H. L. Costa, P. M. Lonardo, and D. A. Lucca. Advances in engineered surfaces for functional performance. *CIRP Annals - Manufacturing Technology*, 57(2):750–769, 2008.

[12] A. Buda and A. Jarynowski. *Life time of correlations and its applications*. Andrzej Buda Wydawnictwo Niezależne, [Głogów], 2010.

[13] M. Burgsteiner. Rendering of the mold design: Konzepte zur Entformungskraftmessung von Mikrostrukturen: Montanuniversität, Internal report, 2012.

[14] M. Burgsteiner, F. Müller, G. Berger, and T. Lucyshyn. Entwicklung eines Werkzeugs zur Entformungskraftmessung von Mikrostrukturen: Montanuniversität, Internal report, 2010.

[15] M. Burgsteiner and T. Struklec. Konzepte: Konzepte zur Entformungskraftmessung von Mikrostrukturen: Montanuniversität, Internal report, 2011.

[16] Center for Devices and Radiological Health. Classify Your Medical Device - Is The Product A Medical Device?

[17] R.-D. Chien. Hot embossing of microfluidic platform. *International Communications in Heat and Mass Transfer*, 33(5):645–653, 2006.

[18] R.-D. Chien. Micromolding of biochip devices designed with microchannels. *Sensors and Actuators A: Physical*, 128(2):238–247, 2006.

[19] G. W. Critchlow, R. E. Litchfield, I. Sutherland, D. B. Grandy, and S. Wilson. A review and comparative study of release coatings for optimised abhesion in resin transfer moulding applications. *International Journal of Adhesion and Adhesives*, 26(8):577–599, 2006.

[20] L. Cunha, M. Andritschky, K. Pischow, Z. Wang, A. Zarychta, A.S Miranda, and A.M Cunha. Performance of chromium nitride and titanium nitride coatings during plastic injection moulding. *Surface and Coatings Technology*, 153(2-3):160–165, 2002.

[21] P. A. Dearnley. Low friction surfaces for plastic injection molding dies-an experimental case study. *Wear*, (225-229):1109–1113, 1999.

[22] K. Delaney, Kennedy D., and Bissacco G. Investigating Polymer-Tool Steel Interfaces to Predict the Work of Adhesion for Demoulding Force Optimisation. *School of Mechanical and Transport Engineering*, 2011.

[23] Duncan Dowson. *History of tribology.* Addison-Wesley Longman Limited, 1979.

[24] Y. Duan, Y. Li, Y. Ding, and D. Li. Effect of surface roughness and release layer on anti-adhesion performance of the imprint template. *Applied Surface Science*, 257(8):3220–3225, 2011.

[25] Europaeisches Parlament. Richtlinie 98/79/EG des Europäischen Parlaments und des Rates vom 27. Oktober 1998 über In-vitro-Diagnostika. 1998.

[26] European Commission. Revision of the medical device directives, 2010.

[27] G. Fu, N. H. Loh, S. B. Tor, B. Y. Tay, Y. Murakoshi, and R. Maeda. Analysis of demolding in micro metal injection molding. *Microsystem Technologies*, 12(6):554–564, 2006.

[28] G. Fu, S. Tor, N. Loh, B. Tay, and D. E. Hardt. A micro powder injection molding apparatus for high aspect ratio metal micro-structure production. *Journal of Micromechanics and Microengineering*, 17(9):1803–1809, 2007.

[29] G. Fu, S. B. Tor, N. H. Loh, and D. E. Hardt. Micro-hot-embossing of 316L stainless steel micro-structures. *Applied Physics A*, 97(4):925–931, 2009.

[30] G. Fu, S. B. Tor, N. H. Loh, B. Y. Tay, and D. E. Hardt. The demolding of powder injection molded micro-structures: analysis, simulation and experiment. *Journal of Micromechanics and Microengineering*, 18(7):075024, 2008.

[31] B. Geissler. Processing and blending of TPE: Montanuniversität, Internal report, 2014.

[32] J. Greener and R. Wimberger-Friedl, editors. *Precision Injection Molding.* Carl Hanser Verlag GmbH & Co. KG, München, 2006.

[33] C. A. Griffiths, S. Bigot, E. Brousseau, M. Worgull, M. Heckele, J. Nestler, and J. Auerswald. Investigation of polymer inserts as prototyping tooling for micro injection moulding. *The International Journal of Advanced Manufacturing Technology*, 47(1-4):111–123, 2010.

[34] C. A. Griffiths, S. S. Dimov, E. B. Brousseau, C. Chouquet, J. Gavillet, and S. Bigot. Micro-injection moulding: surface treatment effects on part demolding. *Multi-Material Micro Manufacture*, 2008.

[35] C. A. Griffiths, S. S. Dimov, E. B. Brousseau, C. Chouquet, J. Gavillet, and S. Bigot. Investigation of surface treatment effects in micro-injection-moulding. *The International Journal of Advanced Manufacturing Technology*, 47(1-4):99–110, 2010.

[36] A. E. Guber, M. Heckele, D. Herrmann, A. Muslija, V. Saile, L. Eichhorn, T. Gietzelt, W. Hoffmann, P. C. Hauser, J. Tanyanyiwa, A. Gerlach, N. Gottschlich, and G. Knebel. Microfluidic lab-on-a-chip systems based on polymers - fabrication and application. *Chemical Engineering Journal*, 101(1-3):447–453, 2004.

[37] Y. Guo, G. Liu, Y. Xiong, and Y. Tian. Analysis of the demolding forces during hot embossing. *Microsystem Technologies*, 13(5-6):411–415, 2007.

[38] Y. Guo, G. Liu, Y. Xiong, and Y. Tian. Study of the demolding process—implications for thermal stress, adhesion and friction control. *Journal of Micromechanics and Microengineering*, 17(1):9–19, 2007.

[39] A. C. Hall, M. T. Dugger, S. V. Prasad, and T. Christensen. Sidewall morphology of electroformed LIGA parts-implications for friction, adhesion, and wear control. *Journal of Microelectromechanical Systems*, 14(2):326–334, 2005.

[40] C. A. Harrington, C. Rosenow, and J. Retief. Monitoring gene expression using DNA microarrays. *Current Opinion in Microbiology*, 3(3):285–291, 2000.

[41] S. Haubenwallner, M. Katschnig, U. Fasching, S. Patz, C. Trattnig, N. Andraschek, G Grünbacher, M. Absenger, S. Laske, C. Holzer, W. Balika, M. Wagner, and U. Schäfer. Effects of the polymeric niche on neural stem cell characteristics during primary culturing. *Journal of materials science. Materials in medicine*, 25(5):1339–1355, 2014.

[42] M. Heckele and W. Bacher. Hot embossing - The molding technique for plastic microstructures. *Microsystem Technologies*, (4), 1998.

[43] M. Heinze. Wear resistance of hard coatings in plastics processing. *Surface and Coatings Technology*, 105(1-2):38–44, 1998.

[44] R. C. Hibbeler. *Engineering Mechanics*. Pearson, Prentice Hall, eleventh edition, 2007.

[45] M. Iwamatsu. The validity of Cassie's law: A simple exercise using a simplified model. *Journal of Colloid and Interface Science*, 294(1):176–181, 2006.

[46] M. Karl and C. Pöschl. Injection mold specifications: Sony DADC, Conferenc call, 2012.

[47] H. Kawata, J. Ishihara, M. Kayama, M. Yasuda, and Y. Hirai. The Dependence of Demolding Characteristics on Side Wall Roughness of Mold in Thermal Imprint. *IEEJ Transactions on Sensors and Micromachines*, 128(8):325–330, 2008.

[48] H. Kawata, M. Matsue, K. Kubo, M. Yasuda, and Y. Hirai. Silicon template fabrication for imprint process with good demolding characteristics. *Microelectronic Engineering*, 86(4-6):700–704, 2009.

[49] O. Kemmann, C. Schaumburg, L. Weber, B. Courtois, S. B. Crary, W. Ehrfeld, H. Fujita, J. M. Karam, and K. W. Markus. Micromolding behavior of engineering plastics. In *Design, Test, and Microfabrication of MEMS/MOEMS*, SPIE Proceedings, pages 464–471. SPIE, 1999.

[50] K. Kendall. Adhesion: Molecules and Mechanics. *Science*, 263(5154):1720–1725, 1994.

[51] Kistler. Kraftmessung mit Messunterlagsscheiben: Product specifications.

[52] K. Koski, J. Hölsä, and P. Juliet. Properties of zirconium oxide thin films deposited by pulsed reactive magnetron sputtering. *Surface and Coatings Technology*, 120-121:303–312, 1999.

[53] C. Lam, R. Wu, D. Li, M. Hair, and A. Neumann. Study of the advancing and receding contact angles: liquid sorption as a cause of contact angle hysteresis. *Advances in Colloid and Interface Science*, 96(1-3):169–191, 2002.

[54] G.-B. Lee, S.-H. Chen, G.-R. Huang, W.-C. Sung, and Y.-H. Lin. Microfabricated plastic chips by hot embossing methods and their applications for DNA separation and detection. *Sensors and Actuators B: Chemical*, 75(1–2):142–148, 2001.

[55] T. Leveder, S. Landis, L. Davoust, and N. Chaix. Optimization of demolding temperature for throughput improvement of nanoimprint lithography. *Microelectronic Engineering*, 84(5-8):953–957, 2007.

[56] A.-C. Liou and R.-H. Chen. Injection molding of polymer micro- and sub-micron structures with high-aspect ratios. *The International Journal of Advanced Manufacturing Technology*, 28(11-12):1097–1103, 2006.

[57] F. London. The general theory of molecular forces. *Transactions of the Faraday Society*, 33:8b, 1937.

[58] D. A. Mair, E. Geiger, A. P. Pisano, Frchet, J. M. J., and F. Svec. Injection molded microfluidic chips featuring integrated interconnects. *Lab on a Chip*, 6(10):1346, 2006.

[59] A. Majumder, A. Ghatak, and A. Sharma. Microfluidic adhesion induced by subsurface microstructures. *Science (New York, N.Y.)*, 318(5848):258–261, 2007.

[60] J. L. Meriam and L. G. Kraige. *Engineering Mechanics: Statics*. Wiley and Sons, 2002.

[61] S. Merino, H. Schift, A. Retolaza, and T. Haatainen. The use of automatic demolding in nanoimprint lithography processes. *Microelectronic Engineering*, 84(5-8):958–962, 2007.

[62] W. Michaeli and R. Gärtner. New demolding concepts for the injection molding of microstructures. *Journal of Polymer Engineering*, 26(2-4):161–177, 2006.

[63] W. Michaeli, A. Spennemann, and R. Gärtner. New plastification concepts for micro injection moulding. *Microsystem Technologies*, 8(1):55–57, 2002.

[64] Micro-Epsilon. Kapazitive Sensoren für Weg, Abstand & Position: Product specifications, 2014.

[65] V. Miikkulainen, M. Suvanto, T. A. Pakkanen, S. Siitonen, P. Karvinen, M. Kuittinen, and H. Kisonen. Thin films of MoN, WN, and perfluorinated silane deposited from dimethylamido precursors as contamination resistant coatings on micro-injection mold inserts. *Surface and Coatings Technology*, 202(21):5103–5109, 2008.

[66] P. B. Monaghan, A. Manz, and W. W. Nichols. Microbiology On-a-Chip. In A. Berg, W. Olthuis, and P. Bergveld, editors, *Micro Total Analysis Systems 2000*, pages 111–114. Springer Netherlands, 2000.

[67] P. Navabpour, D. G. Teer, D. J. Hitt, and M. Gilbert. Evaluation of non-stick properties of magnetron-sputtered coatings for moulds used for the processing of polymers. *Surface and Coatings Technology*, 201(6):3802–3809, 2006.

[68] P. S. Nunes, P. D. Ohlsson, O. Ordeig, and J. P. Kutter. Cyclic olefin polymers: emerging materials for lab-on-a-chip applications. *Microfluidics and Nanofluidics*, 9(2-3):145–161, 2010.

[69] P. O'Leary and M. Harker. An Algebraic Framework for Discrete Basis Functions in Computer Vision: Proceedings. pages 150–157, 2008.

[70] G. Pacher, G. Berger, W. Friesenbichler, and Gruber, D., P. Die Wirkung dynamischer Werkzeugtemperierung auf die Oberflächenqualität von Kunststoffteilen. In *22. Leobener Kunststoff-Kolloquium: Oberlfächen und Grenzflächen in der Polymertechnologie*, pages 101–110. 2013.

[71] Z. Peng, L. Gang, T. Yangchao, and T. Xuehong. The properties of demoulding of Ni and Ni-PTFE moulding inserts. *Sensors and Actuators A: Physical*, 118(2):338–341, 2005.

[72] R. Pethig, Burt, J. P. H., A. Parton, N. Rizvi, M. S. Talary, and J. A. Tame. Development of biofactory-on-a-chip technology using excimer laser micromachining. *Journal of Micromechanics and Microengineering*, 8(2):57, 1998.

[73] A. S. Pouzada, E. C. Ferreira, and A. J. Pontes. Friction properties of moulding thermoplastics. *Polymer Testing*, 25(8):1017–1023, 2006.

[74] H. Pranov, H. K. Rasmussen, N. B. Larsen, and N. Gadegaard. On the injection molding of nanostructured polymer surfaces. *Polymer Engineering & Science*, 46(2):160–171, 2006.

[75] Rudra Pratap and Andy Ruina. *Introduction to Statics and Dynamics*. Oxford University Press, 2002.

[76] O. Rötting, W. Röpke, H. Becker, and C. Gärtner. Polymer microfabrication technologies. *Microsystem Technologies*, 8(1):32–36, 2002.

[77] Yi Sang. Dependence of friction on roughness, velocity, and temperature. *Physical Review E*, 77(3):036123, 2008.

[78] H. Schift. Oral contribution: Paul Scherrer Institut, 5232, Villigen, PSI, 2010.

[79] H. Schift. *NaPa Library of Processes*. NaPANIL-consortium represented by J. Ahopelto, second edition edition, 2012.

[80] W. Schinkoethe and T. Walther. Zykluszeiten verringern: Eine alternative Werkzeugtemperierung beim Mikrospritzgießen. *KU Kunststoffe*, 90(5):62–68, 2000.

[81] N. Schmid. *Untersuchung der Haft- und Entformungskrääfte beim Heißprägen von Mikrostrukturen*. PhD thesis, Fachhochschule Nordwestschweiz: FHNW, Windisch, 2006.

[82] Schmid, J., Jr. The Relationship between the Coefficient of Correlation and the Angle Included between Regression Lines. *The Journal of Educational Research*, 41(4):311–313, 1947.

[83] Z. Song. *Study of demolding process in thermal imprint lithography via numerical simulation and experimental approaches*. PhD thesis, Louisiana State University, 2012.

[84] Z. Song, J. Choi, B. H. You, J. Lee, and S. Park. Simulation study on stress and deformation of polymeric patterns during the demolding process in thermal imprint lithography. *Journal of Vacuum Science & Technology B: Microelectronics and Nanometer Structures*, 26(2):598, 2008.

[85] B. Strohmayer. *Analysis on factors affecting the demolding of microstructured devices in the injection molding process*. PhD thesis, Fachhochschule Nordwestschweiz: FHNW, Leoben, 2015.

[86] S. Takayama, J. C. McDonald, E. Ostuni, M. N. Liang, Kenis, P. J. A., R. F. Ismagilov, and G. M. Whitesides. Patterning cells and their environments using multiple laminar fluid flows in capillary networks. *Proceedings of the National Academy of Sciences*, 96(10):5545–5548, 1999.

[87] U. A. Theilade and H. N. Hansen. Surface microstructure replication in injection molding. *The International Journal of Advanced Manufacturing Technology*, 33(1-2):157–166, 2007.

[88] C.-J. Ting, C.-F. Chen, and C. P. Chou. Subwavelength structures for broadband antireflection application. *Optics Communications*, 282(3):434–438, 2009.

[89] V. Trabadelo, H. Schift, S. Merino, S. Bellini, and J. Gobrecht. Measurement of demolding forces in full wafer thermal nanoimprint. *Microelectronic Engineering*, 85(5-6):907–909, 2008.

[90] H.-D. Wang, B.-S. Xu, J.-J. Liu, and D.-M. Zhuang. Molybdenum disulfide coating deposited by hybrid treatment and its friction-reduction performance. *Surface and Coatings Technology*, 201(15):6719–6722, 2007.

[91] Watlow. Ultramic Advanced Ceramic Heaters: Product specifications.

[92] B. H. Weigl and P. Yager. Microfluidic Diffusion-Based Separation and Detection. *Science*, 283(5400):346–347, 1999.

[93] G. Wolansky and A. Marmur. Apparent contact angles on rough surfaces: the Wenzel equation revisited. *Colloids and Surfaces A: Physicochemical and Engineering Aspects*, 156(1-3):381–388, 1999.

[94] M. Worgull, M. Heckele, and W. K. Schomburg. *Analyse des Mikro-Heißprägeverfahrens*. PhD thesis, Universtität Karlsruhe, Karlsruhe, 2003.

[95] M. Worgull, J.-F. Hétu, K. K. Kabanemi, and M. Heckele. Characterization of Friction during the Demolding of Microstructures Molded by Hot Embossing. *DTIP of MEMS/MOEMS*, 2006.

[96] H. Yamamoto, Y. Ohkubo, K. Ogawa, and K. Utsumi. Application of a chemically adsorbed fluorocarbon film to improve demolding. *Precision Engineering*, 33(3):229–234, 2009.

[97] L. Yi, W. Xiaodong, and Y. Fan. Microfluidic chip made of COP (cyclo-olefin polymer) and comparion to PMMA (polymethylmethacrylate) microfluidic chip. *Journal of Materials Processing Technology*, 208(1-3):63–69, 2008.

[98] Y. E. Yoo, T. H. Kim, D. S. Choi, S. M. Hyun, H. J. Lee, K. H. Lee, S. K. Kim, B. H. Kim, Y. H. Seo, H. G. Lee, and J. S. Lee. Injection molding of a nanostructured plate and measurement of its surface properties. *Current Applied Physics*, 9(2):e12–e18, 2009.

[99] S.-H. Yoon, N.-G. Cha, J. S. Lee, J.-G. Park, D. J. Carter, J. L. Mead, and Barry, C. M. F. Effect of processing parameters, antistiction coatings, and polymer type when injection molding microfeatures. *Polymer Engineering & Science*, 50(2):411–419, 2010.